2016

Effect of real time aging and cyclic fatigue on fused and cemented machined veneers to Y-TZP zirconia

BOSTON UNIVERSITY

HENRY M. GOLDMAN SCHOOL OF DENTAL MEDICINE

DISSERTATION

EFFECT OF REAL TIME AGING AND CYCLIC FATIUGE ON FUSED AND CEMENTED MACHINED VENEERS TO Y-TZP ZIRCONIA

ABDULRAHMAN JAFAR M. ALHADDAD

Bachelor of Dental Medicine and Surgery, King Abdulaziz University, 2007

Postgraduate Certificate in Prosthodontics, Boston University, 2016

Submitted in partial fulfillment of the requirements for the degree of

Doctor of Science in Dentistry

In the Department of Restorative Science and Biomaterials

2016

READER'S APPROVAL

First Reader

Dr. Russell Giordano II, D.M.D., D.M.Sc.
Associate Professor and Director of Biomaterials
Department of Restorative Science and Biomaterials

Second Reader

Dr. Richard Pober, Sc.D.
Associate Research Professor
Department of Restorative Science and Biomaterials

Third Reader

Dr. Gurkan Goktug D.M.D, DDS
Director Prosthodontics Resident Lab, Assistant Professor
Department of Restorative Science and Biomaterials

CHAIRMAN'S APPROVAL

Chairman's Approval

Dr. Dan Nathanson, D.M.D., M.S.D.
Professor and Chairman
Department of Restorative Science and Biomaterials

DEDICATIONS

To my father: Jafar M. Alhaddad, the first teachers who instilled in me the value of knowledge, morale and progress. He will forever be in my memory and in my future of all the practices and values I provide to my children and their kids as they become adults.

To my mother: Fatimah M. Alhebshi, the women who I admire and love unconditionally for the surmounted difficulties to make my world a better place.

To my beautiful wife, who have supported me through the pillars in life.

To my brothers and sisters, who believed in me and encouraged the strength within.

ACKNOWLEDGMENTS

All praise is for God, who gave me the strength and courage to plod on this path in the pursuit for knowledge. May God help me to remember, to praise, and to worship him and to direct this knowledge in helping others through their educational journey.

I cannot forget to pay my true respect and appreciation to the outstanding people who helped me accomplish this research. Their major role in helping me to gain a deeper understanding of biomaterials, especially as it relates to my specialty.

I would like to thank Dr. Giordano, my research advisor and my mentor, who helped me with everything. Thank you for accepting me into this research program. I have learned a lot regarding ceramics, which I have never known before.

I would like to thank Dr. Pober, who was there for me every step teaching me and answering every single question and taught me how to do research.

I must acknowledge my kids: Albatool and Omar who I was lucky to have, and who have made my life in Boston more prosperous, meaningful, and enjoyable.

My gratitude to the Government of the Kingdom of Saudi Arabia for their unrelenting support. I could not have come here for studying without their support.

Many thanks to King Abdul-Aziz University, school of dental medicine who taught me everything I knew in dentistry and graduated the doctor who I am today and accepted me to be one of their faculty members.

Thanks to Dr. Nathanson for accepting me in the program and believing in me to be a great scientist and prosthodontist.

I would like to give special thanks to Dr. Gurkan Goktug who guided me throughout the five years of the prosthodontics department. It was not an easy task, but you are a mentor, colleague and true friend.

I would like to acknowledge Mr. Johnny Sihakhamfong and Dr. Ghassan Al-Ayoub for making the last few years in the dental school great as friendship and brotherhood are hard to come by in a foreign country.

Recognition to Mr. Ron L'Herault, Dr. Claire Zhang, and Dr. Yuwei Fan for guiding me in the proper techniques in the biomaterial laboratory.

Thanks to Mrs. Leslie Baker and Milly Koo for assisting me in organizing this thesis defense and helping with all the paper works.

Finally, I would like to thank all my friends who were standing by my side and giving me the helpful additional support.

EFFECT OF REAL TIME AGING AND CYCLIC FATIUGE ON FUSED AND CEMENTED MACHINED VENEERS TO Y-TZP ZIRCONIA

ABDULRAHMAN JAFAR M. ALHADDAD

Boston University, Henry M. Goldman School of Dental Medicine, 2016

Major Professor: Russell A. Giordano II, Professor of Biomaterials

ABSTRACT

Objectives: The objectives of this study was to determine the differences in failure load between cemented and fused machined veneers to zirconia while observing the effects of real time aging on failure load between cemented and fused machined veneers to zirconia. The study was to examine the differences in aging and fatigue resistance amongst a machined glass-ceramic veneer and a machined feldspathic porcelain veneer.

Materials & Methods: VITA In Ceram YZ zirconia blocks were used as a substructure framework for the three unit fixed partial denture. The veneering material was either milled IPS e.max CAD (glass-ceramic) or milled VITABLOCS Triluxe Forte (feldspathic porcelain). The types of linking material between the substructures and veneering material were either fusing or cementation. Observations were compared between aged and non-aged specimens divided into two main groups; (a) non-aged group (b) aged for three years at room temperature. Each group has two subgroups; fused and cemented which are further divided into static and cyclic fatigue at 20K, 60K and 80K. Specimens were subjected to load to failure test using universal test machine. 40% of failure load was calculated for the cyclic fatigue subgroups. In order to examine the difference in failure load between the static and fatigued specimens, the Tukey-Kramer HSD test was used to analyze the data.

Results and Conclusions: The VITABLOCS Triluxe Forte (feldspathic porcelain) fused to YZ zirconia showed significantly lower failure load values compared to all the other groups ($p<0.05$). The non-aged VITABLOCS Triluxe Forte cemented to YZ zirconia (static and cyclic) showed significantly higher load to failure than the aged cemented Triluxe fatigued groups ($p<0.05$). There is no significant difference in failure load between IPS e.max CAD fused and IPS e.max CAD cemented to YZ zirconia framework ($p>0.05$). The aged IPS e.max CAD fatigued (20K, 60K and 80K cycles) cemented to YZ zirconia showed lower significant difference in failure load among all the other IPS e.max groups. ($p<0.05$).

TABLE OF CONTENTS

List of Tables

List of Figures

List of Graphs

INTRODUCTION

The term ceramic refers to a non-metallic inorganic material treated at high temperature. Ceramics are similar to glass by means of structure with an arrangement of crystal lattice that extends in all directions. The main objective of this literature is to review ceramic dental materials, including their most relevant physical and mechanical properties with different cementation techniques. Restorative materials within dental ceramics have shortcomings due to the inability to withstand functional loads that are present in the oral cavity. Discussions and debates exist to further develop solutions in dental treatment planning; i.e. material used for posterior long-span (3 Unit Bridge) fixed partial prosthetic restorations. With ceramics improvements over the years, it currently displays lower fracture toughness when compared with other restorative materials, such as metals. The aim is to compare the failure load of cementation and fusion technique of different machined veneers. Additionally, the study evaluated the effect of cyclic fatigue on failure load while identifying failures pattern and behavior of all-ceramic crowns by visual inspection.

All-ceramic restorations have become more popular in esthetics and full restorative dental planning, as they are comparable in appearance and strength to that of a natural tooth. Ceramic has many advantages because of its biocompatibility from its thermal conductivity, electrical insulators and chemical inertness to harmful elements that oral cavity endures. Ceramic restorations also provide esthetic and translucency properties providing better color stability and wear resistance compared to porcelain fused to metal. From a patient's point of view, authorized dental restorative procedures are dependent on the needs of the tooth i.e. eating and the visual i.e. smile needs.

The substructure zirconia (VITA In-Ceram YZ) has gained popularity in the last few years due to the combination with its veneering material such as lithium disilicate (IPS e.max) or VITABLOCS (Triluxe). Despite major improvement from previous materials, the current all-ceramic materials common complications are associated with fractures.

The era of digital dentistry has provided CAD/CAM technology with intraoral cameras to replicate scanning and 3-D milling. It has well enhanced time efficiency, visibility with transparency of the ideal tooth shade and the overall dental oral health industry. In present day, the technology of in-office CAD/CAM is available for simple to complex all-ceramic restorations such as; inlays, onlays, crowns and veneers. The now all-ceramic era is introducing high performance veneer ceramic systems to support and standardize single-visit chairside techniques. It is essential to understand the fundamental mechanics of failure in dental ceramics, especially under repetitive function that lead to fatigue failure. The CAD/CAM systems are a disruptive technology that is opening the door for new techniques of using partially stabilized zirconia as a core/framework material.

ZIRCONIA-BASED MATERIAL

Ceramic materials can successfully replace damaged and missing teeth, improving a patient's dental functionality and appearance. Zirconia is the oxidized form of zirconium (Zr) that imitates the qualities of natural teeth. The properties in the material is not cytotoxic which leads to a low bacterial adhesiveness and not vulnerable to corrosion. However, despite strength

under compression, it is unpredictable when it comes to fractures as it does not exhibit any deformation prior to failure as what can occur with a PFM restoration.

Zirconia exists in three major crystal phases: monoclinic, tetragonal, and cubic. Zirconia is in the monoclinic phase at room-temperature when it is stable. If temperatures are from 1170°C - 2369°C, zirconia transforms into the tetragonal intermediate phase and at 2370°C and higher, the material exists in the cubic phase.

Zirconia is able to sustain the tetragonal phase at room temperature when stabilizers such as ceria (CeO2, Cerium oxide), magnesia (MgO, Magnesium oxide), Calcia (CaO, Calcium oxide) or Yttria (Yttrium Oxide) are added. The concentration of the stabilizer plays a decisive role in the performance of this material under fatigue and the addition of yttrium results in partially stabilized tetragonal zirconia, which is the most attractive composition for "transformation toughening". The tetragonal to monoclinic uprising is of great scientific significance, due to the martensitic nature of the reaction.

The change from tetragonal to monoclinic phase is termed transformation-toughening. Upon temperature cooling from tetragonal to monoclinic, the property of zirconia undergoes a composition change with manipulation in the microstructure. Zirconia undertakes a change in the way its atoms are stacked at different temperatures, known as polymorphic transformation. As it is heated, shrinkage of one percent occurs and then a 2-5 % of expansion takes place. Normally as the volume increases, it creates compressive stresses at the crack tip that counteract the external tensile stresses and retards crack growth. Transformation-toughening assists for flexural strength providing data that are ranging between 800-1200 MPa with a fracture toughness ranging between 6-8 MPa, meeting the mechanical requirements for high stress posterior restorations. [16]

Phase transformation is commonly connected with stress concentration at the damage location where the initial residual stress starts. The coefficient of thermal expansion between the core and veneer layers can be relaxed during phase transformation as the monoclinic crystal has a larger volume than tetragonal. [47]

DENTAL CERAMICS

Most ceramic materials are composed of inorganic compounds that require baking at high temperature to fuse small particles together to form a crown or a pre-formed ceramic block used in CAD/CAM techniques. Dental ceramics began in the early 1960s with the introduction of metal-ceramic crowns. Fabrication of these crowns relied on application and firing of veneering porcelain to a metal substructure to produce an appealing crown. With progress, different types of ceramic are offered to handle the needs of the developing dental science and practices. Ceramics are classified according to their fabrication, processing and firing temperature.

Yttrium cation-doped tetragonal zirconia polycrystals (3Y-TZP)

The biomedical grade 3Y-TZP contains 3mol% yttria as a stabilizer. Restorations are fabricated either by soft machining of pre-sintered blanks at high temperatures, or by hard machining of fully sintered blocks. Transformation rate varies to the grain size and if incorrect it will lead to reduced fracture toughness. The microstructure of 3Y-TZP ceramics for dental applications consists of small grains with high flexural strength.

VITA In-Ceram YZ

VITA YZ are porously pre-sintered zirconium dioxide blocks consisting of Y-TZP, which then are CAD/CAM milled, sintered at 1530 Celsius in a high temperature furnace. In-Ceram YZ cubes when sintered have approximated of 20% shrinkage. The results from the sintering process are a dense free structure. The use of yttrium oxide partially stabilized

zirconium oxide crystals in In-Ceram YZ has shown to increase their flexural strength and increase the toughness fracture. Tetragonal crystals in these zirconium oxide ceramics are metastable and transformed into larger monoclinic crystals with the application of stress from cracks or flaws.

VITABLOCS Triluxe

Triluxe blocks are multi-chromatic feldspar ceramic with an integrated three layer of shade intensity. Manufactured from the basis of Mark II ceramic, the production procedure color saturation levels (chroma) and various translucency levels combined for the characteristic of natural dentition. The benefits to the shade are from the neck to the incisal edge. The strength of the material approximated at 130 MPa when polished, and above 160 MPa when glazed, somewhat higher than many press-able materials.[30].

IVOCLAR Vivadent IPS e.max (Lithium Di-silicate)

Lithium di-silicate glass ceramic ($Li_2Si_2O_5$) is an all-ceramic system used in the fabrication of single and multiunit dental restorations. It has gained acceptance for shade similarity and great mechanical properties. IPS e.max is composed of quartz, lithium dioxide, phosphor oxide, alumina, potassium oxide, and other properties. The flexural strength varies depending on the type of fabrication method with an approximate of 160 – 400MPa. [28].

In 2006, lithium di-silicate was reintroduced by Ivoclar Vivadent as press-able ingots (IPS e.max Press) and partially crystalized milling blocks (IPS e.max CAD). The material contained 70% lithium di-silicate crystals embedded in a glassy matrix. Due to its flexural strength with a value of 300 - 400MPa, it eliminated the risk of veneering porcelain chip when applied to monolithic restoration. IPS e.max CAD was also introduced as a lithium di-silicate glass-ceramic block for CADCAM tech with manufacturing process based on glass technology.

This new technology used optimized processing parameters, which avert the formation of defects in the bulk of the ingot. Altered from press-able, the machine-able lithium di-silicate blocks are processed through two-stage crystallization, controlled double nucleation.

The step includes the precipitation of lithium-meta-silicate crystals (Li2SiO3). The intermediate lithium-meta-silicate crystal structure supports easy milling, without extreme bur damage, while sustaining tolerances and marginal integrity. After the initial firing phase, lithium meta-silicate crystals (60 wt. %) and lithium di-silicate crystals (40 wt. %) are formed. The blocks are light bluish color with low MPa flexural strength approximating at 130-150 MPa, which can ease the milling process. The last stage is the heat-treating step to perform after the milling process is completed, in a porcelain furnace at approximately 850 °C. The temperature meta-silicate dissolves and lithium di-silicate crystallizes in relation to a low coefficient thermal expansion (10.5 Å~ 10-6/K). This result in a fine-grain glass-ceramic with 70 % crystal volume incorporated into a glass matrix. The 70% crystal phase of this unique glass-ceramic replicates natural tooth shades and now gives an improved flexural strength ranging from 360 MPa to 400 MPA. Light reflection is excellent due to the crystal arrangement providing superior aesthetic results and great resistance to thermal shock.

Failure Modes of All-Ceramic Restoration

Failures in dental ceramic prostheses are often related with veneer defects. The defects found are possible flaws that could have been from the fabrication, preparation, or post-placement. Unfortunately, these are unseen to the naked eye as they take the form of microveneer/micro-fractures. It may have occurred from machining, sandblast damage or from wear and contact damage on the occlusal surface. As the flaws are generally the form of micro cracks of sub-millimeter scale, valuable clues as to the origin cannot be provided until post-

failures. Influenced by environmental factors, fatigue-induced failure depends on material ductility. Mode of fractures depends mainly on the ceramic combination used.

Types of Failures:

- Adhesive – Interface Failure
- Cohesive – Failure with the core material
- Veneer (veneer) – Mechanical rather than adhesion of the veneer material

LITERATURE REVIEW

Fracture Strength of Aged Monolithic and Bilayer Zirconia-Based Crowns

Crowns are used to protect weak teeth, restore misshapen, discolored or broken ones and to cap implants, root canals and the teeth that anchor either end of a bridge. They're more likely to be needed by people who grind their teeth or clench their jaws, two common activities that lead to fractures and cracks. And in many cases they need to be replaced, sometimes more than once, over the course of a lifetime. Lameria et al, describes in the article "Fracture Strength of Aged Monolithic and Bilayer Zirconia-Based Crowns".

With the upbringing of metal-free restorations, the demand to evolve posterior crowns and fixed dental prostheses (FDPs) reveals the susceptibility of those to various failure modes. To improve the fracture strength of an all ceramic, the use of Yttria-stabilized tetragonal zirconia polycrystals (Y-TZP) is used to heighten the flexural strength for fixed partial prostheses (FPPs) for areas of high masticatory loads. [6.] Bilayer system strength relies upon the core as well as the veneer material. Though with two layers, it tends to fail prematurely although the core being Y-TZP, strong and tough with a veneered translucent and brittle porcelain. The article initially describes a bilayer having several disadvantages, from multistep manufacturing process to low toughness of the veneer material, and the weak bond between veneer layers and coping. These ceramic prostheses veneered with porcelain rarely undergo framework fracture but chipping and cracking of the esthetic structure is the most commonly reported complication. Clinical survival rate of zirconia-based veneer restorations can be as high as 79–100% after 5 years and chipping of the veneer layer is mostly reported for bilayers crowns in powder build-up technique. [6.]

A substitute to a bilayer system is to exchange the veneer/core bilayer with a monolithic restorative system. Fabricating zirconia monolithic could improve the mechanical stability and increases the range of indications of those prostheses as bilayers are two factors. As we know

from readings above, Zirconia presents three different crystal configurations pending on the temperature: monoclinic: 1170°C, tetragonal: 1170°C to 2370°C, and cubic: above 2370°C. When cooling after sintering, volume undergoes expansion of 3-5%, which is associated to the transition from tetragonal to monoclinic phase. Oxides are added to zirconia to stabilize the tetragonal and stronger phase at room temperature. Yttrium is known as the stabilizer to primarily give the superior mechanical properties of zirconia inhibiting crack propagation.

However, due to unfavorable phase transformation at room temperature, and "low temperature degradation" (LTD). Aging occurs through an uncontrolled slow transformation of superficial grains from tetragonal-to-monoclinic phase in contact with water. The water penetration causes further phase transformation consequently provides a loss of mechanical strength. The application of full-contour zirconia restorations is currently discussed as an alternative to bilayer veneered system based on the brittle veneer layer. Lameria et all states that even though reducing the possibility of early fracture by eliminating the weak phase in the bilayer system, phase transformation is still a concern, since the direct contact with saliva under masticatory loads may aggravate the water penetration and crack propagation. Although, monolithic crowns present higher fracture strength, it cannot be foreseen with aging as monolithic depends on the phase transformation and water penetration which is not understood fully at the present time.

Monolithic Versus Bilayered Restorations: A Closer Look

The mechanism of bonding esthetic ceramic to a zirconia substructure was investigated to recognize the quality of the bond. The bilayer non-metal restoration bond strength between veneering ceramic and zirconia framework substructures is a concern as it is substituting metal to porcelain. Chipping, has been reported to occur at a rate of 13 percent during a three-year

observation and in a follow-up study for a five year period, it increased to 15.2 percent. [31]. Current dental laboratory practices accept sandblasting to increase surface area roughness and undercuts for effective bonding and mechanical strength by initiating a phase transition. Phase transition is when tetragonal zirconia becomes monoclinic zirconia resulting in a lower coefficient of thermal expansion. What examined were the different surface treatments on the bond strength of veneering ceramics to zirconia core.

Their study evaluated the effects of treating the zirconia surface by polishing, sandblasting, silica coating and applying a liner. They also considered the impact of regeneration firing, which entails firing the zirconia framework for 15 minutes at 1,000 degrees Celsius prior to veneering. Helvey et al. states that in all specimens, the weakest link was not the interface, but the veneering ceramic itself concluding that neither increased surface roughness nor application of a liner did not improve strength. The report presented fractures were five times more prevalent with ceramic formulations than on metal. The study was to investigate the effect of zirconia types as a replacement of metal for the bond strength to veneer ceramics. Results were significantly weaker bond strength in pigment zirconia framework compared to the white zirconia frameworks.

In Vitro Evaluation of Low-Temperature Aging Effects and Finishing Procedures on the Flexural Strength and Veneer Stability of Y-TZP Dental Ceramics

The purpose of the study was to determine the influence of airborne-particle abrasion and polishing, on the flexural strength and the microveneer constancy of In-Ceram Y-TZP ceramic material. There were 310 specimens, with 61 in the control group and the rest in each experimental group. The data showed that several low-temperature aging treatments had no negative effects on the flexural strengths of Y-TZP ceramic from In-Ceram YZ ceramic blocks.

Once aged in Ringer's solution for different times at 37°C, zirconia specimens did not experience strength degradation after 1 year similar to a test with higher temperature but less time. The LTD phenomenon is primarily in a humid environment at a range of 65°C to 500°C. Temperatures in the range of 65°C can be detected in the mouth during function. This research confirmed no substantial change in bending strength after 30 months of LTD treatment.

Weibull analysis, related to the flaw-size distribution has been reported to relate to the probability of failure. Low (m) values linked to wide flaw-size distributions. The (m) values of the 9 tested groups were within the range of 5 to 15 quoted for dental ceramics, 33 some groups showed smaller Weibull modulus values comparing to the control group. The breaking strengths of the specimens were variable, with a range of values from 546.4 to 1108.9 MPa. The lowest flexural strength value recorded 546.4 MPa above 500 MPa, exceeding the occlusal loads. [41].

At a temperature of 250°C, the transformation of tetra to mono was more pronounced at 100°C. It was identified to be localized on the surface, producing little effect on flexural strength. No direct effects on flexural strength were observed. The high mean flexural strengths of all aged groups, when compared with the control group, suggest that the veneer transformation occurred at the external surface only. The influence of the abrasive airborne particles on the surface of Y-TZP ceramics although can produce surface flaws. The actual depth of the surface flaws induced by airborne-particle abrasion does not exceed the thickness of the compressive surface layer. The airborne-particle-abraded specimens dropped from 950.2 to 861.3 MPa after immersion in boiling water for 7 days, in contrast with the group of control that did not show any degradation. The airborne-particle abrasion process is accountable for the strength degradation. The transformed monoclinic phase, after airborne-particle abrasion, creates a layer of compressive stresses, which counteracts the strength degradation caused by the flaws induced by airborne-

particle abrasion. [41] The standard deviation 166.8 MPa of the airborne-particle-abraded/aged group was the highest among all tested groups but the Weibull modulus (m=5.6) was the lowest, signifying less dependability to clinical performance. Impact flaws might advance stress intensifiers with airborne-particle-abraded ceramics, lowering the strength over time.

With regard to polishing, it appears that the load applied was not capable of inducing transformation and that the temperature increase during the polishing procedure was not high enough to cause any reverse transformation. [41] Polishing could hypothetically minimize flaws on the external surface produced during the milling procedure, subsequent in higher flexural strength. Additional studies should be directed to measure the depth of the phase transformation to discuss the role of aging and finishing procedures on the long-term strength of Y-TZP ceramic materials under cyclic loading.

Effect of Air-Abrasion on the Retention of Zirconia Ceramic Crowns Luted with Different Cements Before and After Artificial Aging

In Shahin et al., mean values of retention ranged from 2.8 to 7.1 MPa after 3 days and from 1.6 to 6.1 MPa after artificial aging. [42]. Luting material had an important effect on crown retention with the adhesive providing a significant high retention. Air-abrasion also increased crown retention, although artificial aging reduced retention. Crown retention in the present study was similar to that of previous studies with zirconia ceramic crowns. The luting agents had a mean retention of 5.1, 6.1, and 5.0 MPa correspondingly. Due to the differences in experiments of the premolars used, the type of cements, means of group retention displayed varying standard deviations. Adhesive resin cement group standard deviations were lesser than in groups with conventional cements, while standard deviations improved after artificial aging. Due to using natural teeth, standard deviations were relatively high in most of the study groups. The adhesive

resin showed a significant higher retention than glass ionomer and zinc phosphate, the hypothesis, that zirconia ceramic crown retention is not influenced by the luting material must be rejected.

The air-abrasion did not affect the crown retention regardless of cement with the group presenting significantly higher retention than non-abraded groups. The increase of retention corresponds to the increase of micro-roughness of the air-abraded zirconia. Surface roughness improved the micromechanical meshing of luting agents to ceramic surfaces. In assumption, the hypothesis that air-abrasion does not influence crown retention has to be rejected. Retention was considerably reduced in retention after aging using thermo-cycling and masticatory simulation. Stresses encouraged by long-term thermal cycling and masticatory simulation are responsible for the reduction of retention simulated clinical conditions. This can be explained by material fatigue as consequence of micro leakage, changes in the elastic modulus, and plastic deformation over the time under thermal cycling and mechanical loading. [42] As a result, the third hypothesis that artificial aging does not influence crown retention has to be rejected.

In groups with zinc phosphate and glass ionomer cements, the failure was typically the cement that stayed on both crown and tooth or on the crown. Groups with adhesive resin cement, the mode of failure was that the cement remained mostly attached to the crown surface. SEM assessment of the failure mode presented that there were still fragments of the adhesive resin across the whole dentin surface and particularly filled in the dentin tubules, which can be measured as cohesive failure. Consequently in verdict, higher crown retention corresponded to more cohesive failures within the luting material.

Bonding Between Layering Materials and Zirconia Frameworks

To achieve a robust bond, the coefficient of thermal expansion (CTE) of the framework material and layering porcelain should closely resemble. On metal–ceramic systems, the layering porcelain should have a lower CTE than metal as it will result in a necessary residual compressive stress in the layering porcelain. To prevent fragment breakage of the layering porcelain, specific materials have been developed with slightly lower or identical CTE. If the porcelain has a higher CTE, the result will be a veneer delamination and extensive micro-crack formation. The mismatch in CTE approximated at 2.0 × 10−6/°C between the zirconia frameworks and layering material, will result in spontaneous de-bonding of the layering porcelain after firing. [43]. Shear bond strength of zirconia/veneer composites with a CTE mismatch from 0.75 to 1.7 × 10−6/°C. Other studies found no connection between shear bond strength and CTE of zirconia and layering porcelain.

Ceramic liners are often used to cover the white color of zirconia frameworks and increase the bonding between the two. Reports of negative effects on bond strength due to the use of such liner materials should be considered as combination with press-on ceramics will decrease the bond strength. There is also indication to the conflicts that shows the application of a liner instead enhances the bond strength between some layering porcelains and a zirconia framework.

Fracture Resistance and Failure of Posterior FDP fabricated with Two Zirconia CADCAM

Among the available selections for fixed dental prosthesis (FDP), ceramic is a unique alternative for posterior teeth. Even with advance of resin cements and adhesive systems, the increase of clinical use of all ceramic restorations has raised a concern related to longevity. This

article presents a study of the analyses for fracture resistance of two zirconia systems: Procera and Lava. The study indicated that for both zirconia systems, the veneer porcelain fractures first before the framework. There is a significant difference in load fracture from the veneer and the framework. The Procera group revealed primarily adhesive failure between the zirconia core and the veneer ceramic in 6 specimens. The Lava group presented a failure pattern from mostly cohesive fracture occurring within the porcelain veneer rather than at the porcelain-zirconia interface. The effect of fracture for the veneering porcelain could be due to many factors such as thermal expansion coefficients between core and ceramic, flexural strength of the veneering ceramic, firing shrinkage of ceramic, porcelain thickness, surface treatment of the framework, and flaws on veneering and pour wetting by veneering on core. [35].

To evaluate between the two zirconia systems for mechanical properties, a standardize system was put in place for the study. The range of tooth preparation design and dimensions were under careful consideration for the study. The veneer porcelain was fired according to the manufacturer´s, recommendations. The dimensions and layered build-up technique were identical to for an appropriate comparison. The framework design was anatomically shaped and tested under compressive pressure and although not similar to the oral cavity cyclic studies.

The greatest common fracture pattern of tested zirconia-based FDPs was at the loading point being the initiation of fracture in the gingival embrasure. The results supports a previous study listed in the article that the connector design appears to be crucial for the fracture resistance and longevity of zirconia FDPs.

Effect of Surface Pre-Treated Zirconia Ceramic–Resin Cement Micro-tensile Bond Strength

Clinical success depends on the formation of a consistent bond with the luting agent. Development in zirconia ceramic–resin cement interfacial strength was logged after SIE and ST treatments. The use of resin cements in combination with preliminary zirconia surface treatments is recognized. SEM and AFM analysis revealed retentive surfaces and changes in topography may be produced on zirconia dependent on the surface treatment. These treatments enhance retention, providing micro-porosities for the luting agent to penetrate and establish micro-mechanical interlocking. The existing study confirmed differences in surface pattern after substrate conditioning may affect the retention of core ceramics. A Calibra, GMA based was chosen between MDP-based resin cement and the zirconia ceramic, evaluating the actual success of the surface treatments. The high ratio of adhesive failures and the low bond strength values documented in the raw zirconia group confirmed no relations occurred between Calibra and the zirconia substrate. [46].

Airborne-particle abrasion of zirconia surface is the most investigated methods of providing bond strength to zirconia when united with phosphate ester monomer. The low bond strength values attained on zirconia after sandblasting and adhesive and premature failures exposed treatment did not end in the formation of sufficient undercuts to improve the bond strength. Aspects regarding sandblasting procedures are that it induces tetragonal to monoclinic (T to M) phase transformation on zirconia surface to increase the flexural strength. Alongside the grain size, pressure application of sandblasting determined it can enhance surface roughness but did not improve bond strength. This procedure is based on the zirconia surface of an infiltrating agent composed of inorganic oxides. During the procedure the agent is heated at 750 °C and

cooled. The remnants are dissolved in a 5% hydrofluoric solution, leaving the zirconia surface conditioned. The hot etching solution may determine a selective chemical etching of zirconia, creating micro-retentions and increasing the grain boundaries. [46] The noticeably higher cement–ceramic bond strengths evaluated in this study confirm the hypothesis after ST treatment of zirconia. Chemical affinity due to the same composition, resin luting agent and composite may guarantee higher bond strength than to zirconia surface without the application of primers or silanes.

Influence of Cyclic Loading on Fracture Toughness and Load Bearing Capacities

Cyclic loading is considered a repeated or fluctuating force or stress to a location on a veneer component. The loss in toughness that occurs is referred to as fatigue degradation. The article discusses all-ceramic crowns and their failure after years of service. The study reveals in a laboratory evaluation of the mechanical properties, the overall load-bearing capacities were to be considered which replicated the routine occlusal behaviors of the restored teeth. Over time, the mechanical strength of all-ceramic materials could cause micro-flaws in veneer and core ceramics. IPS e.max Press and Lava zirconia core were observed from a before and after fatigue loading using the IF method. The IF method is widely accepted and applied in measuring the K_{IC} of brittle materials, although it is not an accurate method for measuring the true fracture toughness of materials because of the use of empirical parameters. [36]

Fracture mechanics is the field of mechanics concerned with crack propagation. Cracks can redirect, grow in the same direction and can be less resistance parallel to the needle-like crystals. The crack lengths in two directions suggested that cracks propagating resulting in either a bridging or crack deflection. The recent progress of CAD/CAM lithium disilicate has provided a promising method for an optimized pressure-casting process to lessen microveneer defects to

that compared of the e.max press. From above understandings, zirconia has a stress-induced transformation-toughening mechanism when subjugated to high stress, a veneer transformation from the tetragonal to monoclinic phase ($t \rightarrow m$) causes compressive stresses, which oppose the opening of cracks and improve resistance to crack growth. If the fatigue load exceeds a certain threshold, cracks will cause strength degradation in the zirconia ceramics. The primary failure mode is chipping of the veneer with the zirconia core remaining intact regardless of the fatigue loading.

The fatigue test was conducted only in air, with the purpose of studying the influence of cyclic loading on the mechanical properties. A comprehensive conclusion that a high-strength core is more durable, while greater attention should be paid to enhancing the strength of veneer ceramics. From this study, the cyclic load was imitated on a stimulated vertical bite force, neglecting stress caused by mastication movement.

The Firing Procedure Influences Properties of a Zirconia Core Ceramic

Zirconia is considered to be a necessary substitute substructure for a bi-layer crown due to compatibility, strength and tooth-like appearance. The article identifies whether a bi-layered veneer ceramic fused to a strong zirconia core will result in a preferred combination of esthetics and strength. The hypothesis states that heating the zirconia multiple times affect the properties of the restoration.

In the past, it was believed that all-ceramic crowns were considered not long term solutions for posterior tooth. This study was to prove the firing influences the properties of zirconia core ceramic. A reduction was seen in flexural strength and micro-hardness after the first heat treatment. What was understood was that the heat treatment impacts the surface of the ceramic during the initial firing. Subsequent firings do not cause additional effects. [37] To increase

flexural strength, mechanical grinding or sandblasting of the surface of zirconia was performed and suggested the better alternative to polished surfaces. [37] The findings of sandblasting and grinding were supported by other studies indicating that phase transition initiated and reduced the number of monocline shaped grains on the surface. The belief that external forces such as cutting and grinding introduce cracks to the surface of the material and the heating lead to changes in the shape of porosities and impurities. Some authors disagreed with crack propagation of mechanical treatment to the surface area and suggested that heating in actuality initiates a phase transformation to stop crack growth. The assumption of that a veneer change from grinding to thermal heating would give dimensional distortion.

Comparison of Two Bond Strength Testing Methodologies for Bilayered All-Ceramics

Dundar et al. described in his article that specific fracture pattern in shear testing can cause cohesive failure in the substrate which leads to misguided interpretation of actual data. This is an issue as the data could change ranking values. In this study the shear bond strength "SBS" measurement values of veneering ceramics to core ceramics ranged between 23 and 41 MPa. Although not the same values of the MTBS measurement systems, a different core/veneer combination was used and resulted in less MTBS values in the present study (9–15 MPa). The common clinically failed all-ceramic crowns have been shown to fail from the internal surfaces, where the highest tensile stresses and/or largest flaws existed. [38].

The results suggested that bilayered ceramic displayed multifaceted failure modes. This is known to be attributed from many factors such as the thickness of ceramic layers, direction, magnitude and frequency of applied load, residual stresses induced by processing, as well as the differences in thermal expansion coefficients of such ceramics.

Since the use of a core ceramic is not used to form an entire crown, building up the crown with a layering technique introduces voids and flaws. The applied load of the veneer to the core creates stresses that in turn lead to veneer and core cracks. It was stated that the core/veneer ratio in this reading was 3 mm/2 mm and reported that as the core/veneer ratio increased, the crack initiation sites shifted from the veneer to the core. Pretreatment of the core with liners was unsuccessful as it did not do anything with strength. From a previous study, Fleming et al. states that an increase in flexural strength was due to liners being used for masking voids. This study decided to not apply a liner as an attempt to increase their adhesion. With vulnerable due to voids in the veneer to core area, the all-ceramic crown could be susceptible to chemicals, thermal and mechanical stress. The influence of water storage lowers the value when compared to the results from dry testing environment because of the combined influence of water and stress. Based on the mean values obtained by shear testing, Dundar believed that the ranking of the systems were flawed due to SBS bond strength measurement techniques. The study was to observe the adhesion behavior and the types of failure at the core–veneer interfaces but Dundar believed porosities, reduced occlusal thickness, thicker ceramic cores lead to fractures.

Fatigue of Bilayered Ceramics Under Cyclic Loading of Core Veneer Thickness Ratios

Dibner et al. describes in the article that, it is under a false assumption that a bilayered ceramic with a thick core improve fatigue strength. It is proposed that the thicker layer of veneering ceramic may actually improve the fatigue strength. Included in the study are the residual stresses after sintering upon cooling understanding thermal expansion/contraction behaviors of the ceramic layers at room temperature. A compressive-tensile residual stress state

is formed hypothesizing higher protective stresses in the core ceramic. Tensile stresses are found in the veneer and compressive stresses in the core, strengthening the whole bilayered ceramic.

They suggest that the role of residual stresses in fatigue strength determines the role of the coefficient of thermal contraction for the veneer and core, as opposite to the coefficient of thermal expansion for understanding the behavior of bilayered ceramics. Fatigue strength is independent of core thickness and is encouraged to maximize the thickness of the veneering porcelain with a minimum core thickness. Veneering ceramics closely replicate amorphous 3-dimensional structure similar to that of enamel and dentin, while core ceramic materials are particle-filled glass or polycrystalline ceramic with less esthetic and more opaque materials. The theory to maximize the veneering layer will improve the esthetics and patient satisfaction.

Unstable Cracking of Veneering Porcelain on All-Ceramic Crowns and FPD

Many types of FPDs or "bridges" have been used to replace missing teeth. Now, with the introduction of implants, many missing teeth are now being replaced in this manner rather than with FPDs. Swain et al. highlight the importance of FPC and their contribution: thermal expansion mismatch and cooling rate-induced tempering. The outcome of this study is that thick layers of porcelain on copings or frameworks with low thermal diffusivity are further inclined to producing high tensile subsurface residual stresses which may result in chipping.

In most instances where the thermal expansion coefficient of the porcelain is lower than that of the coping material, the compressive stresses develop in the porcelain and cause the surface to be slightly tensile. The unwanted outcome leads to initiation of cracks surface leading to an exposed contact and thermal shock type loading. Numbers of cracking patterns may depend on the indenter radius and whether quasi-static or cycling loading is applied. [69] Equally,

reducing the ceramic material causes a lower tensile strength due to removal of thickness. A bilayer highlights the importance of three factors: cooling rate, thermal expansion coefficient and thickness of the porcelain. The initial results from the study verify the above analysis where unstable cracking observed are on all ceramic crowns (porcelain bonded to Y-TZP) with thickness of 1.5 and 2 mm. The concept of effective thickness highlights the importance of the thermal conductivity of the coping material.

Five-Year Clinical Results of Zirconia Frameworks for Posterior Fixed Partial Dentures

Sailer et al conducted an approaching study to evaluate the success rate of zirconia frameworks for posterior fixed partial dentures (FPD). Fifty-seven 3- to 5-unit posterior FPDs were cemented in with different types of cements. Variolink and Panavia TC cement. It was to evaluate the baseline, from after 6 months to 1-5 years after cementation at the abutment and contralateral teeth. Frameworks were fabricated from pre-sintered zirconia blocks using the Cercon system, to then sintered and veneered with a matching of coefficient thermal expansion. The results were an expected porcelain chipping rate at 15.2% with a success rate of 73.4% at 38 months.

10-year Clinical Outcomes of Fixed Dental Prostheses with Zirconia Frameworks

Sax et al conducted an approaching study to assess long-term clinical success rate and the practical difficulties of zirconia-based posterior fixed partial dentures (FPDs). Forty-five patients received 57 3- to 5-unit zirconia-based FPDs. The frameworks were fabricated from pre-sintered zirconia blocks by CAM machining, then sintered and veneered. At baseline, 6 months, and 1, 2, 3, 5, 8 and 10 years of function, the FDPs were examined for technical and/or biological complications. Twenty-one patients with 26 FDPs were examined: 10.7 +/- 1.3 years. 16 FDPs

were lost to follow-up. 15 FDPs replaced due to technical/biological complications; survival rate: 67%. Three framework fractures, resulting in a 10-year survival rate for the zirconia frameworks of 91.5%. Chipping/fracture of the veneering ceramic was detected in 16 FDPs over 10 years (complication rate 32%). Zirconia-based FDPs exhibited problems such as marginal deficiency or chipping of the veneering ceramic.

Three-Year Clinical Prospective Evaluation of Zirconia-based Posterior FDPs

Beuer et al evaluated posterior three-unit FPDs made of zirconia substructures veneered with press-able glass ceramic. Nineteen patients received 21 FPDs replacing the posterior region. The FPDs were manufactured from pre-sintered zirconia blocks; Cercon, DeguDent, veneered with over-pressed glass-ceramics: Cercon Ceram Express, DeguDent and cemented with glass ionomer cement: Ketac Cem, 3M ESPE. Recalls were performed every 12 months with the mean service time of 40 months. One maxillary FPD exhibited zirconia framework fracture 30 months and the lost retention led to removal at 38 months. The survival probability was 90.5%. They determined that over-pressing technique looks to be consistent in terms of the veneering material.

Fatigue and Fracture Properties of Yttria Partially Stabilized Zirconia Crown Systems

Tsalouchou et al. study was to test in vitro fatigue and fracture properties of the Zirconia Everest core material after being veneered with a sintered or a heat-pressed veneer material. 50 zirconium copings were made using Kavo Everest ZS-blanks the CAD/CAM technology. 2 Groups were used for veneering material. Group 1 – Heat-pressed (IPS e.max ZirPress. Group 2: IPS e.max Ceram. Both were subjected to 50,000 cycles of cyclic loading in water. The result was no difference in the fatigue properties of sintering or heat pressing veneering material.

Core Thickness difference on Post-Fatigue indentation Fracture Resistance of Veneered Zirconia

Alhasanyah et al. studies the core thickness of the post-fatigue fracture resistance of veneer porcelain on zirconia crown. Prepared were three thickness designs: Group A: 0.6-mm thick, Group B: 1.7 mm occlusal, Group C: uniform 1.2 mm thick. CAD/CAM milled. The experiment ran over 100,000 fatigue cycles under 200 N maximum forces. The result lead to extra-thick occlusal core of 1.7 (Group B) significantly reduce the veneer chipping and fracture of zirconia crowns.

OBJECTIVES

The objectives of this study were:

1. Examine differences in aging and fatigue resistance between a machined glass-ceramic veneer and a machined feldspathic porcelain veneer.
2. Determine the differences in failure load between cemented and fused machined veneers to zirconia.
3. Determine the effect of real time aging on the failure load of cemented and fused machined veneers to zirconia.
4. Examine the differences in failure mechanism between fused and cemented veneers.

MATERIALS AND METHODS

The materials used in this study can be reviewed in (Table 1) with the physical properties listed in (Table 2).

Figures	Material	Brand Name	Composition wt.%
Figure 1	Zirconia Framework	Vita In-Ceram YZ (Vita Zahnfabrik, Germany)	Pre-sintered yttria-stabilized zirconium oxide ZrO_2 >90%, Y_2O_3 5%, HfO_2 < 3%, Al_2O_3, SiO_2 < 1%
Figure 2	Milled Ceramics	VITABLOCSS® TriLuxe Forte (Vita Zahnfabrik, Bad Sackingen, Germany)	Mixture of feldspathic crystalline particles embedded in glassy matrix SiO2: 56-64, AI2O3: 20-23, Na2O: 6-9, K2O: 6-8, CaO: 0,3-0,6 TiO2: 0,0-0,1
Figure 3	Milled Ceramics	IPS e. max CAD (Ivoclar Vivadent, Liechtenstein).	Lithium disilicate glass-ceramic SiO_2 57.0 – 80.0%, Li_2O 11.0 – 19.0%, K_2O 0.0 – 13.0%, P_2O_5 0.0 – 11.0%, ZrO_2 0.0 – 8.0 %, ZnO 0.0 – 8.0%, Al_2O_3 0.0 – 5.0%, MgO 0.0 – 5.0%, Coloring oxides 0.0 –0.8%
Figure 4	Fusing Porcelains	Vita VM9	Feldspathic Porcelain
Figure 5	Fusing Porcelains	IPS e. max CAD Crystall./Connect (Ivoclar Vivadent, Liechtenstein).	Fusing glass-ceramic SiO_2 50.0 - 65.0%, Al_2O_3 8.0 - 22.0%, Na_2O 6.0 - 11.0%, K_2O 4.0 - 8.0%, ZnO 1.0 - 3.0%, Other oxides 5.0 - 17.5%. Pigments 0.1 - 3.0%
Figure 6	Luting Cement	Multilink Automix (Ivoclar Vivadent, Liechtenstein)	Adhesive Luting Composite Multilink Automix Base / Catalyst Dimethacrylate and HEMA 30.5 / 30.2 Barium glass filler and Silica filler 45.5 / 45.5 Ytterbium triflouride 23.0 / 23.0 Catalysts and Stabilizers 1.0 / 1.3 Pigments <0.01 / - Multilink Primer A Water 85.7%, Initiators 14.3% Multilink Primer B Phosphoric Acid acrylate 48.1%, Hydroxyethyl methacrylate 48.1%, Methacrylate mod. Polyacrylic acid 3.8%, Stabilizers <0.02% Monobond Plus Ethanol 50-100%, Trimethoxysilylpropyl methacrylate ≤ 2.5% Methacrylated phosphoric acid ester ≤ 2.5%

Table 1: Materials and Figures 1-6 explained.

Figure 1: Vita In-Ceram YZ block

Figure 4: Vita VM9

Figure 2: VITABLOCS TriLuxe Forte

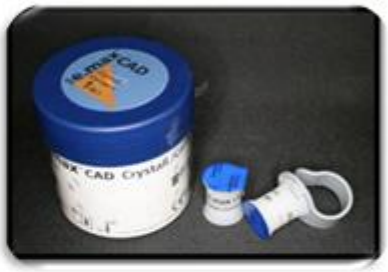

Figure 5: Fusing glass-ceramic capsules, IPS e. max CAD Crystall/Connect

Figure 3: IPS e.max CAD

Figure 6: Multilink Automix Resin Cement (Ivoclar Vivadent)

Material	**Coefficient of Thermal expansion** **($10^{-6} \cdot K^{-1}$)**	**Flexural Strength** **(MPa)**	**Fracture Toughness** **(**$MPa \cdot m^{1/2}$)	**Modulus of Elasticity** **(GPa)**
In-Ceram YZ	25-500°C 10.5	>900	5.9	210
VM9	25–500°C 9.0–9.2	100		
VITABLOCSs Triluxe forte	25-500°C 9.4	154		45
IPS e. max CAD	100-400°C 10.2 100-500°C 10.5	360 - 400	2.25	95
IPS e. max CAD Crystall./Connect	100-400°C 9.5 100-500°C 9.2	160		65

Table 2: Physical properties of materials used in the study

Preparation of Zirconia framework:

Standard aluminum die (Figure 7) was placed on a metal holder (Figure 8) then sprayed with IPS contrast spray lab side (Ivoclar Vivadent, Liechtenstein) (Figure 9) and scanned using Sirona inEos Blue scanner (Sirona, Bensheim Germany) (Figure 10). The Zirconia substructure frameworks (Figure 11) were designed using the Sirona Multilayer technique for three unit fixed partial dentures by the Sirona InLab 3D software V3.80. Afterwards, milling was completed by Sirona's CEREC inLab MC XL milling machine (Sirona, Bensheim Germany) (Figures 12). Pre-sintered zirconia blocks were milled into 20-25% enlarged frameworks with 30 μm virtual cement space (Figures 13). Milled zirconia frameworks were thoroughly cleaned and dried, then sintered in Vita ZYrcomat T furnace (Vita Zahnfabrik, Germany) (Figure 14) following manufacturer's instructions (Table 3).The external surface of all zirconia frameworks were sandblasted with 50-μm alumina particles (Aluminum oxide 50μm, Renfert GmbH industriegebiet, Hilzingen, Germany) using approximately 2.5 bar pressure. Then the frameworks were cleaned in an ultrasonic unit for approximately 5 minutes, rinsed thoroughly with water spray and dried with oil-free air.

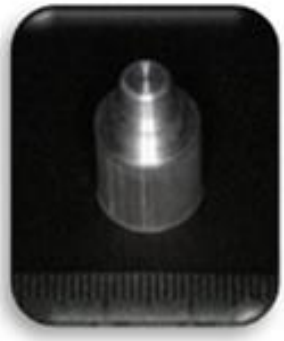

Figure 7: Standard Aluminum Die

Figure 10: Sirona InEos Blue Scanner

Figure 8: Metal Holder with Dies

Figure 11: Framework design

Figure 9: IPS Contrast Spray Lab-side

Figure 12: Sirona CEREC inLab

Figure 13: Milled Zirconia Frame Before Sintering

Figure 14: Vita ZYrcomat T Furnace

Sintering Steps	Rising time	Rising rate	End temperature	Holding time
Vita In-Ceram YZ	1.5 h	17°C/minute	1530°C	2 h

Table 3: Sintering steps for zirconia copings

Fabrication of IPS e.max CAD:

IPS e.max CAD block (Ivoclar Vivadent, Liechtenstein) was milled based on the Sirona Multilayer technique of substructure via Sirona InLab 3D software V3.81 (Figure 15) using Sirona's CEREC inLab MC XL milling machine (Sirona, Bensheim Germany).

For the cementation groups:

Glaze paste (IPS e.max® Ceram Glaze paste, Ivoclar Vivadent AG) was mixed with liquid (IPS e.max® Ceram Glaze and Stain Liquid, Ivoclar Vivadent AG) (Figure 16) to the desired consistency and applied evenly on the entire surface of each specimen. The combination firing (crystallization/glaze) (Table 4) was performed according to the manufacturer's recommendations using Programat CS (Ivoclar Vivadent, Liechtenstein) (Figure 17). Then the fitting surface of the veneer was etched using 5% hydrofluoric acid (IPS Ceramic etching gel, Ivoclar Vivadent, Liechtenstein) (Figure 18) for 20 seconds then thoroughly rinsed with water, cleansed in ultrasonic cleaner for 5 minutes and dried with oil-free air. Monobond plus (Figure 19) was applied to the pre-treated surface with a brush and let it react for 60 seconds. Subsequently, it was dispersed with a strong stream of air. A thin layer of luting composite resin (Multilink Automix, Ivoclar Vivadent, Liechtenstein) (Figure 20) was applied on the inner surface of the veneer and then seated on the zirconia framework with finger pressure. Excess cement was removed and each bridge was kept under a static load of 30 N (3kg) for 10 minutes in a loading apparatus (Figure 21). Two measurements on the FPD were recorded (before and after applying the cement) using a digital micrometer (Mitutoyo Corp. Japan) (Figure 22) to make sure there was no significant height change during the cementation.

Figure 15: Veneer Design

Figure 16: IPS e.max Glazing System

Figure 17: Programat CS Furnace

Stand-by temp. °C/°F	Closing Time min.	Heating rate °C/°F /min	Firing temp. °C/°F	Holding Time min.	Heating rate °C/°F /min	Firing temp. °C/°F	Holding time min.	Vacuum 1 1_1 °C/°F 1_2 °C/°F	Vacuum 2 2_1 °C/°F 2_2 °C/°F	Long term cooling °C/°F
403/757	6.00	60/108	820/1508	2:00	30/54	840/1544	7:00	550/820 1022/1508	820/840 1508/1540	700/1292

Table 4: Crystallization and glaze firing chart for IPS e.max CAD

Figure 18: IPS Ceramic Etching Gel

Figure 21: Cemented bridges under loading apparatus

Figure 19: Monobond Plus, Silane Coupling Agent

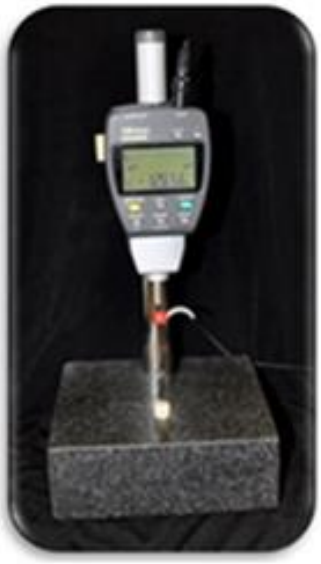

Figure 22: Digital Micrometer

Figure 20: Multilink Automix syringe

For the fusing group:

IPS e.max CAD Crystal/Connect was applied into the internal surface of the veneer and evenly distributed using Ivomix vibrator (Ivoclar Vivadent, Liechtenstein) (Figure 23). The Vita In-Ceram YZ framework was fitted into the veneer with slight pressure using the Ivomix to help distribute the fusing material. Excess fusing glass ceramic was removed. Inspection of the IPS e. max CAD Crystall/Connect was a concern for the material to be evenly distributed to assure there is enough fusing material between the veneer and the zirconia framework. Three measurements were recorded on the FPD (before adding the fusing porcelain, after adding the fusing porcelain but before sintering, and after sintering) using a digital micrometer (Mitutoyo Corp. Japan) to make sure there was no significant height change during the fusing process. The glaze paste (IPS e.max® Ceram Glaze paste, Ivoclar Vivadent AG) was mixed with liquid (IPS e.max® Ceram Glaze and Stain Liquid, Ivoclar Vivadent AG) following the manufacturer's instructions and applied evenly on the surface of each specimen. It was then subjected to crystallization firing using Programat P300/G2, (Ivoclar Vivadent, Liechtenstein). This firing served to sinter/fuse the fusing glass-ceramic (Table 5).

Furnaces Programat	Stand-by temp. °C/°F	Closing Time min.	Heating rate °C/°F /min	Firing temp. °C/°F	Holding Time min.	Heating rate °C/°F /min	Firing temp. °C/°F	Holding time min.	Vacuum 1 1_1 °C/°F 1_2 °C/°F	Vacuum 2 2_1 °C/°F 2_2 °C/°F	Long term cooling °C/°F	Cooling rate t_1 °C/°F
Fusing/ Crystallization	403/757	6.00	90/162	820/1508	00:10	30/54	840/1544	7:00	550/820 1022/1508	820/840 1508/1540	700/1292	0
Glaze firing	403/757	6.00	90/162	820/1508	00:10	30/45	840/1544	3:00	550/820 1022/1508	820/840 1508/1540	700/1292	0

Table 5: Fusing/Crystallization firing for IPS e. max CAD

Figure 23: Ivomix Vibrator

Fabrication of VITABLOCSS TriLuxe Forte:

VITABLOCSS TriLuxe Forte (Vita Zahnfabrik, Bad Sackingen, Germany) were milled based on Sirona Multilayer technique of substructure via Sirona InLab 3D software V3.81 using Sirona's CEREC inLab MC XL milling machine (Sirona, Bensheim Germany).

For the cementation groups:

The veneers were glazed by Vita Akzent Glaze spray (Figure 24) and fired according to the manufacturer's recommendations for glaze firing chart (Table 6) using a Vacumat 6000M vacuum furnace (Vita-Zahnfabrick, Bad Sackingen, Germany) (Figure 25). Then the fitting surface of the veneer was etched using 5% hydrofluoric acid (IPS Ceramic etching gel, Ivoclar Vivadent, Liechtenstein) for 60 seconds then thoroughly rinsed with water spray, cleansed in ultrasonic cleaner for 5 minutes and dried with oil-free air. Monobond plus was applied to the pre-treated surface with a brush and allowed to react for 60 seconds. Next, it was spread with a strong stream of air. A thin layer of luting composite resin (Multilink Automix, Ivoclar Vivadent, Liechtenstein) was applied on the inner surface of the veneer and then seated on the zirconia framework with finger pressure. Excess cement was removed and each bridge was kept under a static load of 30 N (3kg) for 10 minutes in a loading apparatus. Two measurements were recorded (before and after applying the cement) on the FPD using a digital micrometer (Mitutoyo Corp. Japan) to make sure there was no significant height change during the cementation.

Figure 24: Vita Akzent Glaze Spray

Figure 25: Vacumat 6000M

Firing Steps	Drying Temp. °C	Drying Time min.	Rising time min.	Rising rate °C/min	Final Tem. °C	Holding time min.	Cooling temp. °C	Vacuum min.
Glaze firing with Vita Akzent	500	4.00	5.15	80	920	1.00	-	-

Table 6: Glaze firing steps for VITABLOCS Triluxe Forte

For the fusing group:

VITABLOCS TriLuxe Forte (Vita Zahnfabrik, Bad Sackingen, Germany) were milled based on Sirona Multilayer technique of substructure via Sirona InLab 3D software V3.81 using Sirona's CEREC inLab MC XL milling machine (Sirona, Bensheim Germany).

These veneer caps were fitted onto zirconia frameworks. The veneer and the framework were joined using Vita VM9 feldspathic porcelain. Vita VM9 porcelain was mixed with modeling liquid, applied into the internal surface of the veneer cap and evenly distributed using Ivomix vibrator (Ivoclar Vivadent, Liechtenstein), then In-Ceram YZ framework was fitted into the veneer with slight pressure and excess fusing glass ceramic was removed. VM9 fusing material must be evenly squeezed out of the entire circular fusing joint, to make sure there was enough fusing material in between veneer and zirconia framework. Three measurements were recorded (before adding the fusing porcelain, after adding the fusing porcelain but before sintering, and after sintering) using a digital micrometer (Mitutoyo Corp. Japan) to make sure there was no significant height change before and after addition of fusing porcelain. After that, the glazing material was applied using Vita Akzent glazing spray, then they were subjected to fusing firing in Vacumat 6000 porcelain furnace (Vita Zahnfabrik, Germany) (Table 7).

Firing Steps	Drying Temp. °C	Drying Time min.	Rising time min.	Rising rate °C/min	Final Temp. °C	Holding time min.	Cooling temp. °C	Vacuum min.
Fusing firing	500	6.00	6:40	66	940	3.00	200	6:40

Table 7: Fusing firing for VM9/ Glazing VITABLOCS Triluxe Forte

Cementation on the aluminum dies

All bridges were cemented conventionally onto their aluminum dies using resin composite cement (Multilink Automix, Ivoclar Vivadent). Steps for cementation were followed by manufacturer's specification. Excess cement was removed and each restoration was kept under a static load of 30 N (3kg) for 10 minutes in a loading apparatus.

All specimens were kept in a dry area before being stored in an incubator (Figure 26) and distilled water under the condition of 37°C for 24 hours before the mechanical testing.

Aging process:

All the specimens of aging group kept in a dry area at room temperature for three years before being stored in distilled water at the incubator under the condition of 37°C for 24 hours before the mechanical testing.

Figure 26: Incubator

Testing Group

In Ceram Zirconia + Triluxe Forte (Figure 27)

Cemented

1. Non-aged
    - Static group
    - Cyclic (20K,60K and 80K cycles)
2. Aged
    - Static group
    - Cyclic (20K,60K and 80K cycles)

Fused

1. Non-aged
    - Static group
    - Cyclic (20K,60K and 80K cycles)
2. Aged
    - Static group

In Ceram Zirconia + e.max (Figure 28)

Cemented:

1. Non-aged
    - Static group
    - Cyclic (20K,60K and 80K cycles)
2. Aged
    - Static group
    - Cyclic (20K,60K and 80K cycles)

Fused: In Ceram Zirconia + e.max

1. Non-aged
    - Static group
    - Cyclic (20K,60K and 80K cycles)
2. Aged
    - Static group

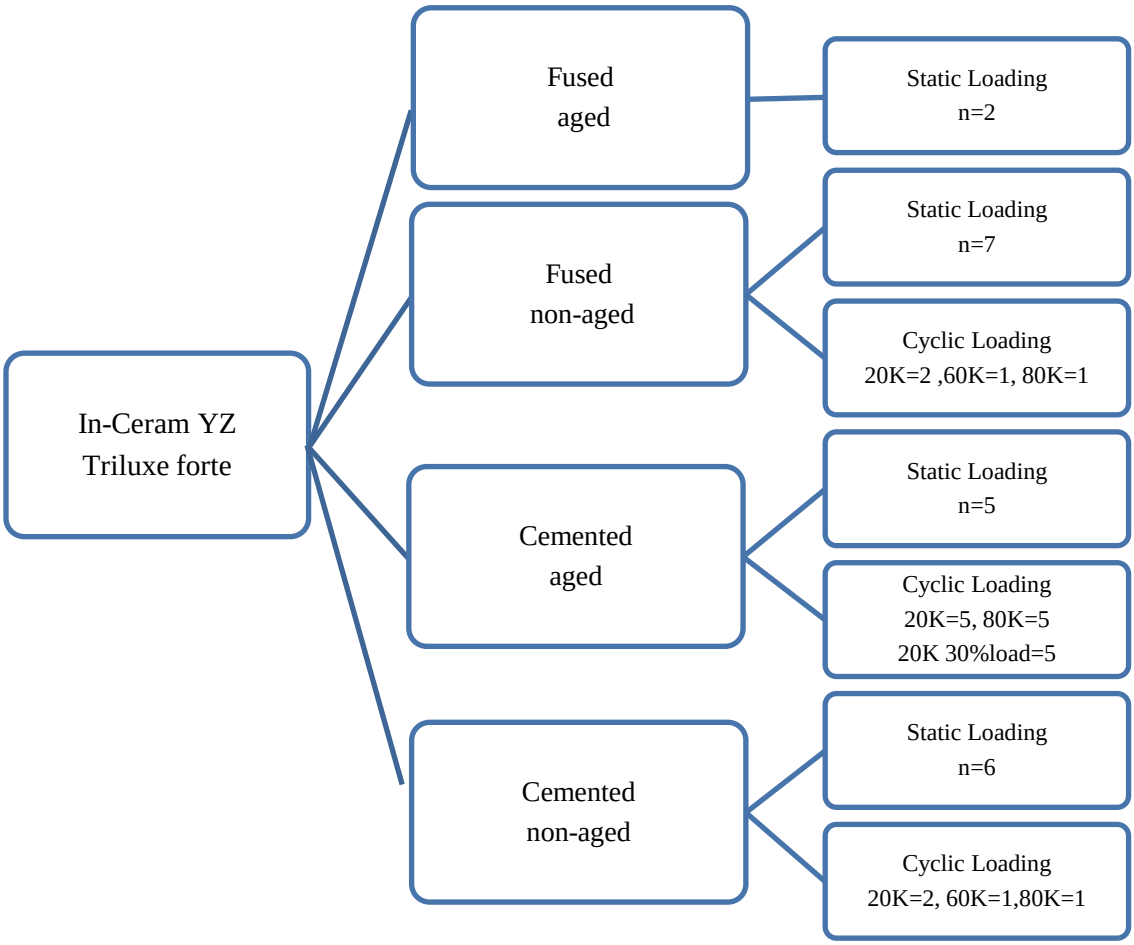

Figure 27: Study design, YZ-Triluxe Forte

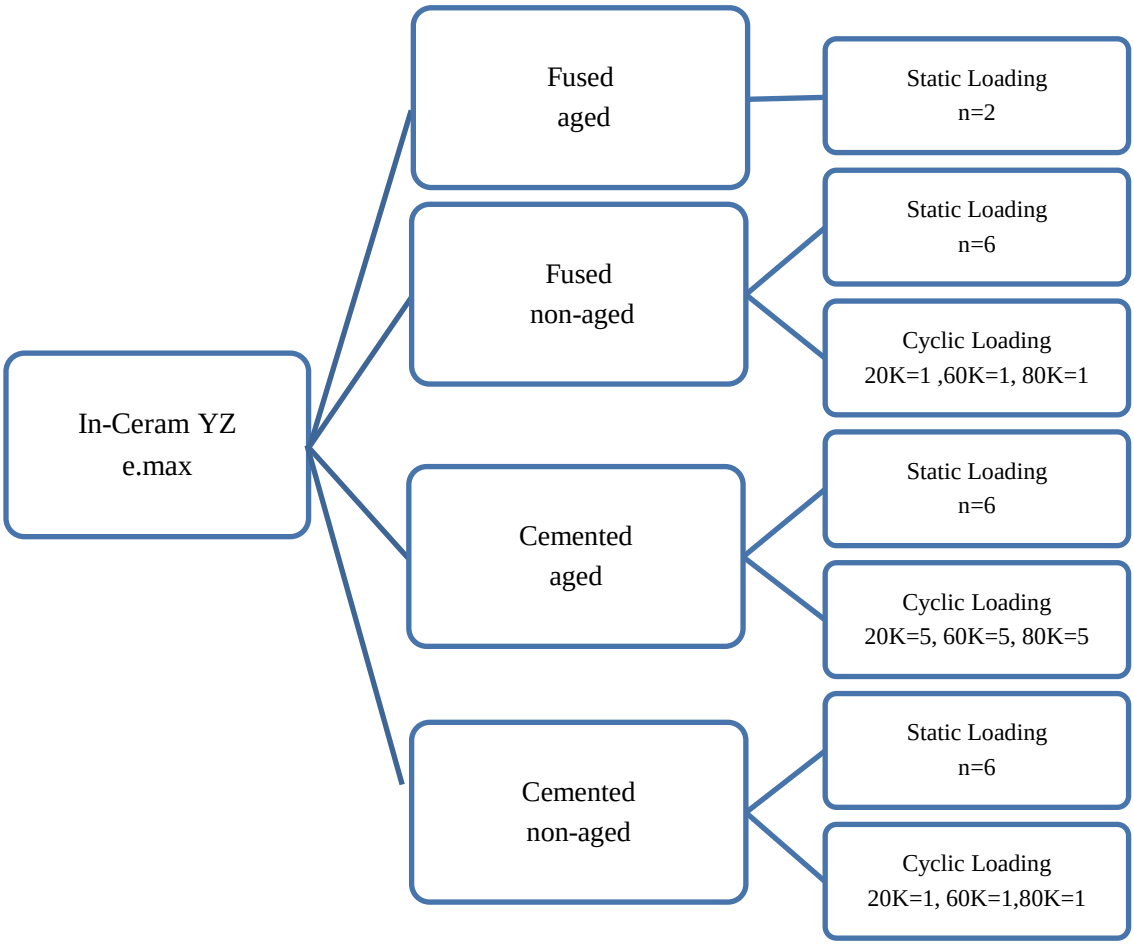

Figure 28: Study design, In-Ceram YZ–e.max

Mechanical Testing:

Failure Load Test

Load at failure was recorded at the point where a sharp drop in the load occurred. Each specimen was individually mounted in a testing jig and loaded in universal testing machine (Model 4202, Instron Co., Norwood, MA)(Figure 29) at 0.5 mm/minute rate until fracture (failure load). The Instron machine was connected to a computer with a specifically designed program (BlueHill 3 software, Instron Worldwide Headquarters, Norwood, MA). This software controlled the testing machine and recorded the breakage load and crown deflection.

A steel ball, 4.7 mm diameter, placed on the occlusal central fossa of the FPD pontic. A thin plastic sheet (0.1mm) placed between the ball and the test specimen to prevent local stress concentration. Failure defined as occurrence of visible cracks, porcelain chipping, or acoustic events accompanied by a drop in the load by 20%.

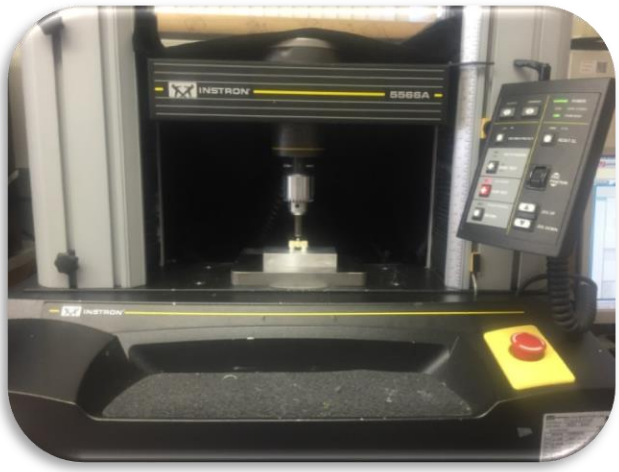

Figure 29: Universal testing machine

Cyclic Fatigue Test:

This group was subjected to many cyclic test; 20K, 60K and 80K at a frequency rate of 1 Hz in a cyclic fatigue device (Pober Industries, Waban MA) (Figures 30) in a distilled water bath. The load applied on each specimen was 40% of the mean fracture load of each material. The load applied at the center of the pontic of FPD by a 4.7 mm steel ball. After cyclic loading was completed, each specimen was examined to detect any cracks or defects. The survived specimen was subjected to failure load test. The failure loads were measured in newtons and compared with statics groups. Failure modes, cohesive failure (total fracture extending through the veneer and coping), adhesive failure (veneer delamination) or veneer failure (veneer crack) observed and recorded after each test.

Figure 30: Cyclic loading apparatus, Pober Industries, Waban MA

Microstructure Examination:

Energy Dispersive Spectroscopy (EDS)

EDS performed to study the chemical composition of the materials. The specimens cleaned with isopropyl alcohol for 10 seconds. Then the specimens were sputter coated with carbon using Agar SEM carbon coater (Agar scientific, Elektron Technology UK) (Figure 31). EDS (Hitachi SU6600- High Resolution Analytical FE-SEM) (Figure 31) performed in the SEM using an accelerating voltage of 15 kV for elemental analysis on the zirconia framework.

Figure 31: Agar sputter coating machine

Figure 32: Hitachi SU6600- High Resolution Analytical FE-SEM

RESULTS

Effect of cyclic fatigue on failure load on aged and non-aged e.max cemented to YZ zirconia:

Effect of cyclic fatigue on failure load on aged (A) and non-aged (NA) e.max cemented (CEM) to YZ zirconia		
Groups	**Failure Load (Newton)**	**SIG DIFF**
E.MAX CEM NA	2740	A
20,000 cycles	2168	A
60,000 cycles	2062	A
80,000 cycles	2911	A
E.MAX CEM A	2374	A
20,000 cycles	675	B
60,000 cycles	481	B
80,000 cycles	Failed in cyclic fatigue test	C

Table 8: Effect of cyclic fatigue on failure load on aged and non-aged e.max cemented to YZ zirconia.

When viewing non-aged e.max veneer cemented to the YZ zirconia group, we found that there is no statistically significant difference between the static and the cyclic fatigue groups. Also, there was no statistically significant difference within non-aged cyclic fatigue e.max veneer cemented to YZ zirconia groups ($p>0.05$).When comparing aged e.max veneer cemented to YZ zirconia, we found there is a significant difference between the static group and the cyclic fatigue groups ($p<0.05$).

When comparing aged e.max veneer cemented to YZ zirconia, there was no significant difference between cyclic fatigue groups of 20K and 60K cycles. There is a significant difference between cyclic fatigue of 80K cycles and the groups fatigued for 60K and under cycles (60K and 20K) ($p<0.05$).

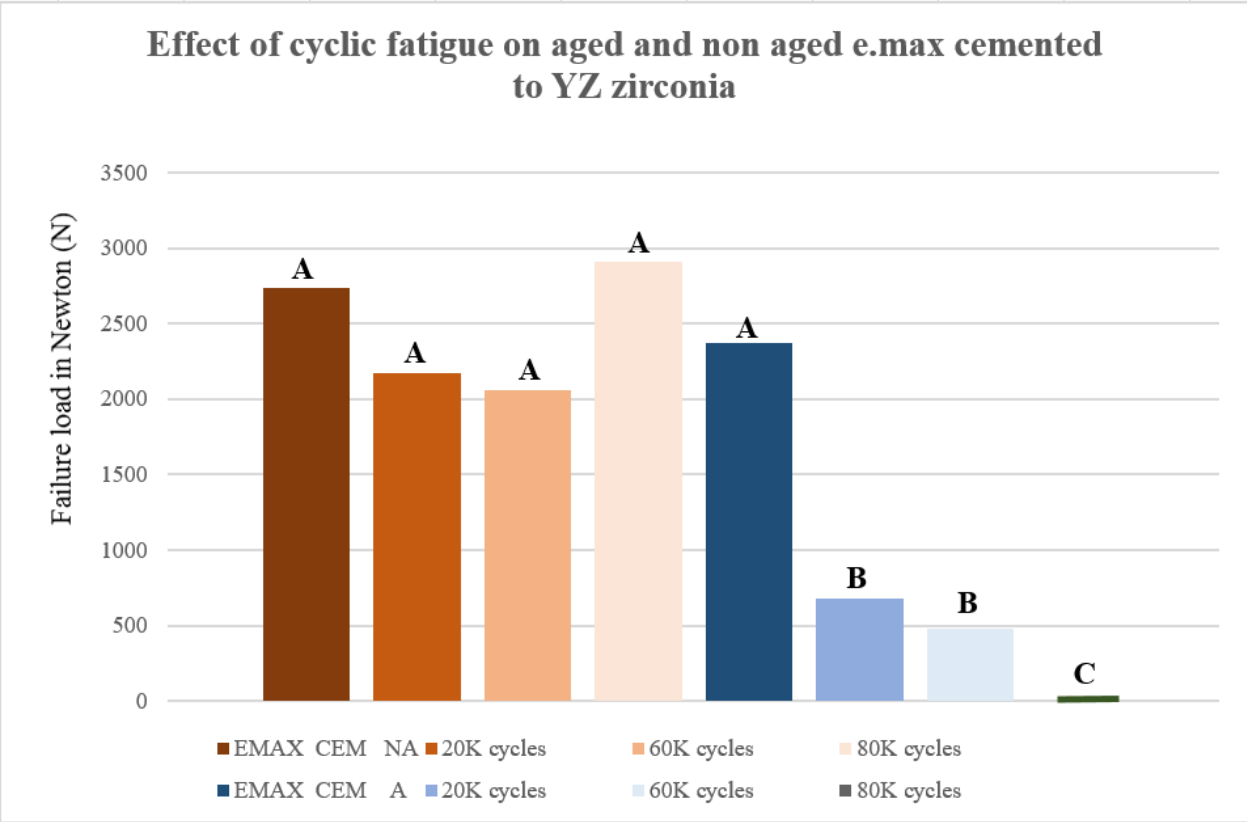

Graph 1: Effect of cyclic fatigue on failure load on aged and non-aged e.max cemented to YZ zirconia.

Groups	**SIG DIFF**
E.MAX CEM NA	A
20K cycles	A
60K cycles	A
80K cycles	A
E.MAX CEM A	A
20K cycles	B
60K cycles	B
80K cycles	C
***Groups not connected by same letter are significantly different.	

Table 9: The difference of effect of cyclic fatigue failure load on aged and non-aged e.max cemented to YZ zirconia analysis using the Tukey-Kramer HSD test.

Effect of cyclic fatigue on aged and non-aged e.max fused to YZ zirconia:

Effect of cyclic fatigue on failure load on aged (A) and non-aged (NA) e.max fused to YZ zirconia		
Groups	**Failure Load (Newton)**	**SIG DIFF**
E.MAX FUSE NA	2678	A
20,000 cycles	1909	A
60,000 cycles	2190	A
80,000 cycles	1824	A
E.MAX FUSE A	2374	A

Table 10: Effect of cyclic fatigue on failure load on aged and non-aged e.max fused to YZ zirconia

When observing e.max veneer fused to YZ zirconia, there is no significant difference between aged e.max fused to YZ zirconia and non-aged static cyclic fatigue groups ($p>0.05$).

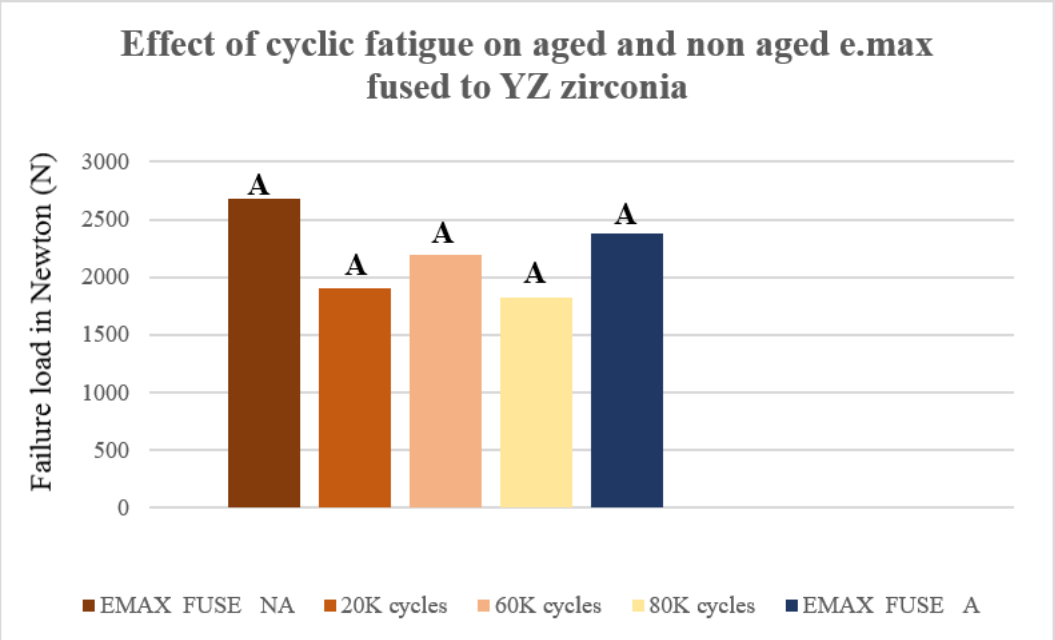

Graph 2: Effect of cyclic fatigue on failure load on aged and non-aged e.max fused to YZ zirconia

Groups	**SIG DIFF**
E.MAX FUSE NA	A
20K cycles	A
60K cycles	A
80K cycles	A
E.MAX FUSE A	A
***Groups not connected by same letter are significantly different.	

Table 11: The difference effect of cyclic fatigue failure load on aged and non-aged e.max fused to YZ zirconia analysis using the Tukey-Kramer HSD test.

Effect of cyclic fatigue failure load on aged and non-aged e.max cemented and fused to YZ zirconia:

Effect of cyclic fatigue failure load on aged (A) and non-aged (NA) e.max cemented (CEM) and fused to YZ zirconia		
Groups	**Failure Load (Newton)**	**SIG DIFF**
E.MAX CEM NA	2740	A
20,000 cycles	2168	ABCD
60,000 cycles	2062	ABCD
80,000 cycles	2911	ABC
E.MAX CEM A	2374	AB
20,000 cycles	675	BCD
60,000 cycles	481	CD
80,000 cycles	Failed in the cyclic fatigue	D
E.MAX FUSE NA	2678	A
20,000 cycles	1909	ABCD
60,000 cycles	2190	ABCD
80,000 cycles	1824	ABCD
E.MAX FUSE A	2433	ABCD

Table 12: Effect of cyclic fatigue on failure load on aged and non-aged e.max cemented and fused to YZ zirconia

There was no significant difference between non-aged (static and fatigued) e.max veneer cemented and non-aged (static and cyclic) fused to YZ zirconia groups ($p>0.05$).

In addition, we found a significant difference between aged e.max fused to YZ zirconia, non-aged (static and cyclic) cemented to YZ zirconia and aged fatigued e.max cemented to YZ zirconia ($p<0.05$).

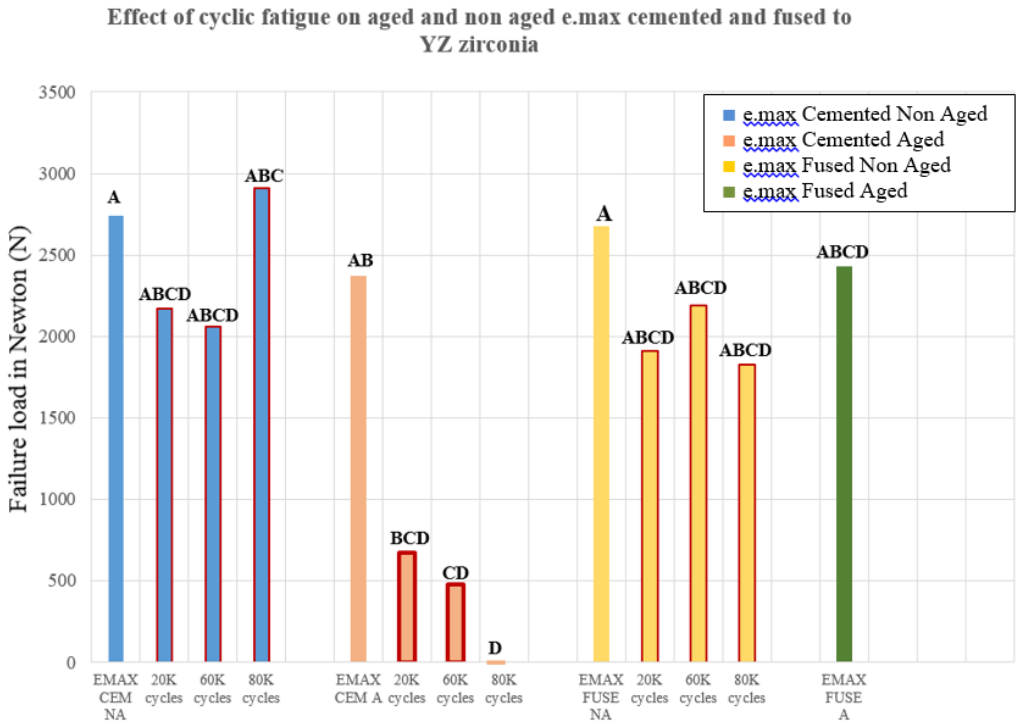

Graph 3: Effect of cyclic fatigue failure load on aged and non-aged e.max cemented and fused to YZ zirconia

Groups	**SIG DIFF**
E.MAX CEM NA	A
20K cycles	ABCD
60K cycles	ABCD
80K cycles	ABC
E.MAX CEM A	AB
20K cycles	BCD
60K cycles	CD
80K cycles	D
E.MAX FUSE NA	A
20K cycles	ABCD
60K cycles	ABCD
80K cycles	ABCD
E.MAX FUSE A	ABCD
*** Groups not connected by same letter are significantly different.	

Table 13: The difference of cyclic fatigue failure load on aged and non-aged e.max cemented and fused to YZ zirconia analysis using the Tukey-Kramer HSD test.

Effect of cyclic fatigue failure load on aged and non-aged Triluxe cemented to YZ zirconia:

Effect of cyclic fatigue failure load on aged (A) and non-aged (NA) Triluxe cemented (CEM) to YZ zirconia		
Groups	**Failure Load (Newton)**	**SIG DIFF**
TRILUXE CEM A	1805	A
20,000 cycles	Failed in cyclic fatigue	B
60,000 cycles	Failed in cyclic fatigue	B
80,000 cycles	Failed in cyclic fatigue	B
20,000/30% load of failure	1468	Not applicable
TRILUXE CEM NA	1950	A
20,000 cycles	2218	A
60,000 cycles	1910	A
80,000 cycles	1765	A

Table 14: Effect of cyclic fatigue on failure load on aged and non-aged Triluxe cemented to YZ zirconia

When observing aged Triluxe veneer cemented to YZ zirconia, there was a significant difference between the static aged Triluxe cemented to YZ and the fatigued aged Triluxe cemented to YZ zirconia groups (20K, 60K and 80K cycles) ($p<0.05$).

There is no significant difference between the static non-aged Triluxe veneer cemented to YZ zirconia and non-aged fatigued Triluxe cemented to YZ zirconia groups (20K, 60K and 80K cycles) ($p>0.05$).

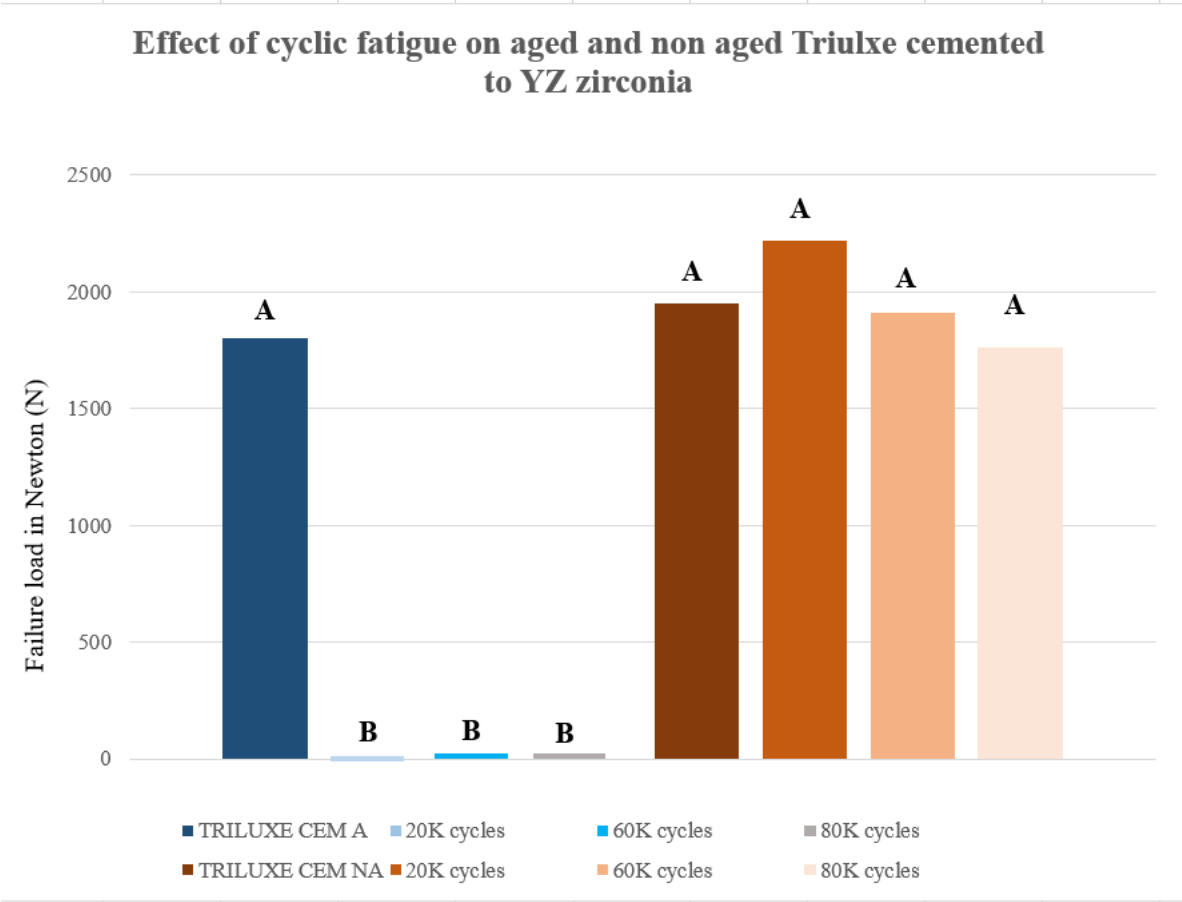

Graph 4: Effect of cyclic fatigue failure load on aged and non-aged Triluxe cemented to YZ zirconia

Groups	SIG DIFF
TRILUXE CEM A	A
20K cycles	B
60K cycles	B
80K cycles	B
TRILUXE CEM NA	A
20K cycles	A
60K cycles	A
80K cycles	A
***Groups not connected by same letter are significantly different.	

Table 15: The difference of cyclic fatigue failure load on aged and non-aged Triluxe cemented to YZ zirconia analysis using the Tukey-Kramer HSD test.

Effect of cyclic fatigue failure load on aged and non-aged Triluxe fused to YZ zirconia:

Effect of cyclic fatigue failure load on aged (A) and non-aged (NA) Triluxe fused to YZ zirconia		
Groups	**Failure Load(Newton)**	**SIG DIFF**
TRILUXE FUSE NA	966	A
20,000 cycles	787	A
60,000 cycles	628	A
80,000 cycles	561	B
TRILUXE FUSE A	1044	A

Table 16: Effect of cyclic fatigue on failure load on aged and non-aged Triluxe fused to YZ zirconia.

When viewing the aged and non-aged Triluxe veneer fused to YZ zirconia, there was a significant difference between the 80K fatigued non-aged Triluxe fused to YZ zirconia and aged, non aged (static, fatigued 60K cycles and under) Triluxe fused to YZ zirconia ($p<0.05$).

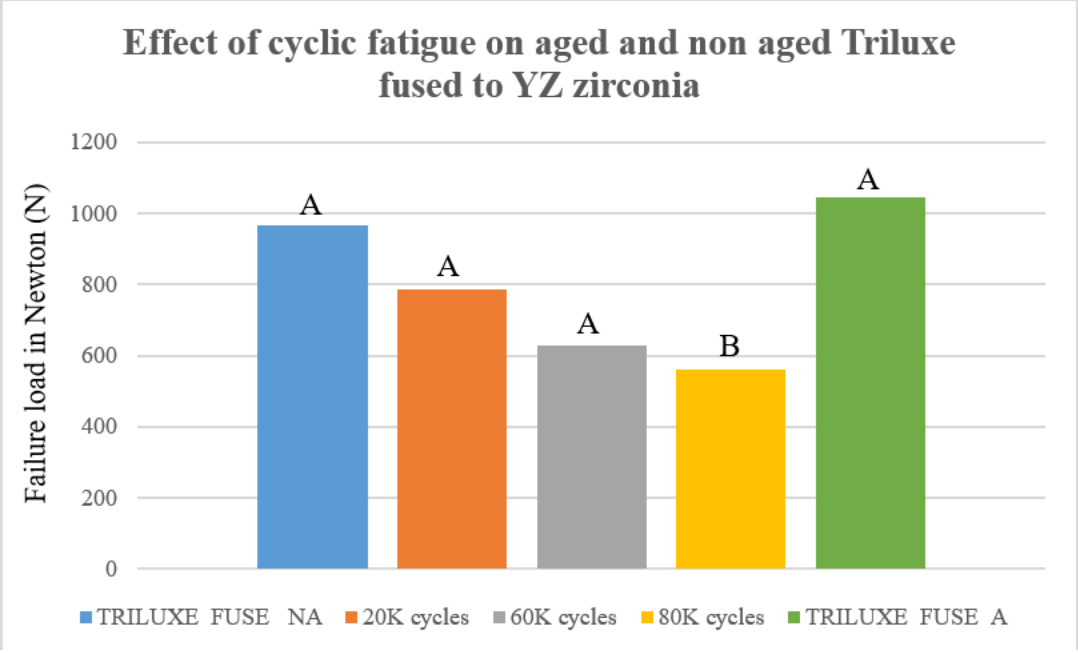

Graph 5: Effect of cyclic fatigue failure load on aged and non-aged Triluxe fused to YZ zirconia

Groups	SIG DIFF
TRILUXE FUSE NA	A
20K cycles	A
60K cycles	A
80K cycles	B
TRILUXE FUSE A	A
*** Groups not connected by same letter are significantly different.	

Table 17: The difference of cyclic fatigue failure load on aged and non-aged Triluxe fused to YZ zirconia analysis using the Tukey-Kramer HSD test.

Effect of cyclic fatigue on failure load on aged and non-aged Triluxe cemented and fused to YZ zirconia:

Effect of cyclic fatigue on failure load on aged (A) and non-aged (NA) Triluxe cemented (CEM) and fused to YZ zirconia		
Groups	**Failure Load (Newton)**	**SIG DIFF**
TRILUXE CEM A	1805	AB
20,000 cycles	Failed in the cyclic fatigue	E
60,000 cycles	Failed in the cyclic fatigue	E
80,000 cycles	Failed in the cyclic fatigue	E
20,000/30% load of failure	1468	Not applicable
TRILUXE CEM NA	1950	A
20,000 cycles	2218	A
60,000 cycles	1910	AB
80,000 cycles	1765	ABC
TRILUXE FUSE NA	966	CD
20,000 cycles	787	CD
60,000 cycles	628	D
80,000 cycles	561	D
TRILUXE FUSE A	1044	BCD

Table 18: Effect of cyclic on fatigue failure load on aged and non-aged Triluxe cemented and fused to YZ zirconia.

There was a significant difference when comparing between the non-aged Triluxe veneer cemented to YZ zirconia and the non-aged Triluxe veneer fused to YZ zirconia ($p<0.05$). Moreover, there was a significant difference between the fatigued (20K, 60K and 80K cycles) aged Triluxe cemented to YZ zirconia and all the other groups ($p<0.05$).

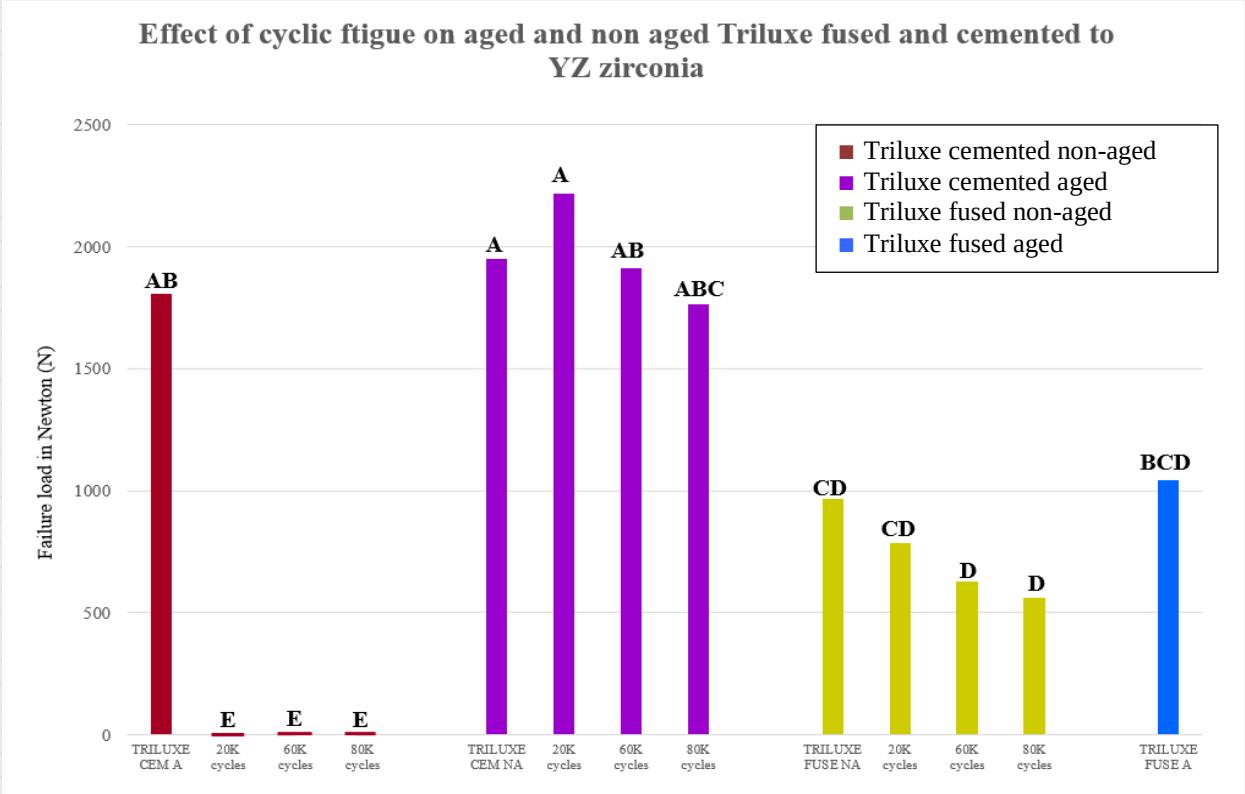

Graph 6: Effect of cyclic fatigue on failure load on aged and non-aged Triluxe cemented and fused to YZ zirconia

Groups	**SIG DIFF**
TRILUXE CEM A	AB
20K cycles	E
60K cycles	E
80K cycles	E
TRILUXE CEM NA	A
20K cycles	A
60K cycles	AB
80K cycles	ABC
TRILUXE FUSE NA	CD
20K cycles	CD
60K cycles	D
80K cycles	D
TRILUXE FUSE A	BCD
***Groups not connected by same letter are significantly different.	

Table 19: The difference of cyclic fatigue failure load on aged and non-aged Triluxe cemented and fused to YZ zirconia analysis using the Tukey-Kramer HSD test.

Effect of cyclic fatigue on failure load on non-aged Triluxe and e.max fused to YZ zirconia:

Effect of cyclic fatigue on failure load on non-aged (NA) Triluxe and e.max fused to YZ zirconia		
Groups	**Failure Load (Newton)**	**SIG DIFF**
E.MAX FUSE NA	2678	A
20,000 cycles	1909	AB
60,000 cycles	2190	AB
80,000 cycles	1824	AB
TRILUXE FUSE NA	966	B
20,000 cycles	787	B
60,000 cycles	628	B
80,000 cycles	561	C

Table 20: Effect of cyclic fatigue on failure load on non-aged Triluxe and e.max fused to YZ zirconia

When comparing the non-aged e.max veneer fused to YZ zirconia group and non-aged Triluxe veneer fused to YZ zirconia group, there was a significant difference between the non-aged e.max veneer fused to YZ zirconia group and non-aged (static and fatigued) Triluxe veneer fused to YZ zirconia groups ($p<0.05$). In addition, there was a significant difference between the non-aged fatigued e.max fused o YZ zirconia and the 80K fatigued non-aged Triluxe fused to YZ zirconia ($p<0.05$).

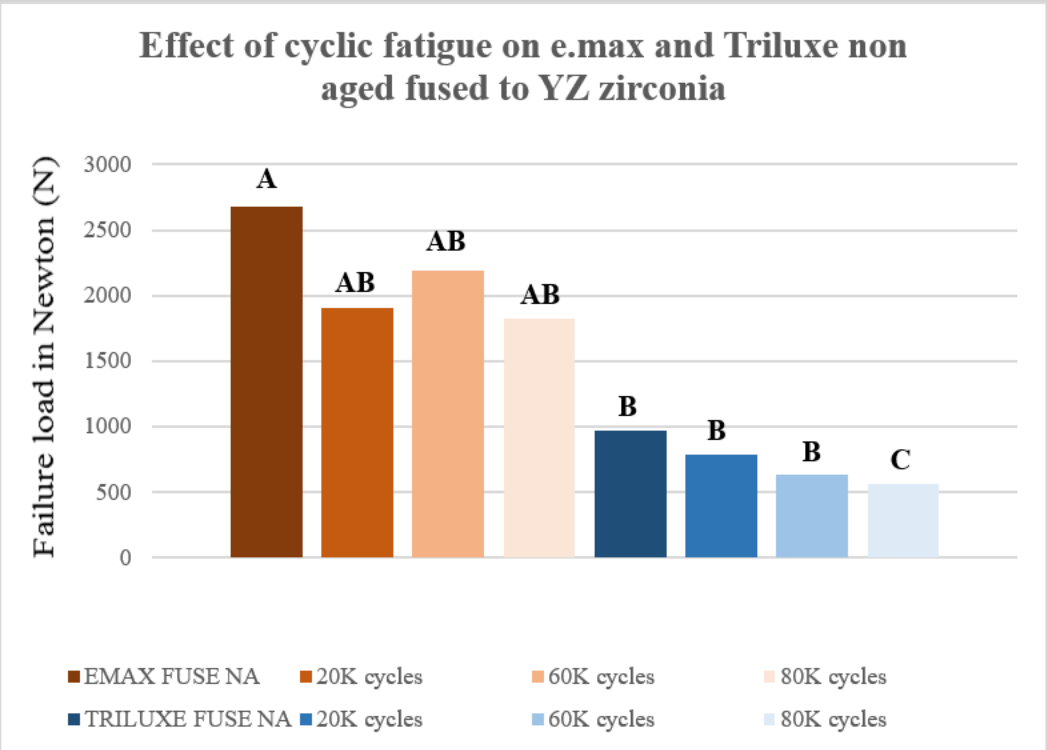

Graph 7: Effect of cyclic fatigue on failure load on non-aged Triluxe and e.max fused to YZ zirconia

Groups	**SIG DIFF**
E.MAX FUSE NA	A
20K40	AB
60K40	AB
80K40	AB
TRILUXE FUSE NA	B
20K40	B
60K40	B
80K40	C
***Groups not connected by same letter are significantly different	

Table 21: The difference of non-aged e.max and Triluxe fused to YZ zirconia groups analysis using the Tukey-Kramer HSD test.

Effect of cyclic fatigue on failure load on non-aged e.max and Triluxe cemented to YZ zirconia:

Effect of cyclic fatigue on failure load on non-aged (NA) e.max and Triluxe cemented (CEM) to YZ zirconia		
Groups	**Failure Load (Newton)**	**SIG DIFF**
E.MAX CEM NA	2740	A
20,000 cycles	2168	A
60,000 cycles	2062	A
80,000 cycles	2911	A
TRILUXE CEM NA	1950	A
20,000 cycles	2218	A
60,000 cycles	1910	A
80,000 cycles	1765	B

Table 22: Effect of cyclic fatigue on failure load on non-aged e.max and Triluxe cemented to YZ zirconia

When comparing between the non-aged e.max veneer cemented to YZ zirconia group and the non-aged Triluxe veneer cemented to YZ zirconia, there was a statistical significant difference between the non-aged (static and fatigue) e.max cemented to YZ zirconia and the 80K fatigued non-aged Triluxe cemented to YZ zirconia ($p<0.05$).

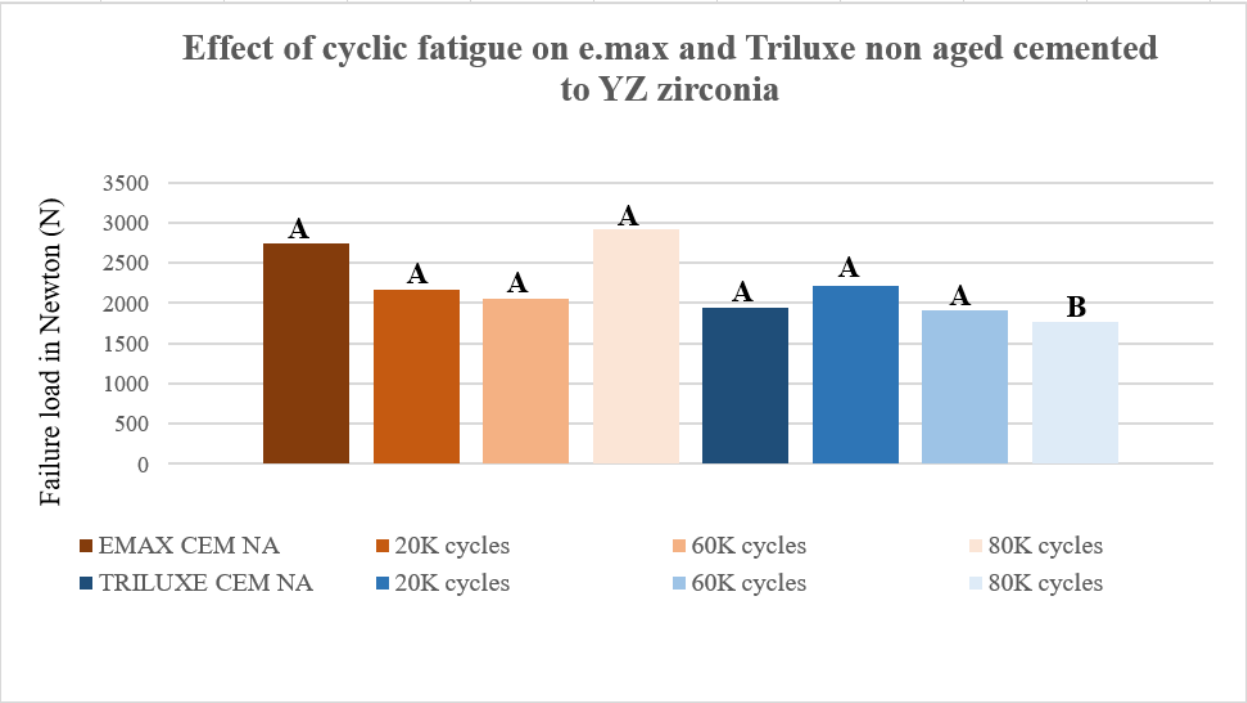

Graph 8: Effect of cyclic fatigue failure load on non-aged e.max and Triluxe cemented to YZ zirconia.

Groups	**SIG DIFF**
E.MAX CEM NA	A
20K cycles	A
60K cycles	A
80K cycles	A
TRILUXE CEM NA	A
20K cycles	A
60K cycles	A
80Kcycles	B
***Groups not connected by same letter are significantly different	

Table 23: The difference of non-aged e.max and Triluxe cemented to YZ zirconia groups analysis using the Tukey-Kramer HSD test.

Comparison of non-aged e.max and Triluxe cemented and fused to YZ zirconia groups:

Comparison of non-aged (NA) e.max and Triluxe cemented (CEM) and fused to YZ zirconia		
Groups	**Failure Load (Newton)**	**SIG DIFF**
E.MAX CEM NA	2740	A
E.MAX FUSE NA	2678	A
TRILUXE CEM NA	1950	AB
TRILUXE FUSE NA	966	B

Table 24: Mean of failure load of non-aged e.max and Triluxe cemented and fused to YZ zirconia

When we compare between the non-aged e.max veneer (cemented or fused) to YZ zirconia and Triluxe veneer (cemented or fused) to YZ zirconia, there was a statistically significant difference between non-aged Triluxe veneer fused to YZ zirconia group and non-aged e.max veneer (cemented or fused) to YZ zirconia ($p<0.05$).

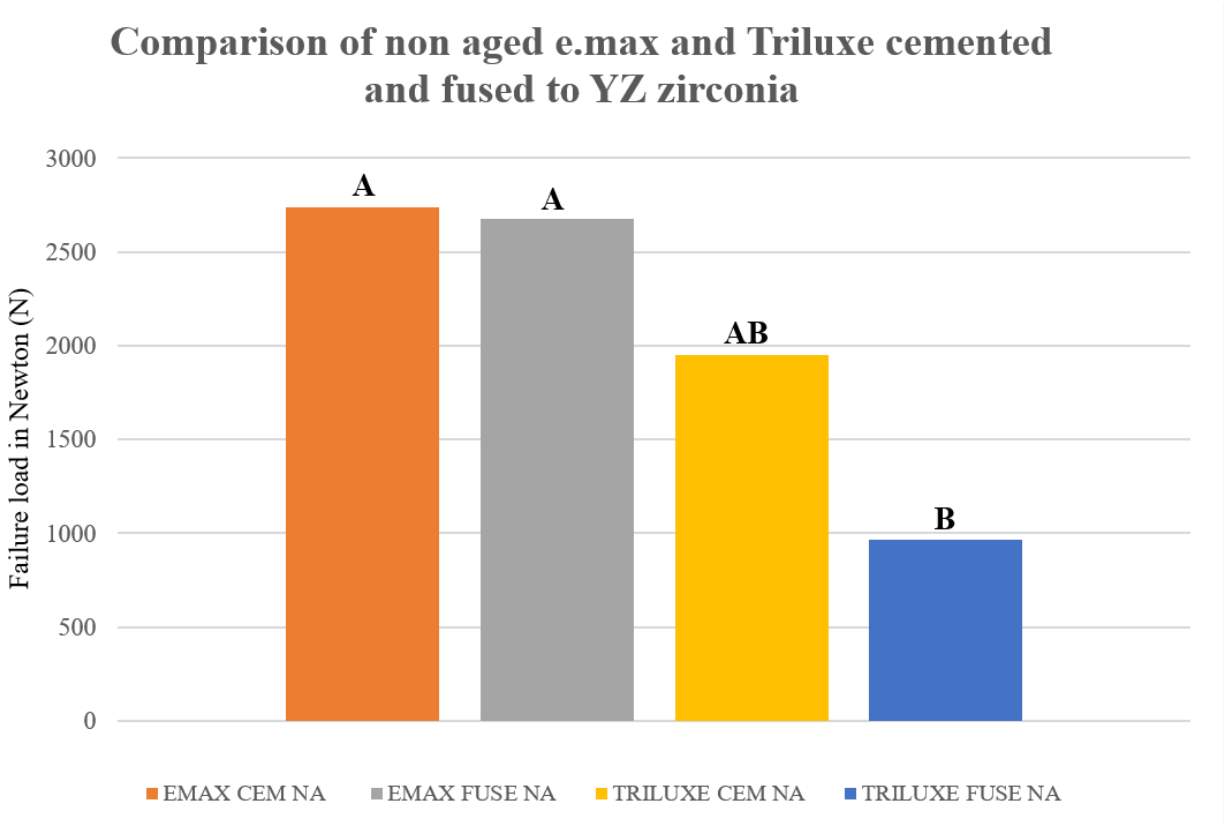

Graph 9: Comparison of non-aged e.max and Triluxe cemented and fused to YZ zirconia groups

Groups	**SIG DIFF**
E.MAX CEM NA	A
E.MAX FUSE NA	A
TRILUXE CEM NA	AB
TRILUXE FUSE NA	B
*** Groups not connected by same letter are significantly different.	

Table 25: The difference of non-aged e.max and Triluxe cemented and fused to YZ zirconia groups analysis using the Tukey-Kramer HSD test.

MODE OF FAILURE

e.max fused to YZ group:

Site	Cohesive failure	Adhesive failure	Veneer failure
Pontic	0	5	1
Connector	1	0	0
Coping	1	0	0
Pontic & connector	2	0	0
Connector & coping	1	0	0
Pontic , connector & coping	0	0	0

Table 26: Mode of Failure of YZ e.max fused group

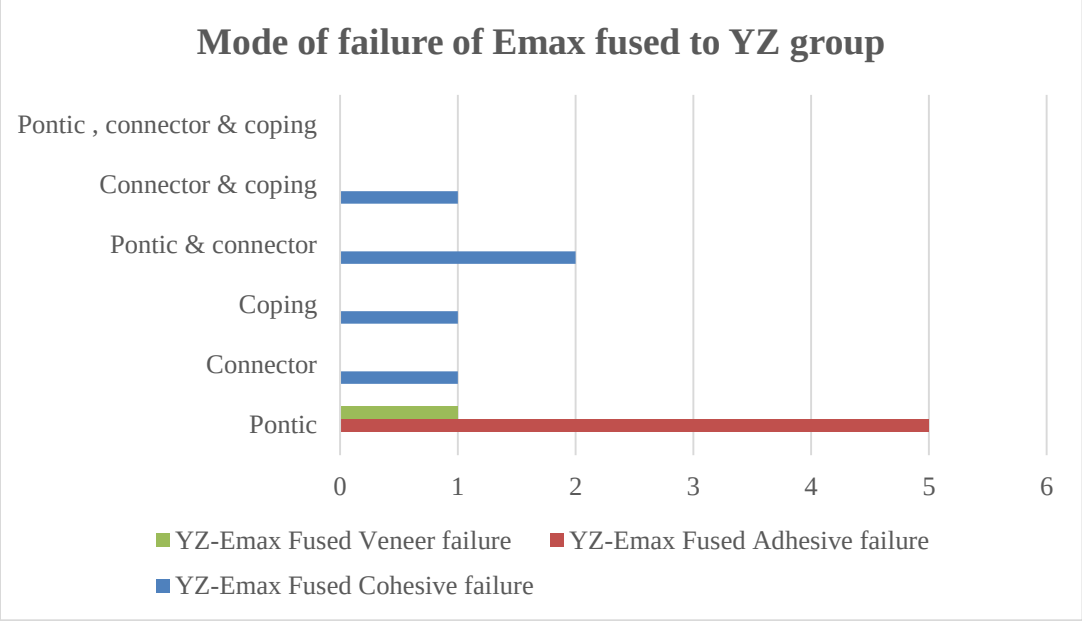

Graph 10: Mode of failure of E.max fused to YZ zirconia

In YZ-e.max fused group, there were five incidences of adhesive failure at the pontic area and two incidences of cohesive failure at the pontic and connector area together. There was one incidence of cohesive at coping, connector and connector & coping area as well as one other incidence of veneer failure at the pontic area. (Figures 33-38)

e.max fused to YZ group:

Figure 33: Sample# 1 (YZ-e.max Fused)

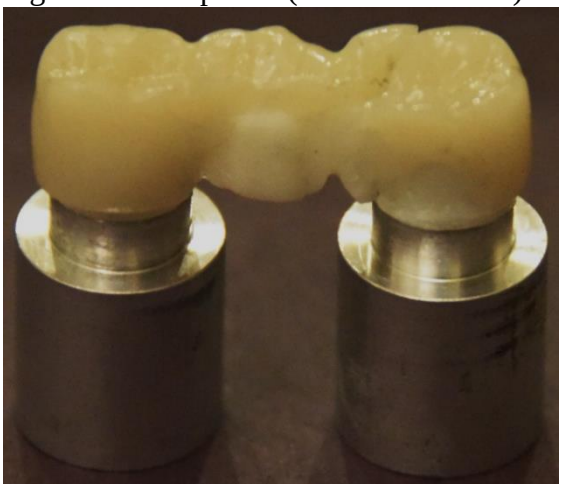

Figure 34: Sample# 2(YZ-e.max Fused)

Figure 35: Sample# 14 (YZ-e.max Fused)

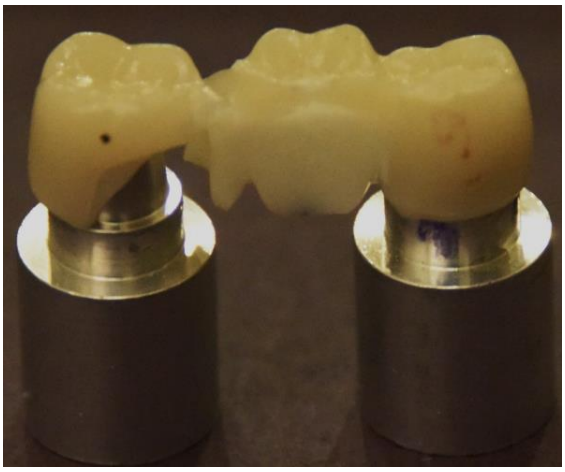

Figure 36: Sample# 9 (YZ-e.max Fused)

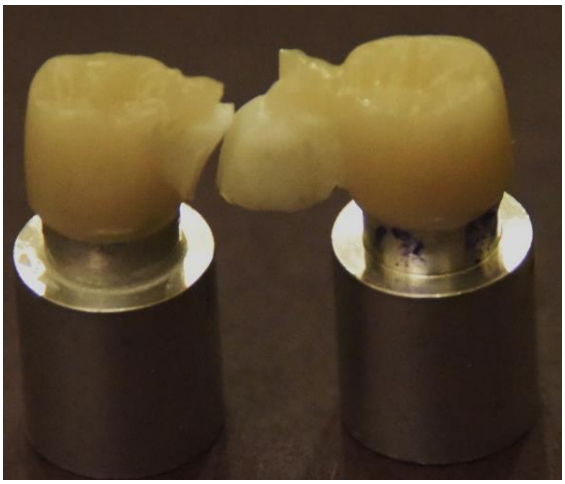

Figure 37: Sample# 13 (YZ-e.max Fused)

Figure 38: Sample# 10 (YZ-e.max Fused)

e.max cemented to YZ group:

Site	Cohesive Failure	Adhesive Failure	Veneer failure
Pontic	1	1	0
Connector	0	0	0
Coping	0	0	0
Pontic & connector	0	0	0
Connector & coping	0	0	0
Pontic , connector & coping	0	4	0

Table 27: Failure mode of YZ e.max cemented group

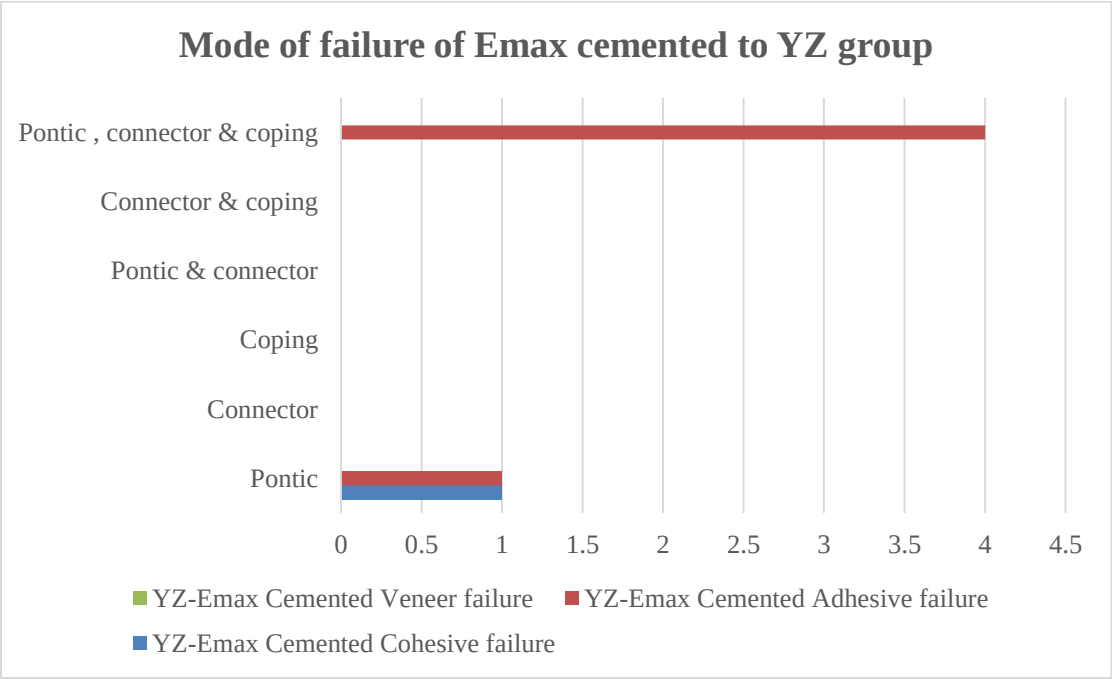

Graph 11: Mode of failure of e.max cemented to YZ zirconia

In the YZ-e.max cemented group there are four incidences of adhesive failure in the pontic, connector & coping area as well as an incidence of 1 specimen of adhesive and cohesive at the pontic area (Figures39-43)

e.max cemented to YZ group:

Figure 39: Sample# 13 (YZ-e.max cemented)

Figure 40: Sample# 12 (YZ-e.max cemented)

Figure 41: Sample# 11 (YZ-e.max cemented)

Figure 42: Sample# 1 (YZ-e.max cemented)

Figure 43: Sample# 8 (YZ-e.max cemented)

Triluxe fused to YZ group:

Site	Cohesive failure	Adhesive failure	Veneer failure
Pontic	0	1	0
Connector		0	0
Coping	0	0	0
Pontic & connector	0	0	0
Connector & coping	0	0	0
Pontic , connector & coping	0	4	0

Table 28: Failure mode of YZ-Triluxe fused group

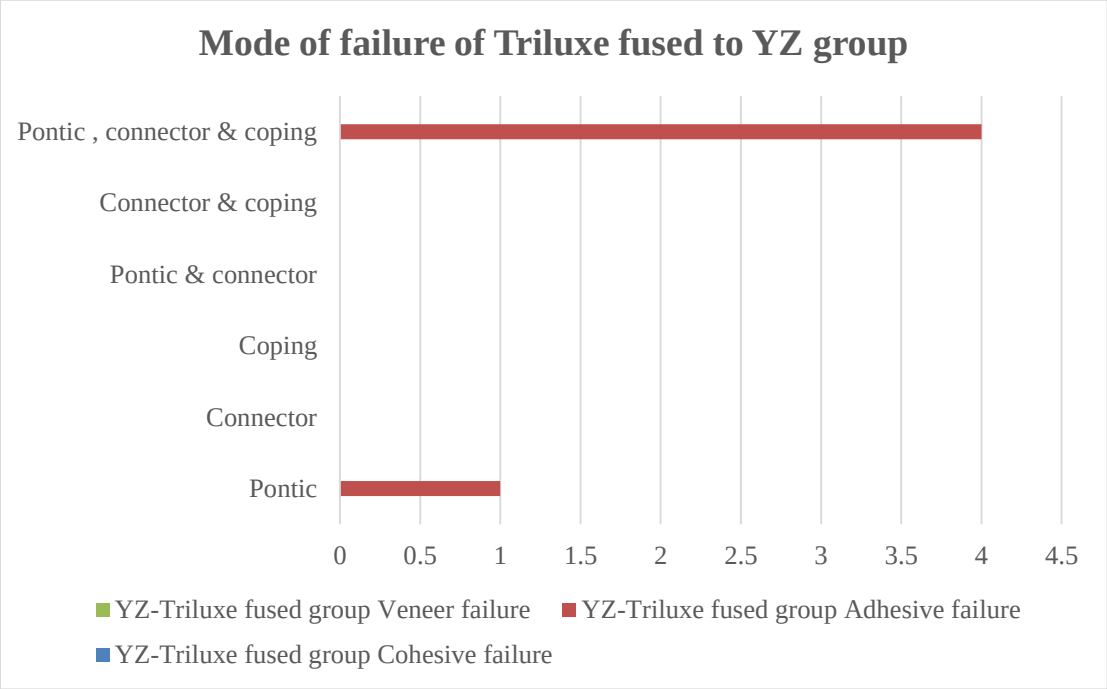

Graph 12: Mode of failure of Triluxe fused to YZ zirconia

In YZ-Triluxe fused group there are four incidences of adhesive failure at the pontic, connector & coping area as there is one incidence of adhesive failure at the pontic area (Figures44-48)

Triluxe fused to YZ group:

Figure 44: Sample# 13 (YZ -Triluxe, fused)

Figure 45: Sample# 8 (YZ-Triluxe, fused)

Figure 46: Sample# 14 (YZ-Triluxe fused)

Figure 47: Sample# 16 (YZ-Triluxe fused)

Figure 48: Sample# 11 (YZ-Triluxe fused)

Triluxe cemented to YZ group:

Site	Cohesive failure	Adhesive failure	Veneer failure
Pontic	0	2	0
connector	0	0	0
Coping	0	0	0
Pontic & connector	1	1	0
connector & coping	0	0	0
Pontic , connector & coping	0	3	0

Table 29: Failure mode of YZ-Triluxe cemented group

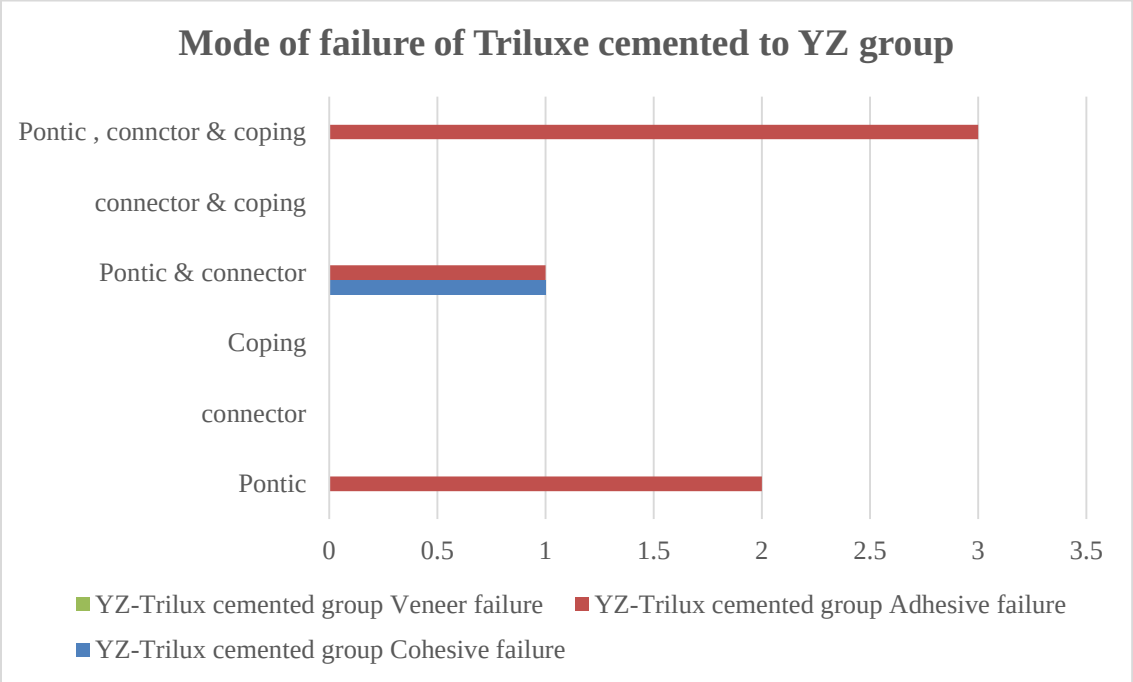

Graph 13: Mode of failure of Triluxe cemented to YZ zirconia

In YZ-Triluxe cemented group there are three incidences of adhesive failure at the pontic, connector & coping area as well as two incidences at pontic area, also we can see one incidence of cohesive and adhesive failure at pontic & connector area (Figures 49-54).

Triluxe cemented to YZ group:

Figure 49: Sample# 13 (YZ-Triluxe cemented)

Figure 50: Sample# 12 (YZ-Triluxe cemented)

Figure 51: Sample# 11 (YZ-Triluxe cemented)

Figure 52: Sample# 1 (YZ-Triluxe cemented)

Figure 53: Sample# 3 (YZ-Triluxe cemented)

Figure 54: Sample# 5 (YZ-Triluxe cemented)

20K cycles 40% of load e.max fused to YZ zirconia:

Sample#	Mode of Failure	Site
16	Cohesive Adhesive	Pontic & connector Pontic

Table 30: Failure mode of 20K cycles 40% of load e.max fused to YZ zirconia

In YZ-e.max fused group that subjected to 20K cycles of the cycle fatigue showed adhesive failure at the pontic and cohesive failure at the pontic & connector area (Figure 55).

Figure 55: Sample# 16 (YZ-e.max fused 20K)

Mode of failure of 20K cycles 40% of load E.max cemented to YZ zirconia:

Sample#	Mode of Failure	Site
2	Cohesive Adhesive	Pontic & connector Pontic

Table 31: Mode of failure of 20K cycles 40% of load E.max cemented to YZ zirconia

In YZ-E.max cemented group that subjected to 20K cycles of the cycle fatigue showed adhesive failure at the pontic and cohesive failure at the pontic & connector area (Figure 56).

Figure 56: Sample# 2 (YZ-e.max cemented 20K)

Mode of failure of 60K cycles 40% of load e.max fused to YZ zirconia:

Sample#	Mode of Failure	Site
12	Cohesive Adhesive	Pontic & connector Pontic

Table 32: Mode of failure of 60K cycles 40% of load e.max fused to YZ zirconia:

In YZ-e.max fused group that subjected to 60K cycles of the cycle fatigue showed adhesive failure at the pontic and cohesive failure at the pontic & connector area (Figure 57).

Figure 57: Sample# 12 (YZ-e.max fused 60K)

Mode of failure of 60K cycles 40% of load e.max cemented to YZ zirconia:

Sample#	Mode of Failure	Site
6	Adhesive	Pontic ,connector & coping

Table 33: Mode of failure of 60K cycles 40% of load e.max cemented to YZ zirconia

In YZ-E.max cemented group that subjected to 60K cycles of the cycle fatigue showed adhesive failure at the pontic, connector & coping area (Figure 58).

Figure 58: Sample# 6 (YZ-e.max cemented 60K)

Mode of failure of 80K cycles 40% of load e.max fused to YZ zirconia:

Sample#	Mode of Failure	Site
3	Adhesive	Pontic ,connector & coping

Table 34: Mode of failure 80K cycles 40% of load e.max fused to YZ zirconia

In YZ-e.max fused group that subjected to 80K cycles of the cycle fatigue showed adhesive failure at the pontic, connector & coping area (Figure 59).

Figure 59: Sample# 3 (YZ-e.max fused 80K)

Mode of failure of 80K cycles 40% of load E.max cemented to YZ zirconia:

Sample#	Mode of Failure	Site
11	Cohesive	Connector & coping

Table 35: Mode of failure 80K cycles 40% of load e.max cemented to YZ zirconia

In YZ-e.max cemented group that subjected to 80K cycles of the cycle fatigue showed a cohesive failure at the connector & coping area (Figure 60).

Figure 60: Sample# 11 (YZ-e.max cemented 80K)

Mode of failure of 20K cycles 40% of load Triluxe fused to YZ zirconia:

Sample#	Mode of Failure	Site
2	Cohesive Adhesive	Coping Pontic, connector & coping
3	Adhesive	Coping, connector & coping

Table 36: Mode of failure 20K cycles 40% of load Triluxe fused to YZ zirconia

In YZ-Triluxe fused group that subjected to 20K cycles of the cycle fatigue showed one incidence of cohesive failure at coping area and two incidences of adhesive failure at the coping, connector & coping area (Figures 61-62).

Figure 61: Sample# 2 (YZ-Triluxe fused 20K)

Figure 62: Sample# 3 (YZ-Triluxe fused 20K)

Mode of failure of 20K cycles 40% of load Triluxe cemented to YZ zirconia:

Sample#	Mode of Failure	Site
1	Veneer	Pontic
8	Adhesive	Pontic

Table 37: Mode of failure 20K cycles 40% of load Triluxe cemented to YZ zirconia

In YZ-Triluxe cemented group that subjected to 20K cycles of the cycle fatigue showed one incidence of cohesive and veneer failure at pontic (Figures 63-64).

Figure 63: Sample# 1 (YZ-Triluxe cemented 20K)

Figure 64: Sample# 8 (YZ-Triluxe cemented 20K)

Mode of failure of 60K cycles 40% of load Triluxe fused to YZ zirconia:

Sample#	Mode of Failure	Site
9	Adhesive	Pontic, connector & coping

Table 38: Mode of failure 60K cycles 40% of load Triluxe fused to YZ zirconia

In YZ-Triluxe fused group that subjected to 60K cycles of the cycle fatigue showed one incidence of adhesive failure at pontic, connector & coping area (Figure 65).

Figure 65: Sample# 9 (YZ-Triluxe fused 60K)

Mode of failure of 60K cycles 40% of load Triluxe cemented to YZ zirconia:

Sample#	Mode of Failure	Site
7	Veneer Cohesive	Coping Pontic, connector & coping

Table 39: Mode of failure 60K cycles 40% of load Triluxe cemented to YZ zirconia

In YZ-Triluxe cemented group that subjected to 60K cycles of the cycle fatigue showed an incidence of veneer failure at coping area and a cohesive failure at pontic, connector & coping area (Figure 66).

Figure 66: Sample# 7 (YZ-Triluxe cemented 60K)

Mode of failure of 80K cycles 40% of load Triluxe fused to YZ zirconia:

Sample#	Mode of Failure	Site
6	Adhesive	Pontic, connector & coping

Table 40: Mode of failure 80K cycles 40% of load Triluxe fused to YZ zirconia

In YZ-Triluxe fused group that subjected to 80K cycles of the cycle fatigue showed one incidence of adhesive failure at pontic, connector & coping area (Figure 67).

Figure 67: Sample# 6 (YZ-Triluxe fused 80K)

Mode of failure of 80K cycles 40% of load Triluxe cemented to YZ zirconia:

Sample#	Mode of Failure	Site
4	Adhesive	Pontic

Table 41: Mode of failure 80K cycles 40% of load Triluxe cemented to YZ zirconia

In YZ-Triluxe cemented group that subjected to 80K cycles of the cycle fatigue showed one incidence of adhesive failure at pontic area (Figure 68).

Figure 68: Sample# 4 (YZ-Triluxe cemented 80K)

Aged 20K cycles e.max cemented to YZ zirconia:

Site	Cohesive failure	Adhesive failure	Veneer failure
Pontic	0	1	0
Connector	0	0	0
Coping	0	0	0
Pontic & connector	0	0	3
Connector & coping	0	0	0
Pontic , connector & coping	0	0	1

Table 42: Mode of failure aged 20K cycles e.max cemented to YZ zirconia

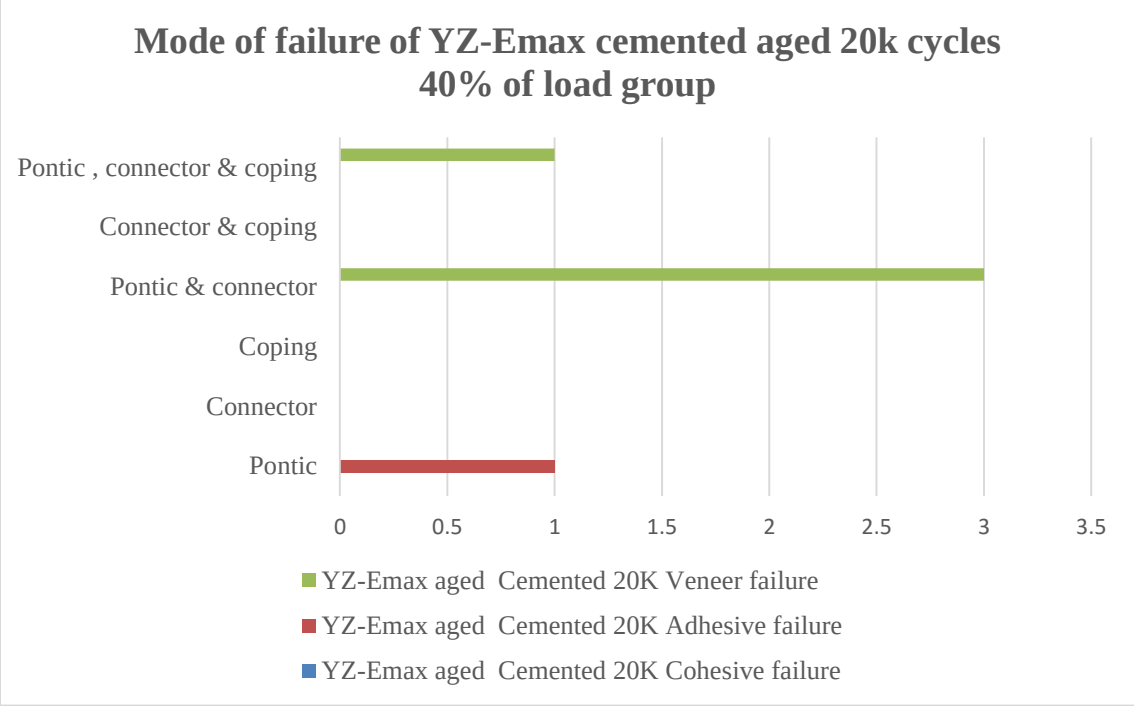

Graph 14: Mode of failure of aged 20K e.max cemented to YZ zirconia

In YZ-e.max cemented aged group that subjected to 20K cycles in cyclic fatigue test; there are three incidences of veneer failure at the pontic & connector area and one at pontic, connector & coping area , as there is one incidence of adhesive failure at the pontic area (Figures 69-73).

Aged 20K cycles e.max cemented to YZ zirconia:

Figure 69: Sample# 14 (YZ-e.max cemented aged 20K)

Figure 70: Sample# 15 (YZ-e.max cemented aged 20K)

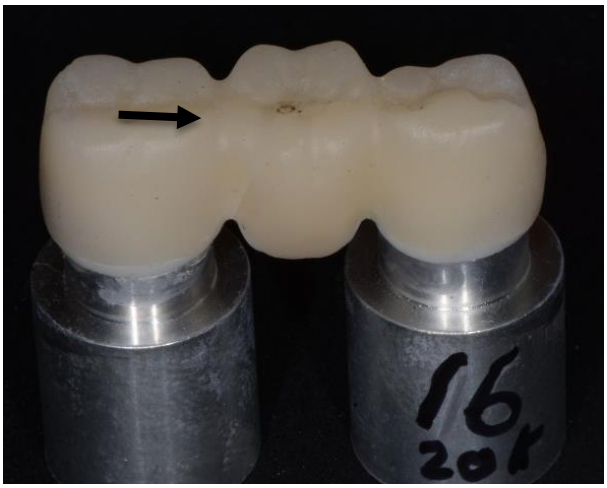

Figure 71: Sample# 16 (YZ-e.max cemented aged 20K)

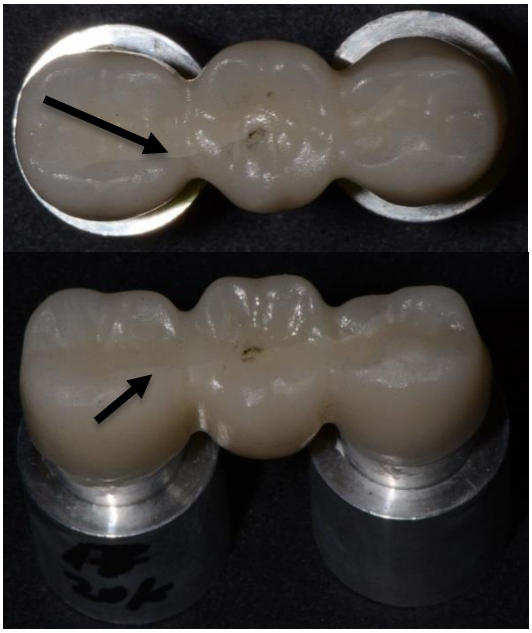

Figure 72: Sample# 17 (YZ-e.max cemented aged 20K)

Figure 73: Sample# 18 (YZ-e.max cemented aged 20K)

Aged 60K cycles e.max cemented to YZ zirconia:

Site	Cohesive failure	Adhesive failure	Veneer failure
Pontic	0	0	0
Connector	0	0	0
Coping	0	0	0
Pontic & connector	0	0	3
Connector & coping	0	0	0
Pontic , connector & coping	0	0	0

Table 43: Mode of failure aged 60K cycles e.max cemented to YZ zirconia

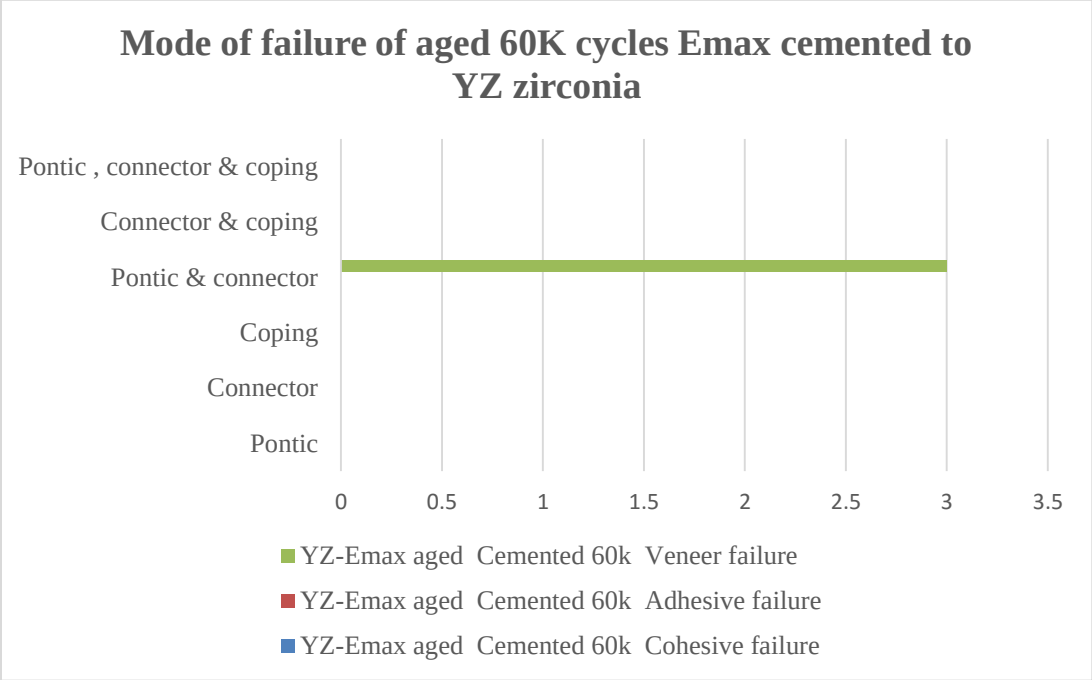

Graph 15: Mode of failure of aged 60K e.max cemented to YZ zirconia

In YZ-e.max cemented aged group that subjected to 60K cycles in cyclic fatigue test; there are three incidences of veneer failure at the pontic & connector area (Figures 74-78).

Aged 60K cycles e.max cemented to YZ zirconia:

Figure 74: Sample# 19 (YZ-e.max cemented aged 60K)

Figure 75: Sample# 20 (YZ-e.max cemented aged 60K)

Figure 76: Sample# 21 (YZ-e.max cemented aged 60K)

Figure 77: Sample# 22 (YZ-e.max cemented aged 60K)

Figure 78: Sample# 23 (YZ-e.max cemented aged 60K)

Mode of Failure of aged 80K cycles e.max cemented to YZ zirconia:

Site	Cohesive failure	Adhesive failure	Veneer Failure
Pontic	0	1	0
Connector	0	0	0
Coping	0	0	0
Pontic & connector	0	0	0
Connector & coping	0	0	0
Pontic , connector & coping	0	4	0

Table 44: Mode of failure aged 80K cycles e.max cemented to YZ zirconia

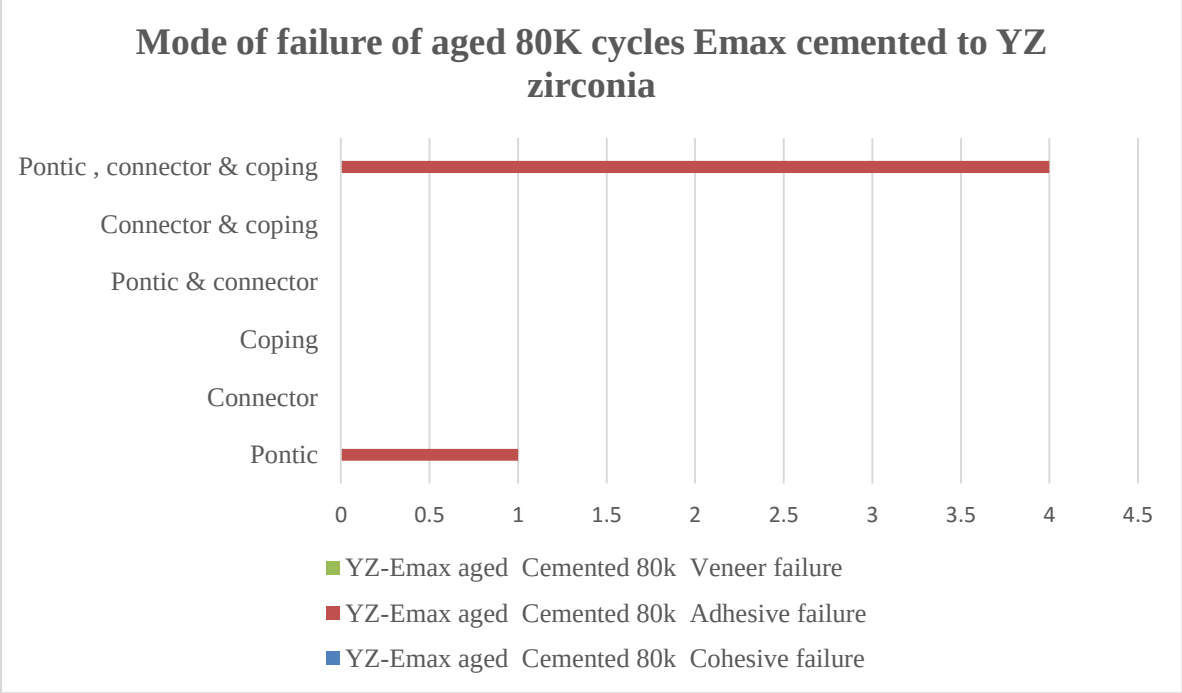

Graph 16: Mode of failure of aged 80K e.max cemented to YZ zirconia

In YZ-E.max cemented aged group that subjected to 80K cycles in cyclic fatigue test; there are four incidences of adhesive failure at the pontic, connector & coping area as well as one incidence of adhesive failure at the pontic area (Figures 79-83).

Mode of Failure of aged 80K cycles e.max cemented to YZ zirconia:

Figure 79: Sample# 24 (YZ-e.max cemented aged 80K)

Figure 80: Sample# 25 (YZ-e.max cemented aged 80K)

Figure 81: Sample# 26 (YZ-e.max cemented aged 80K)

Figure 82: Sample# 27 (YZ-e.max cemented aged 80K)

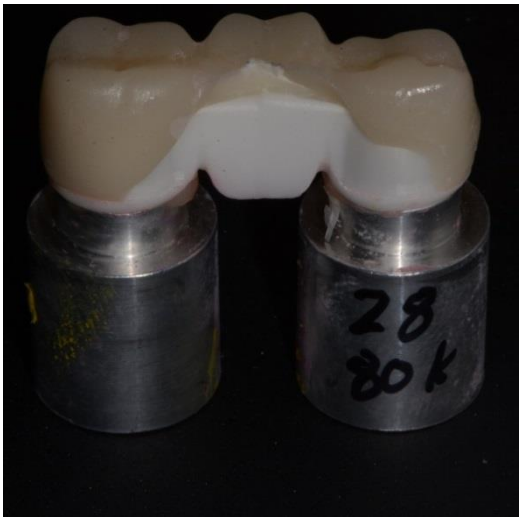

Figure 83: Sample# 28 (YZ-e.max cemented aged 80K)

Mode of failure of aged 20K cycles Triluxe cemented to YZ zirconia:

Site	Cohesive failure	Adhesive failure	Veneer failure
Pontic	0	2	1
Connector	0	0	0
Coping	0	0	0
Pontic & connector	0	0	0
Connector & coping	0	0	0
Pontic , connector & coping	0	6	0

Table 45: Mode of failure aged 20K cycles Triluxe cemented to YZ zirconia

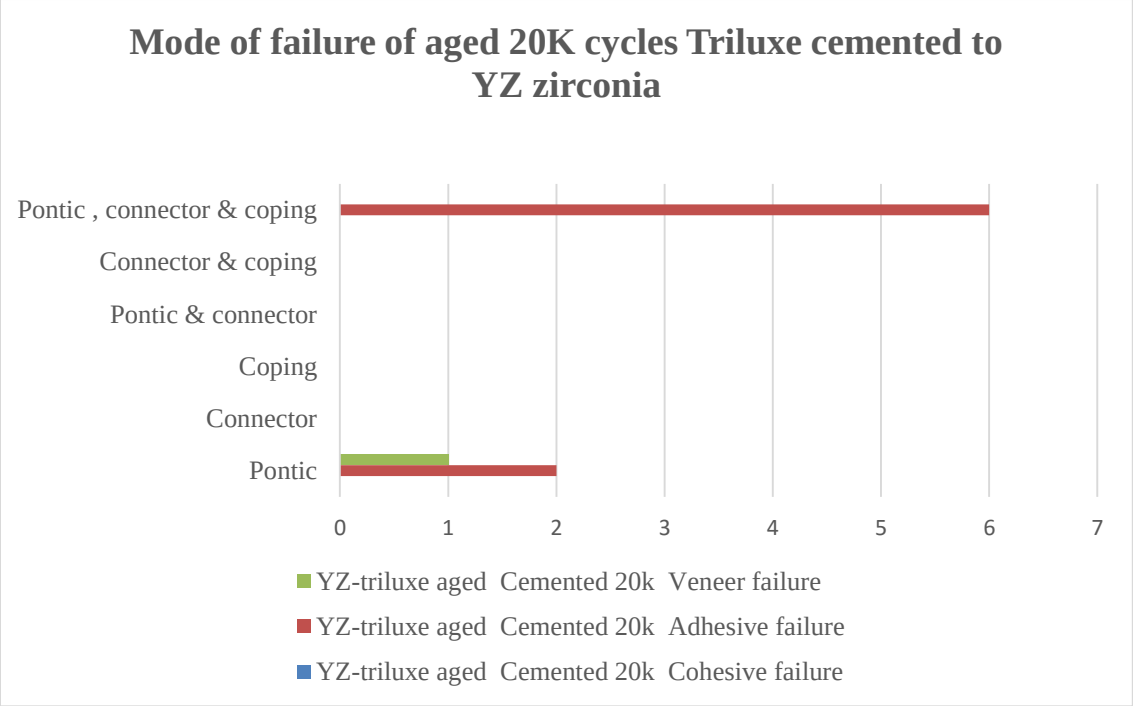

Graph 17: Mode of failure of aged 20K Triluxe cemented to YZ zirconia

In YZ-Triluxe cemented aged group that subjected to 20K cycles in cyclic fatigue test; there are six incidences of adhesive failure at the pontic, connector & coping area and two adhesive failure at the pontic area only as well as one incidence of veneer failure at the pontic area (Figures 84-90).

Mode of failure of aged 20K cycles Triluxe cemented to YZ zirconia:

Figure 84: Sample# 16 (YZ-Triluxe cemented aged 20K)

Figure 85: Sample# 17 (YZ-Triluxe cemented aged 20K)

Figure 86: Sample#18 (YZ-Triluxe cemented aged 20K)

Figure 87: Sample# 19 (YZ-Triluxe cemented aged 20K)

Figure 88: Sample# 25 (YZ-Triluxe cemented aged 20K)

Figure 89: Sample# 26 (YZ-Triluxe cemented aged 20K)

Figure 90: Sample# 27 (YZ-Triluxe cemented aged 20K)

Mode of failure of aged e.max fused to YZ zirconia:

Site	Cohesive failure	Adhesive failure	Veneer failure
Pontic	0	0	1
Connector	0	0	0
Coping	0	0	0
Pontic & connector	1	0	0
Connector & coping	0	0	0
Pontic , connector & coping	0	0	0

Table 46: Mode of failure aged e.max fused to YZ zirconia

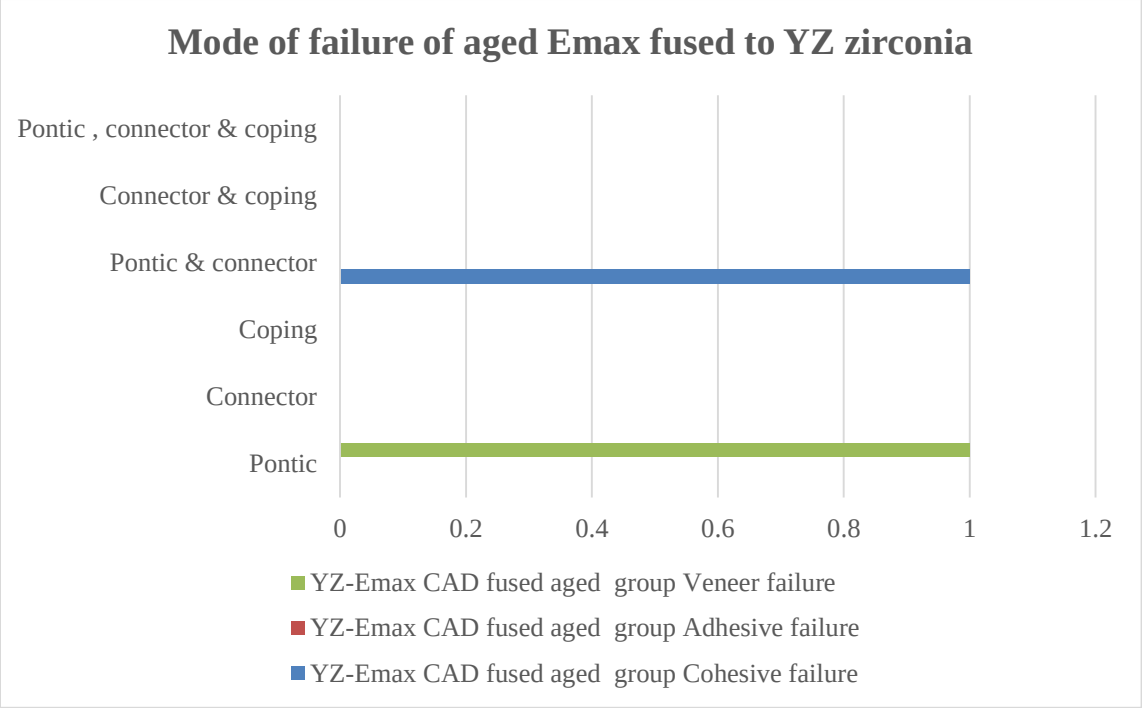

Graph 18: Mode of failure of aged E.max fused to YZ zirconia

In YZ-e.max fused aged group there is one incidence of veneer failure at the pontic area and one incidence of cohesive failure at the pontic & connector area (Figures 91-92).

Mode of failure of aged e.max fused to YZ zirconia:

Figure 91: Sample# 6 (YZ-e.max fused aged)

Figure 92: Sample# 7 (YZ-e.max fused aged)

Mode of Failure of aged Triluxe fused to YZ zirconia:

Site	Cohesive failure	Adhesive failure	Veneer failure
Pontic	0	0	0
Connector	0	0	0
Coping	1	0	0
Pontic & connector	0	0	0
Connector & coping	0	0	0
Pontic , connector & coping	0	2	0

Table 47: Mode of failure aged Triluxe fused to YZ zirconia

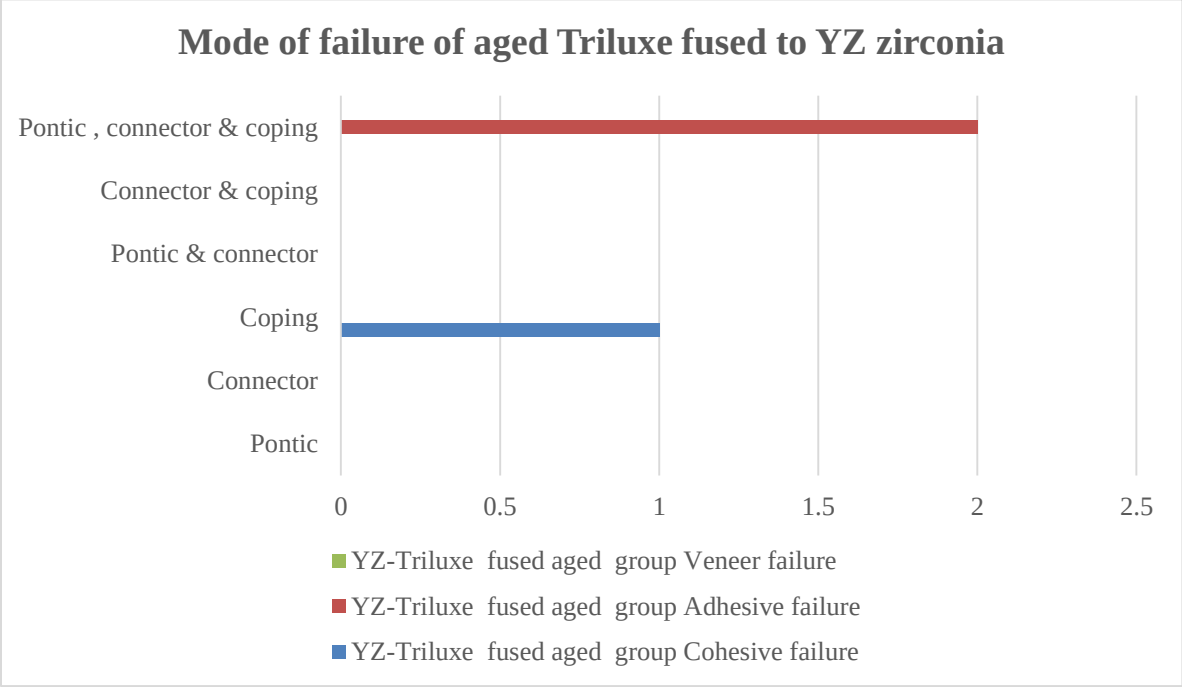

Graph 19: Mode of failure of aged Triluxe fused to YZ zirconia

In YZ-Triluxe fused aged group there is one incidence of cohesive failure at the coping area and two incidences of adhesive failure at the pontic, connector & coping area (Figures 93-94).

Mode of Failure of aged Triluxe fused to YZ zirconia:

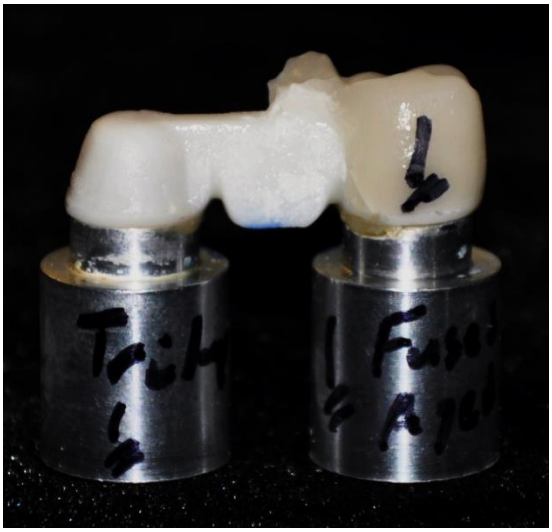

Figure 93: Sample# 1 (YZ-Triluxe fused aged)

Figure 94: Sample# 7 (YZ-Triluxe fused aged)

Mode of failure of aged e.max cemented to YZ zirconia:

Site	Cohesive failure	Adhesive failure	Veneer failure
Pontic	0	1	0
Connector	1	0	0
Coping	0	0	0
Pontic & connector	1	0	0
Connector & coping	0	0	0
Pontic , connector & coping	0	4	0

Table 48: Mode of failure of aged e.max cemented to YZ zirconia

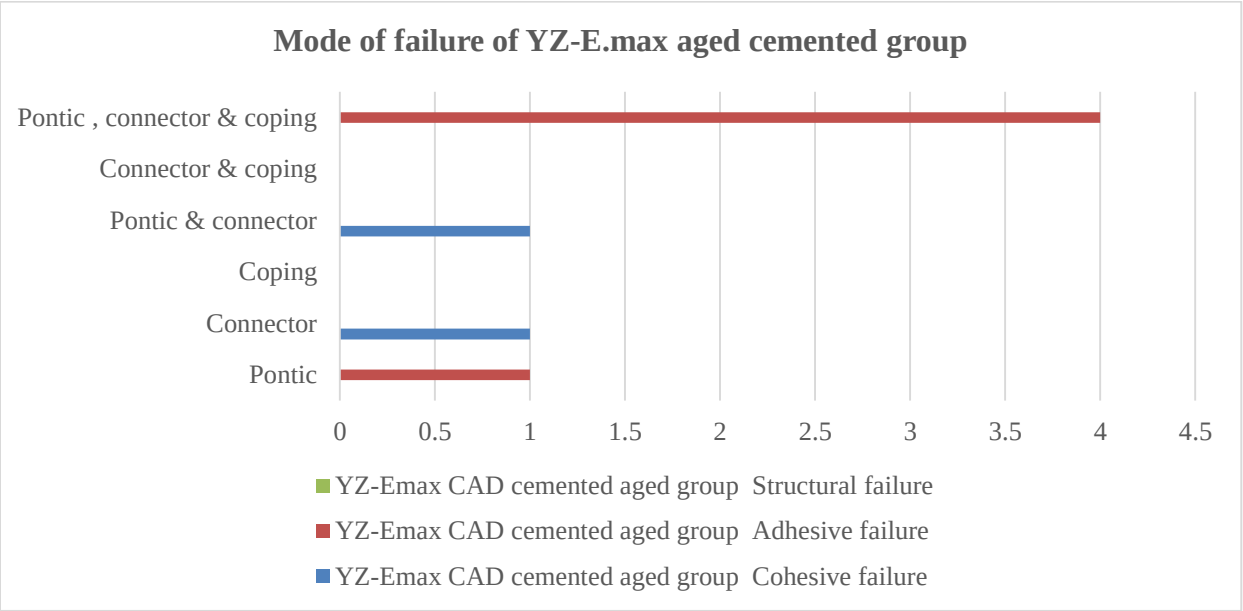

Graph 20: Mode of failure of aged e.max cemented to YZ zirconia

In YZ-e.max cemented aged group there is one incidence of adhesive failure at the pontic area and one incidence of cohesive failure at the connector as well as four incidences of adhesive failure at the pontic, connector & coping area (Figures 95-100).

Mode of failure of aged e.max cemented to YZ zirconia:

Figure 95: Sample# 3 (YZ-e.max cemented aged)

Figure 96: Sample# 29 (YZ-e.max cemented aged)

Figure 97: Sample# 30 (YZ-e.max cemented aged)

Figure 98: Sample# 31 (YZ-e.max cemented aged)

Figure 99: Sample# 32 (YZ-e.max cemented aged)

Figure 100: Sample# 33 (YZ-e.max cemented aged)

Mode of failure of aged 20K cycles 40% of load e.max cemented to YZ zirconia:

Site	Cohesive failure	Adhesive failure	Veneer failure
Pontic	0	0	0
Connector	0	0	0
Coping	0	0	0
Pontic & connector	0	0	0
Connector & coping	0	0	0
Pontic , connector & coping	0	1	0

Table 49: Mode of failure of aged 20K cycles 40% of load e.max cemented to YZ zirconia

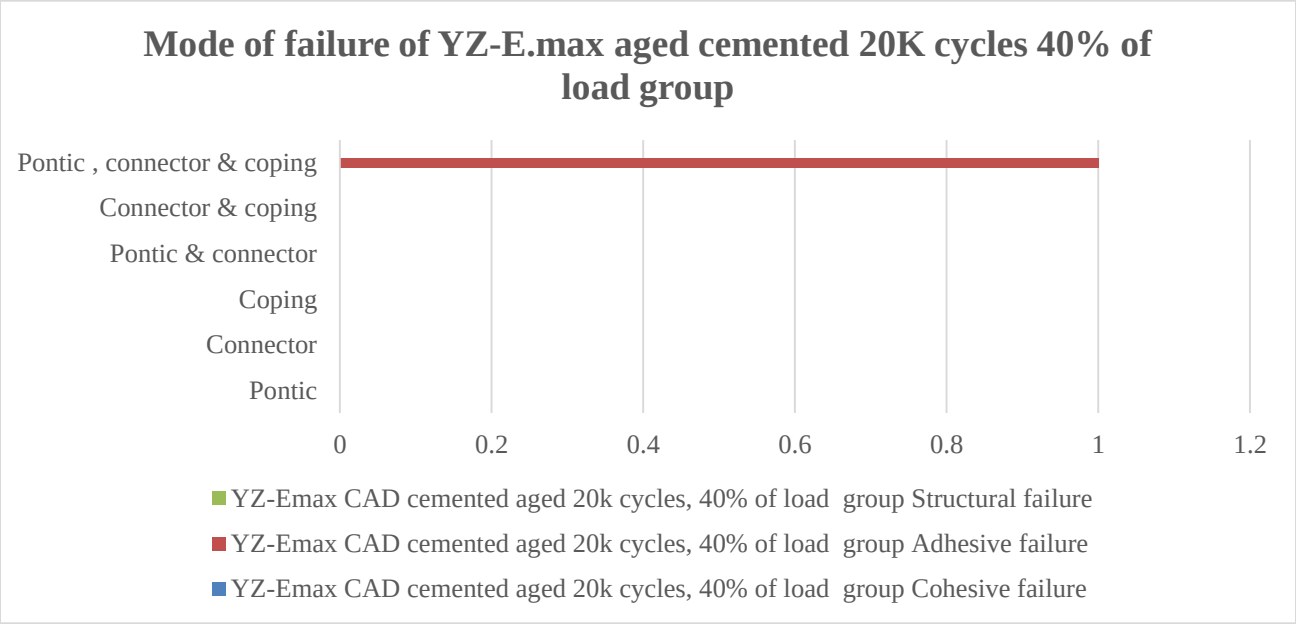

Graph 21: Mode of failure of aged 20K e.max cemented to YZ zirconia

In YZ-e.max aged cemented 20K cycles group there is one sample survived with adhesive failure at the pontic, connector & coping area (Figure 101).

Mode of Failure of aged 20K e.max cemented to YZ zirconia:

Figure 101: Sample# 15 (YZ-e.max cemented aged 20K 40%)

Mode of failure of aged 60K cycles 40% of load cemented to YZ zirconia:

Site	Cohesive failure	Adhesive failure	Veneer failure
Pontic	0	0	0
Connector	1	0	0
Coping	0	0	0
Pontic & connector	0	0	0
Connector & coping	0	0	0
Pontic , connector & coping	0	2	0

Table 50: Mode of failure of aged 60K cycles 40% of load cemented to YZ zirconia

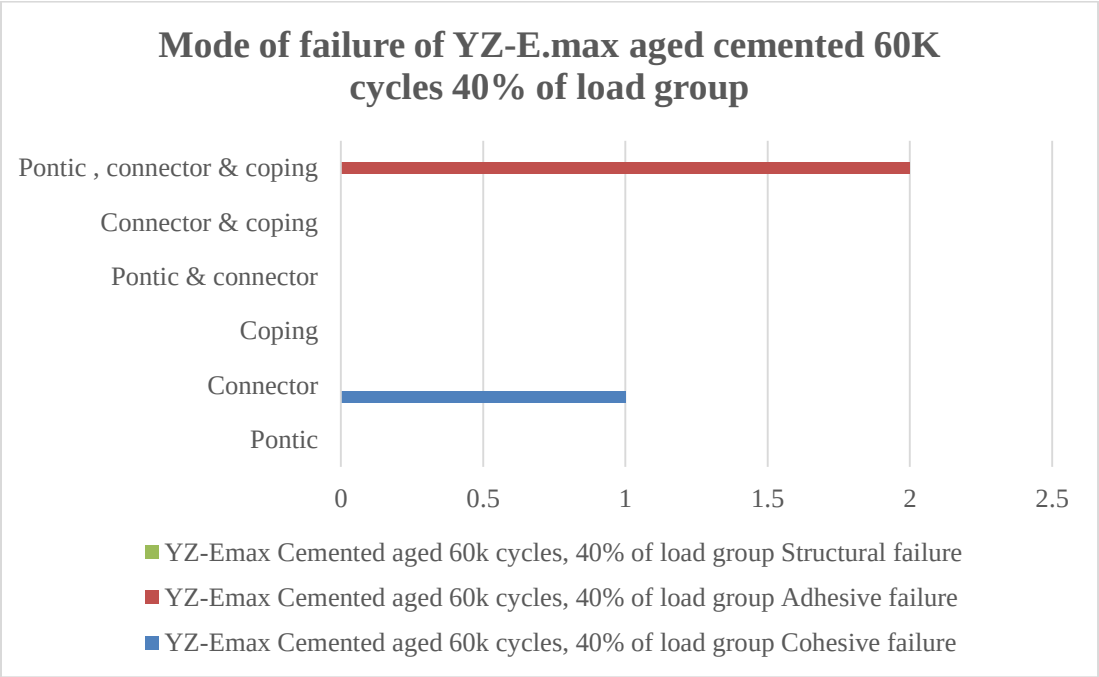

Graph 22: Mode of failure of aged 60K e.max cemented to YZ zirconia

In YZ-e.max cemented aged 60K cycles group there are two samples survived and showed two incidences of adhesive failure at pontic, connector & coping area and one incidence of cohesive failure at connector area (Figures 102-103).

Mode of failure of aged 60K cycles 40% of load cemented to YZ zirconia:

Figure 102: Sample# 19 (YZ-e.max cemented aged 60K 40%)

Figure 103: Sample# 20 (YZ-e.max cemented aged 60K 40%)

Mode of failure of aged 20K cycles 30% of load Triluxe cemented to YZ zirconia:

Site	Cohesive failure	Adhesive failure	Veneer failure
Pontic	0	0	0
Connector	0	0	0
Coping	0	0	0
Pontic & connector	0	0	0
Connector & coping	0	0	0
Pontic , connector & coping	0	2	0

Table 51: Mode of failure of aged 20K cycles 30% of load Triluxe cemented to YZ zirconia

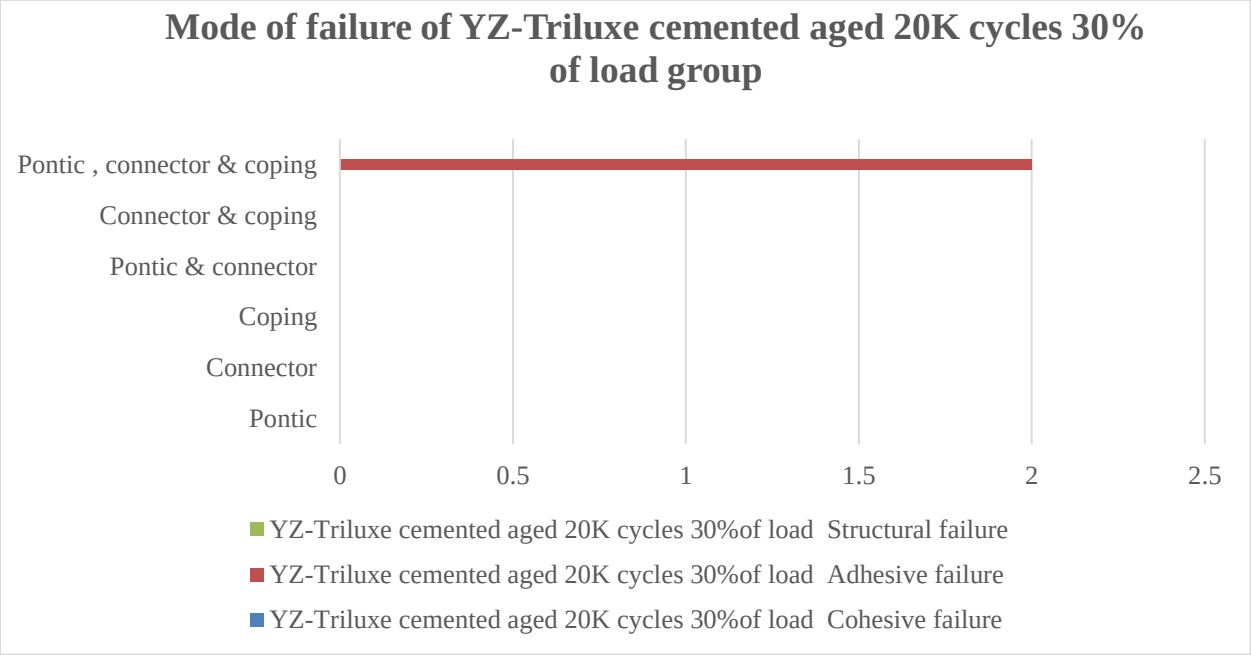

Graph 23: Mode of failure of aged 20K 30% of load Triluxe cemented to YZ zirconia

In YZ-Triluxe cemented aged 20K cycles 30% of load group tow specimens survived and showed after load to failure test an adhesive failure at the pontic, connector & coping area (Figures 104-105).

Mode of failure of aged 20K cycles 30% of load Triluxe cemented to YZ zirconia:

Figure 104: Sample# 20 (YZ-Triluxe aged cemented 20K 30%)

Figure 105: Sample# 22 (YZ-Triluxe aged cemented 20K 30%)

Mode of failure of aged Triluxe cemented to YZ zirconia:

Site	Cohesive failure	Adhesive failure	Veneer failure
Pontic	0	1	0
Connector	0	0	0
Coping	0	0	0
Pontic & connector	2	0	0
Connector & coping	0	0	0
Pontic , connector & coping	0	4	0

Table 52: Mode of failure of aged Triluxe cemented to YZ zirconia

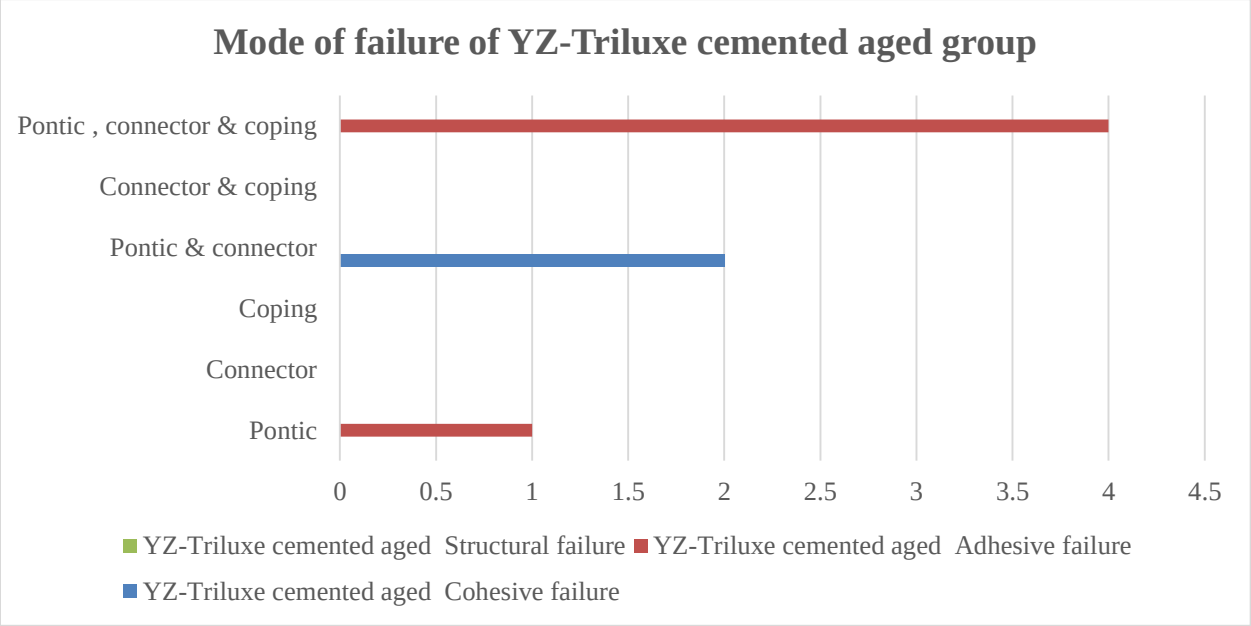

Graph 24: Mode of failure of aged Triluxe cemented to YZ zirconia

In YZ-Triluxe cemented aged group there are two incidence of cohesive failure at the pontic & connector area and one incidence of adhesive failure at the pontic area as well as four incidences of adhesive failure at the pontic connector & coping area (Figures 106-110).

Mode of failure of aged Triluxe cemented to YZ zirconia:

Figure 106: Sample# 30 (YZ-Triluxe cemented aged)

Figure 107: Sample# 31 (YZ-Triluxe cemented aged)

Figure 108: Sample# 32 (YZ-Triluxe cemented aged)

Figure 109: Sample# 33 (YZ-Triluxe cemented aged)

Figure 110: Sample# 34 (YZ-Triluxe cemented aged)

MICROSTRUCTURE EXAMINATION

IPS e.max fused to YZ zirconia group:
a-SEM of IPS e.max fused to YZ zirconia:

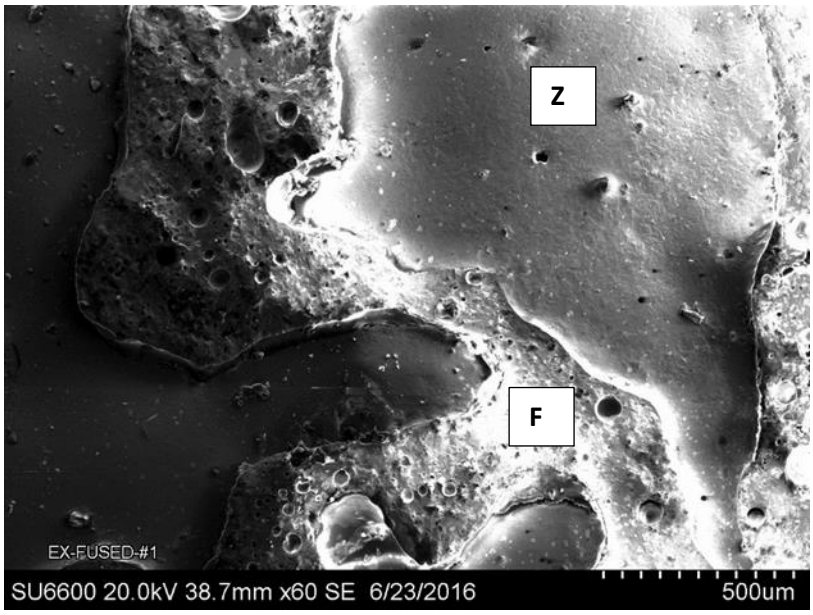

Figure 111: Electron Micrograph of the fracture surface showing adhesive failure of e.max fused to YZ. X60, Z= YZ zirconia, F = fusing material.

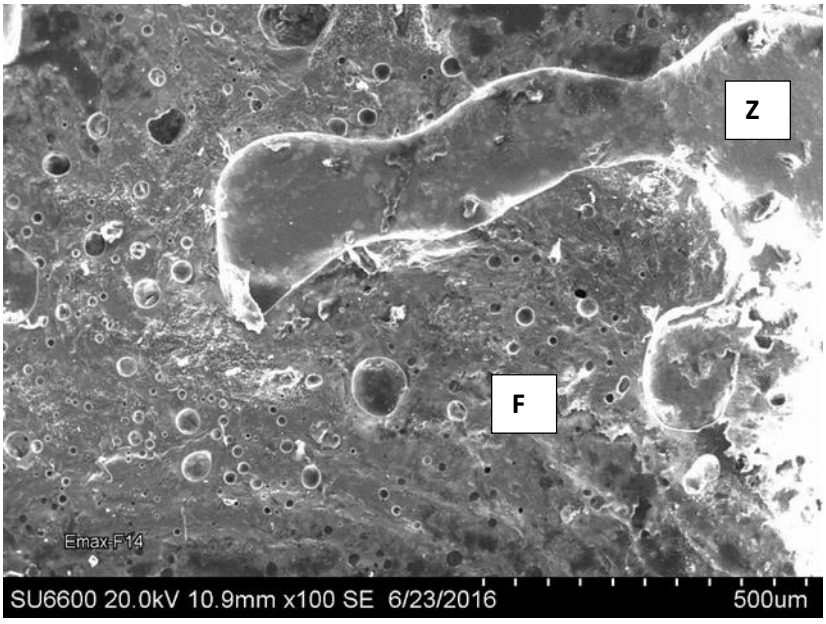

Figure 112: Electron Micrograph of the fracture surface showing adhesive failure of e.max fused to YZ. X100, Z= YZ zirconia, F = fusing material.

b- EDS of IPS e.max fused to YZ zirconia:

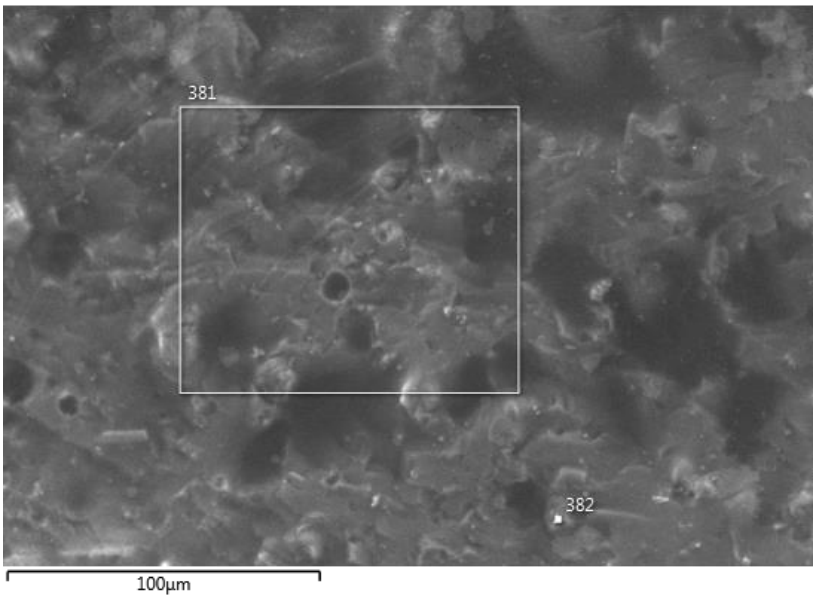

Spectrum 381		
	Wt%	σ
O	42.5	0.4
Si	34.5	0.2
K	11.2	0.1
Al	7.0	0.1
Ca	1.8	0.1
Zn	1.8	0.2
Ti	1.1	0.1

Spectrum 382		
	Wt%	σ
O	42.9	0.4
Si	29.0	0.2
K	15.8	0.2
Al	10.0	0.1
Ca	1.3	0.1
Zn	0.6	0.2
Ti	0.3	0.1

Figure 113: Electron Micrograph of the fracture surface of e.max fused to YZ zirconia x600, EDS analysis; Spectrum 381 & 382 showed elements of glass fusing material.

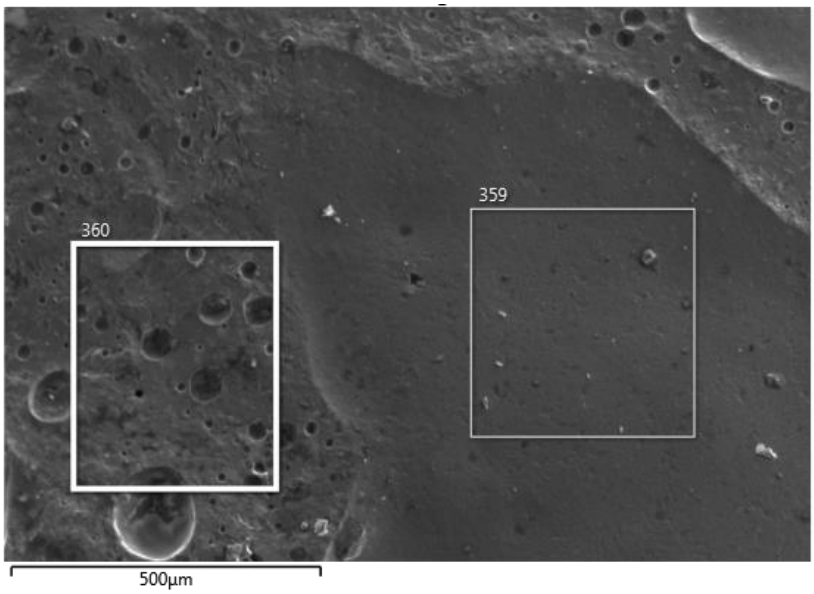

Spectrum 359

	Wt%	σ
O	56.3	0.2
Si	27.2	0.2
K	6.8	0.1
Al	6.6	0.1
Ca	1.2	0.1
Zn	0.8	0.1
Ti	0.5	0.0
Ce	0.5	0.1

Spectrum 360

	Wt%	σ
O	57.5	0.3
Si	26.7	0.2
Al	6.2	0.1
K	6.0	0.1
Zr	1.5	0.2
Ca	1.0	0.1
Ti	0.6	0.1
Zn	0.5	0.1

Figure 114: Electron Micrograph of the fracture surface of e.max fused to YZ zirconia x100 EDS analysis; Spectrum 359 showed elements of glass fusing material only, Spectrum 360 showed elements of glass fusing material and zirconia.

Triluxe cemented to YZ zirconia group:
a-SEM of Triluxe cemented to YZ zirconia:

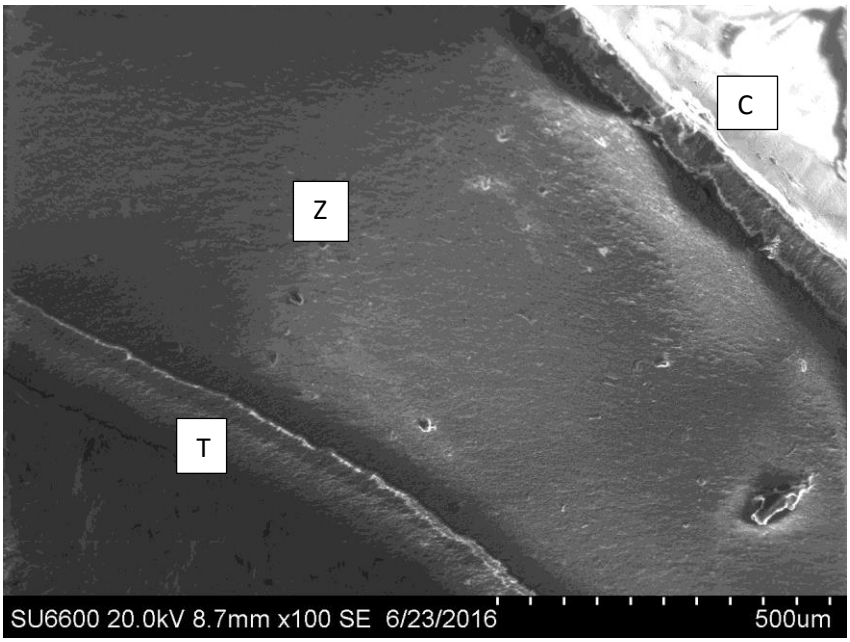

Figure 115: Electron Micrograph of the fracture surface showing cohesive failure of Triluxe cemented to YZ. X100, Z= YZ zirconia, C= resin cement material T=Triluxe veneer.

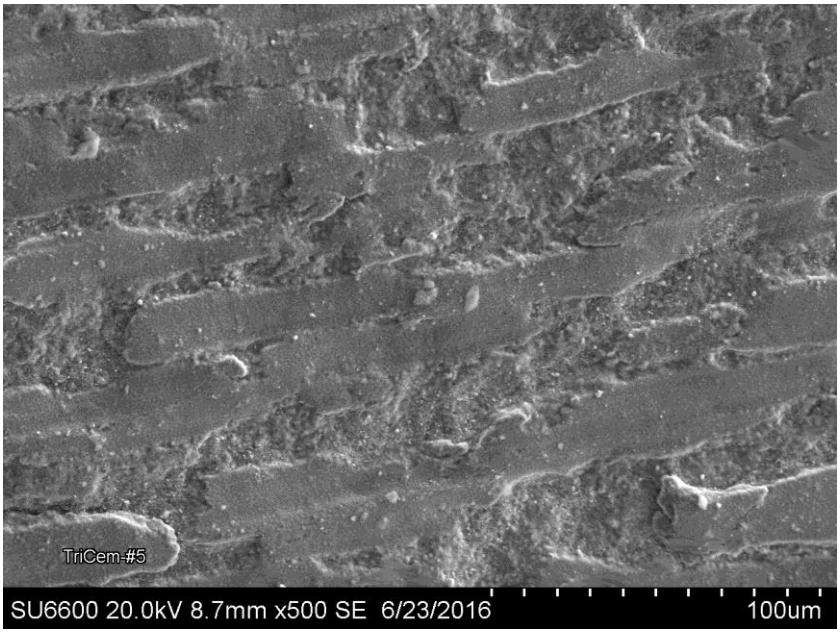

Figure 116: Electron Micrograph for the fracture surface of Triluxe cemented to YZ. x500,

b-EDS of Triluxe cemented to YZ zirconia group:

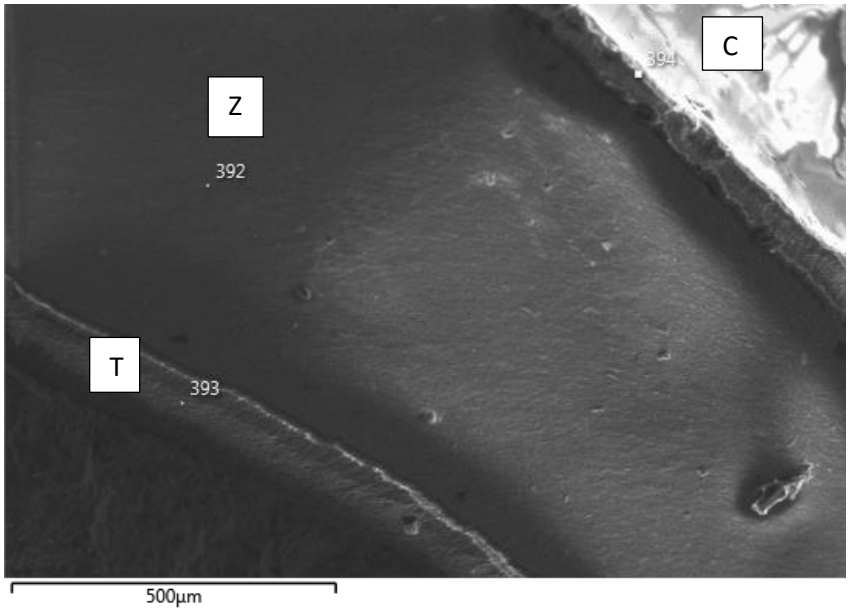

Spectrum 392

	Wt%	σ
Zr	76.1	0.7
O	19.0	0.5
Y	3.7	0.4
Hf	1.2	0.5

Spectrum 393

	Wt%	σ
O	62.7	1.4
Si	22.0	0.9
Al	8.0	0.5
Zr	3.9	1.0
K	3.4	0.4

Spectrum 394

	Wt%	σ
O	37.1	0.4
Si	22.8	0.3
Yb	13.4	0.4
Ba	12.2	0.3
F	8.4	0.5
Al	3.8	0.2
Ca	2.0	0.1
K	0.3	0.1

Figure 117: Electron Micrograph of a fracture surface showing cohesive failure of Triluxe cemented to YZ. X100, Z= YZ zirconia, C= resin cement material T=Triluxe veneer. EDS analysis; Spectrum 392 showed elements of zirconia, Spectrum 393 showed elements of Triluxe forte, Spectrum 394 showed elements of resin cement.

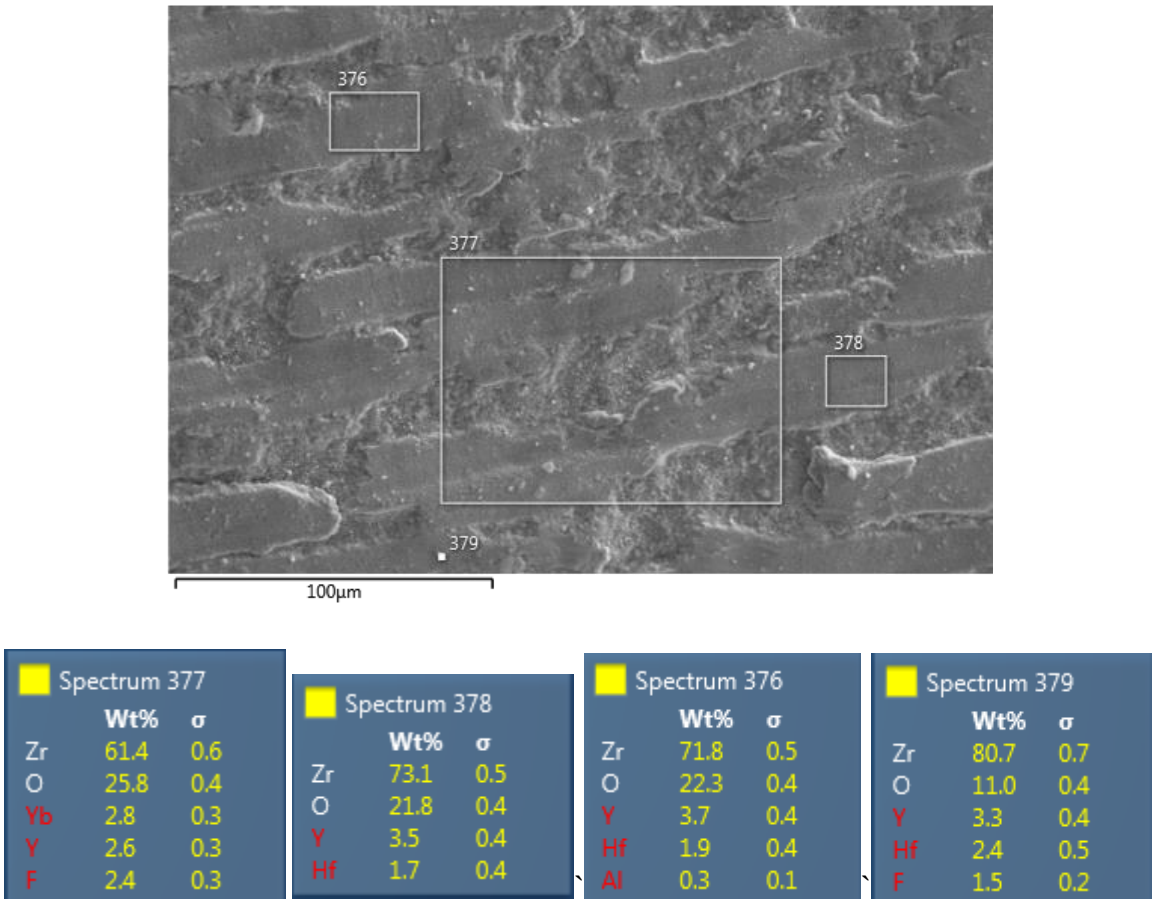

Figure 118: Electron Micrograph of the fracture surface of Triluxe cemented to YZ. x500, EDS analysis; Spectrum 377, 378, 376, 379 showing elements of zirconia

20K cycles Triluxe cemented to YZ zirconia group:
a-SEM and EDS for 20K cycles Triluxe cemented to YZ zirconia:

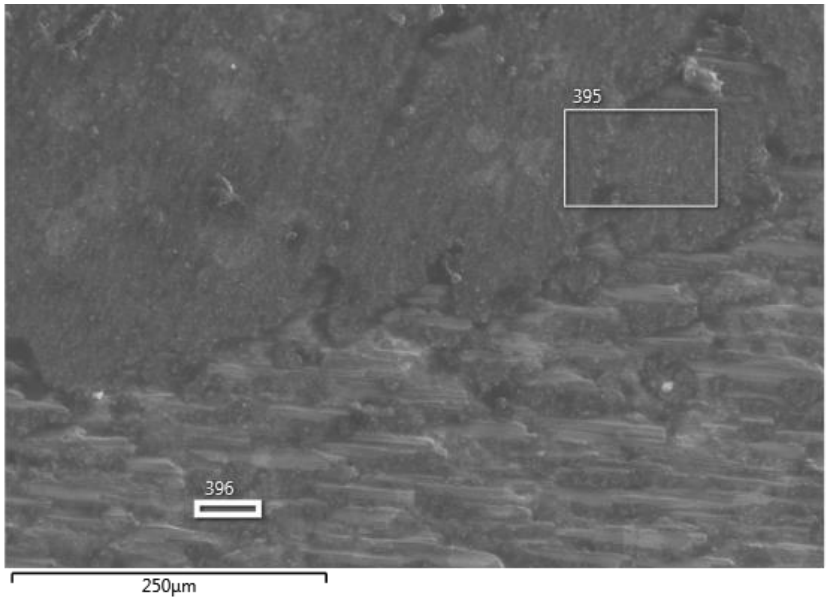

Spectrum 396		
	Wt%	σ
Zr	63.5	0.5
O	32.2	0.4
Y	2.8	0.3
Hf	1.5	0.3

Spectrum 395		
	Wt%	σ
O	36.2	0.5
Si	23.3	0.3
Yb	19.3	0.6
Ba	12.4	0.4
Zr	4.8	0.4
Al	3.2	0.2
Ca	0.8	0.1

Figure 119: Electron Micrograph of the fracture surface of 20K cycles Triluxe cemented to YZ. x500, EDS analysis; Spectrum 396 showed elements of zirconia, Spectrum 395 showed elements of resin cement.

b- EDS layered for 20K cycles Triluxe cemented to YZ zirconia:

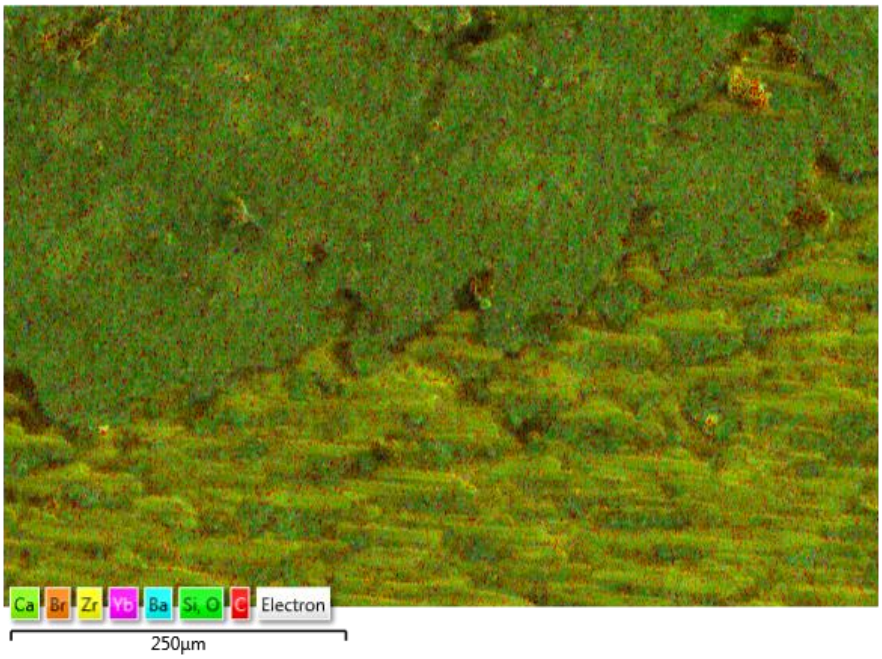

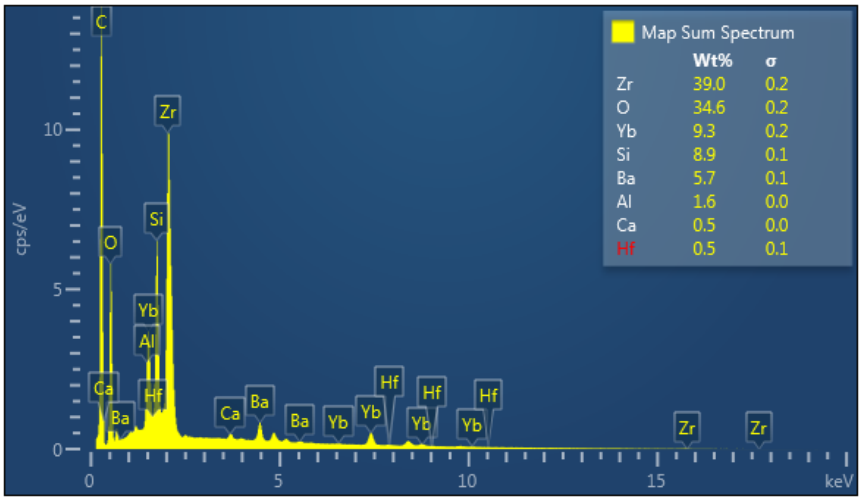

Figure 120: EDS layered of 20K cycles Triluxe cemented to YZ zirconia magnification x500 Showing elements of zirconia and the glass fusing porcelain elements.

Aged Triluxe fused to YZ zirconia group:
a-SEM of Aged Triluxe fused to YZ zirconia group:

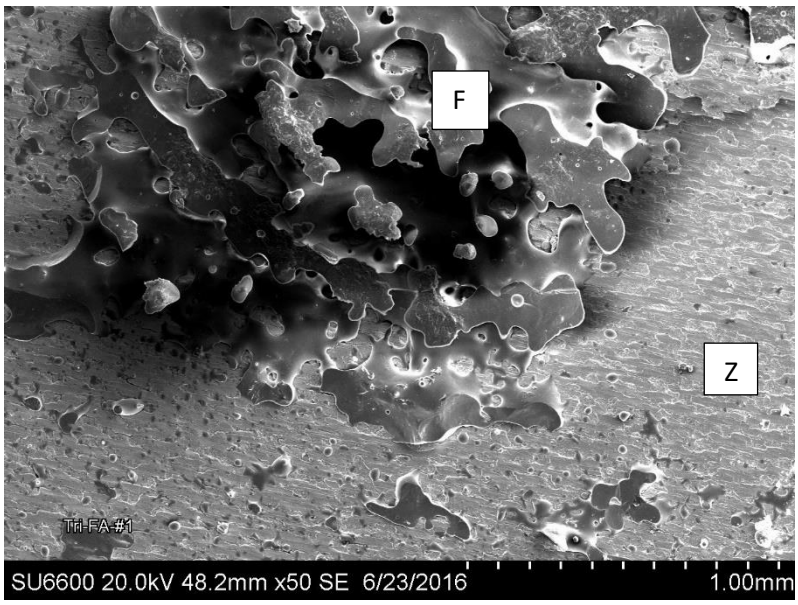

Figure 121: Electron Micrograph of the fracture surface showing adhesive failure of aged Triluxe fused to YZ. x50, Z= YZ zirconia, F= fusing material (VM9)

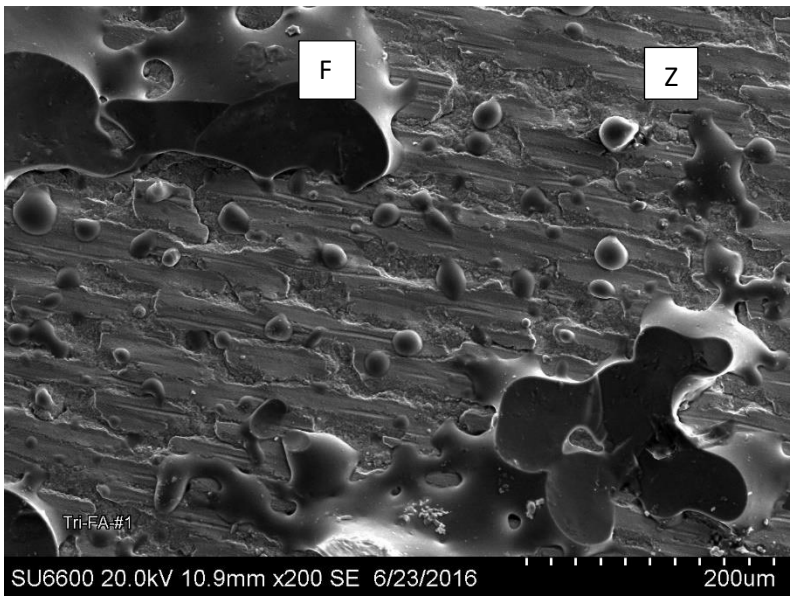

Figure 122: Electron Micrograph of the fracture surface showing adhesive failure mode of aged Triluxe fused to YZ. x200, Z= YZ zirconia, F= fusing material (VM9)

b-EDS of Aged Triluxe fused to YZ zirconia group:

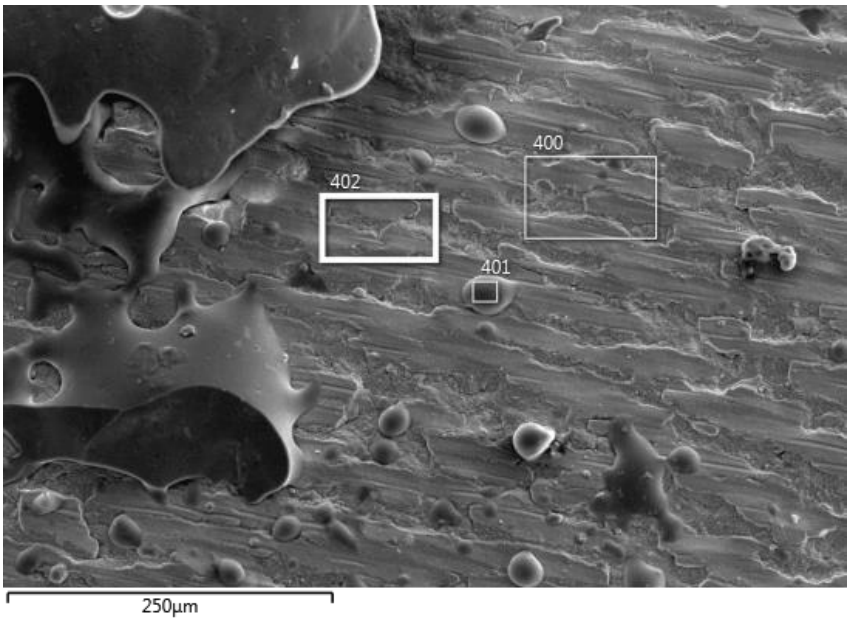

Spectrum 401		
	Wt%	σ
O	51.6	0.4
Si	28.5	0.3
Al	8.4	0.2
K	5.8	0.1
Ba	2.1	0.2
Zr	1.8	0.3

Spectrum 402		
	Wt%	σ
Zr	65.6	0.5
O	29.9	0.4
Y	3.0	0.3
Hf	1.5	0.3

Spectrum 400		
	Wt%	σ
Zr	63.7	0.5
O	31.5	0.4
Y	3.6	0.4
Hf	1.3	0.3

Figure 123: Electron Micrograph of the fracture surface showing adhesive failure of aged Triluxe fused to YZ. x200, EDS analysis; Spectrum 401 showing elements of glass fusing porcelain, Spectrum 402 & 400 showing elements of zirconia.

c-EDS layered of Aged Triluxe fused to YZ zirconia group:

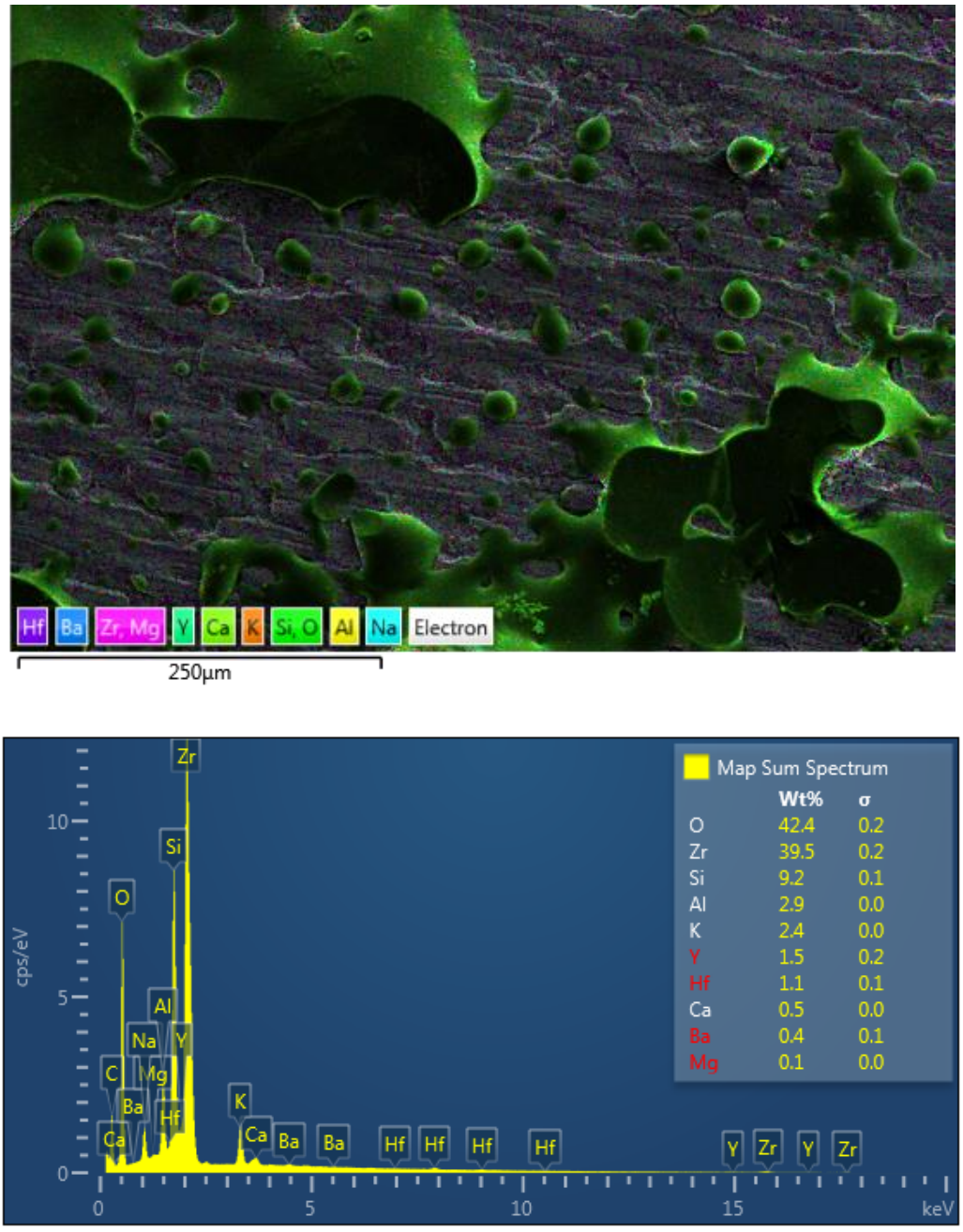

Figure 124: EDS layered of aged Triluxe fused to YZ zirconia magnification x200 Showing zirconia and the glass fusing porcelain elements.

DISCUSSION

Zirconia holds a unique place among all-ceramics due to its excellent mechanical properties. Flexural strength and fracture toughness of zirconia are the highest of the currently used dental ceramics. This allows use in posterior fixed partial dentures and permits a substantial reduction in core thickness. These capabilities are eye-catching in prosthetic dentistry, where strength and esthetics are principal requirements for patient satisfaction.[42]. Even with the exceptional mechanical properties, there are problems with zirconia based all-ceramic restorations. The most common technical difficulty associated with zirconia based all-ceramic restorations is veneer fracture.[74-76]. Chipping of the veneering porcelain, which can be repaired with resin material, has been reported in several clinical studies. [69-79] Several factors play an important role in the chipping of the ceramic for zirconia-supported restorations; (a) strength of the veneering porcelain, (b) bonding between veneering porcelain and zirconia, (c) support from the underlying zirconia core, (d) microstructural defects in veneering porcelain and residual thermal stresses. [58-68]

Triluxe forte was milled and fused to YZ zirconia by means of VM9 fusing porcelain and cemented to YZ zirconia by means of Multilink resin cement. The failure load of aged fatigued Triluxe cemented to YZ zirconia showed a significant difference as compared to non-aged fatigued Triluxe cemented to YZ zirconia. Renan Belli et. al. 2014, found the mechanical degradation of Triluxe Forte is governed by stress corrosion mechanisms, with strength degradation severity being linked to the glass phase amount. This supports our finding that aging and cyclic fatigue cause mechanical degradation of the Triluxe forte.

In this study, it was determined that there is no significant difference between the aged and non-aged Triluxe fused to YZ zirconia. On the other hand, there is a significant difference between (aged and non-aged) Triluxe cemented to YZ zirconia and (aged and non-aged) Triluxe fused to YZ zirconia. This may in part be due to the presence of voids in the fusing layer as well as a mismatch of the coefficient of the thermal expansion of the VM9 fusing material.

For the e.max groups, there is a significant difference between aged e.max cemented to YZ zirconia and aged fatigued e.max cemented to YZ zirconia. Furthermore, as the cycle number increased (20K, 60K and 80K cycles) in the aged fatigued e.max cemented to YZ groups the failure load decreased. This is supported by the work of Renan Belli et. al. 2014 that showed the aging and dynamic (cyclic) fatigue affect the mechanical properties of e.max CAD by stress corrosion mechanisms.

Due to high flexural strength (360 MPa) and modulus of elasticity (95 GPa) of the e.max veneer material, there is a significant difference between non-aged e.max fused to YZ zirconia and non-aged Triluxe fused to YZ zirconia. The higher flexural strength of e.max (360 GPa) may explain the significantly higher failure load of non-aged e.max versus non-aged Triluxe (154 GPa). Also, the fusing material for e.max veneer may be more compatible with respect to thermal expansion and ability to bond with both the e.max and zirconia.

There is no statistical significant difference between the aged, non-aged e.max fused to YZ zirconia, which can be explained after examination of the specimens under the microscope. The e.max fusing material appears to fill the machining grooves on YZ zirconia framework and reinforce the mechanical properties of the specimens as it shown in the electron micrograph pictures of this group. Comparing the non-aged e.max fused veneer group and the

non-aged Triluxe fused veneer group we found that, there is a significant difference between the static non-aged e.max veneer fused to YZ zirconia group and the non-aged static fatigued Triluxe veneer fused to YZ zirconia groups. This can be explained by four factors:

1. Higher mechanical properties of the e.max.
2. Integration of fusing material with YZ zirconia on e.max fused group.
3. The coefficient of thermal expansion mismatch of VM9.
4. The presence of voids in the fusing material in the Triluxe fused YZ zirconia group.

Within the e.max groups, all the specimens of the cemented aged fatigued for 80K cycles failed in the fatigued test. Furthermore, the 60K cyclic aged cemented group showed the lowest failure load in comparison to all other e.max groups. This could be explained by the following factors:

1. Degradation of the mechanical properties of the e.max by stress corrosion mechanism due to effect of real time aging (Renan Belli et. al. 2014).
2. Potential for stress relaxation in the zirconia and phase change from tetragonal phase to monoclinic phase that create stress at the veneer interface (Fahmi et.al. 2012) which represented in the adhesive failure in all the aged e.max groups.

CONCLUSIONS

The following conclusions were drawn:

1. The Triluxe Forte fused to YZ zirconia framework showed lower significant difference in failure load among all the other groups ($p<0.05$).
2. There is higher significant difference between the non-aged Triluxe cemented to YZ zirconia (static and cyclic) and the aged cemented Triluxe fatigued for 60K and above ($p<0.05$).
3. Within the IPS e.max CAD groups, there is lower significant difference in failure load between the aged e.max fatigued (20K, 60K and 80K) cemented to YZ zirconia and all the other groups ($p<0.05$).
4. There is no significant difference in failure load between e.max fused and IPS e.max CAD cemented to YZ zirconia framework ($p>0.05$).

Recommendations:

1. Further study of the effect of real time aging on mechanical properties of the YTZP and dental ceramic material.
2. Further study to improve the compatibility of the coefficient of thermal expansion fusing material used with Triluxe Forte and improve the fusing technique.

REFERENCES

1. Helvey, Gregg DDS, A history of Dental Ceramics. Compendium, May 2010 Volume 31, Issue 4

2. Jones DW. Development of dental ceramics. An historical perspective. Dental Clinics of North America 1985; 29(4):621-44.

3. Kelly JR, Benetti P. Ceramic materials in dentistry: historical evolution and current practice. Australian Dental Journal 2011; 56 1:84-96.

4. Asgar K. Casting metals in dentistry: past--present--future. Advances in Dental Research 1988;2(1):33-43.

5. Kelly JR, Nishimura I, Campbell SD. Ceramics in dentistry: historical roots and current perspectives. Journal of Prosthetic Dentistry 1996; 75(1): 18-32.

6. Deborah PL, Wilkens AS, Frederico AE, De Souza, Grace M. Fracture Strength of Aged Monolithic and Bilayer Zirconia-Based Crowns. BioMed Research International. vol. 2015, Article ID 418641, 7 pages, 2015

7. Leinfelder KF, Kurdziolek SM. Contemporary CAD/CAM technologies: the evolution of restorative systems. Practice Procedure Aesthetic Dentistry 2004; 16(3):224-231.

8. McLean JW, Hughes TH. The reinforcement of dental porcelain with ceramic oxides. British Dental Journal 1965; 119(6):251-67.

9. McLean JW. Science and art of dental ceramics. The nature of dental ceramics and their clinical use. Berlin: Quintessence Publishing Co; 1979.

10. Minguez C, Lyons K. Failure of crowns and bridges--a review of the literature. New Zealand Dental Journal 2007; 103(1):7-13.

11. Oh SC, Dong JK, Luthy H, Scharer P. Strength and microstructure of IPS Empress 2 glass-ceramic after different treatments. International Journal of Prosthodontics 2000;13(6):468-72.

12. Holand W, Schweiger M, Frank M, Rheinberger V. A comparison of the microstructure and properties of the IPS Empress 2 and the IPS Empress glass-ceramics. Journal of Biomedical Materials Research 2000;53(4):297-303.

13. Marquardt P, Strub JR. Survival rates of IPS Empress 2 all-ceramic crowns and fixed partial dentures: results of a 5-year prospective clinical study. Quintessence International 2006; 37(4):253-259.

14. Fabianelli A, Goracci C, Bertelli E, et al. A clinical trial of Empress II porcelain inlays luted to vital teeth with a dual-curing adhesive system and a self-curing resin cement. Journal of Adhesive Dentistry 2006; 8: 427-431.

15. Computer-aided direct ceramic restorations: a 10-year prospective clinical study of Cerec CAD/CAM inlays and onlays. International Journal of Prosthodontics, 15 (2002), pp. 122–128.

16. Li RW, Chow TW, Matinlinna JP. Ceramic dental biomaterials and CAD/CAM technology: State of the art. Journal of Prosthodontics Research 2014; Vol. 58 Issue 4 pp 208-216.

17. Birkby, Ian, "Fabrication and Wear of Yttria Tetragonal Polycrystals", University of Leeds Ph.D. Thesis, 1994.

18. IC Clarke, M Manaka, DD Green, P Williams, G Pezzotti, YH Kim, M Ries, N Sugano, L Sedel, C Delauney, BB Nissan, T Donaldson, GA Gustafson. Current Status of Zirconia Used in Total Hip Implants. J Bone Joint Surgery Am, 2003 Nov; 85 (suppl 4): 73-84.

19. Sundh A, Sjogren G. A comparison of fracture strength of yttrium-oxide- partially-stabilized zirconia ceramic crowns with varying core thickness shapes and veneer ceramics. Journal of Oral Rehabilitation 2004;31(7):682-8.

20. Burgess, John OL, Nathaniel C, Robles A. Comparing Digital and Conventional Impressions. Inside Dentistry, November 2013, Volume 9 Issue 11.

21. Anunmana C, Charoenchitt M, Asvanund C. Gap comparison between single crown and three-unit bridge zirconia substructures. Journal of Advanced Prosthodontics August 2014; 6(4): 253-258

22. Parmigiani, J.P. The role of toughness and cohesive strength on crack deflection at interfaces. Journal of the mechanics and Physics of Solids. February 2006 54(2): 266-287

23. Thonpson, Van P., Rekow, Dianne E. Dental Ceramics and the Molar Crown Testing Ground. Journal of Applied Oral Science. 2004;12(spe):26-36.

24. Regish KM, Sharma D, Prithviraj DR. Techniques of Fabrication of Provisional Restoration: an Overview. International Journal of Dentistry. 2011: 134659.

25. Narasimha R. Ceramics in Dentistry, Sintering of Ceramics - New Emerging Techniques, Dr. Arunachalam Lakshmanan. 2012; 978-953-51-0017-1, InTech, Available from:http://www.intechopen.com/books/sintering-of-ceramics-new-emerging-techniques/ceramics-in-dentistry.

26. Borba M, Cesar PF, Griggs JA, Bona AD. Adaptation of all-ceramic fixed partial dentures. Dental Materials. 2011 (11): 1119-1126.

27. Bozogullari N, Inan, O, Usumez A. Bond strength of adhesively luted ceramic discs to different core materials. Journal of Biomedical Material Research Part A. 2009 (89A) Issue 2: 466-471.

28. VITA., VITA In-Ceram YZ: Working Instructions., 2016 Retrieved April 7, 2016 from www.dt-shop.com/fileadmin/media/ga/05899_ga_enu.pdf.

29. Roedentallab., IPS e.max. CAD., 2016 Retrieved April 7, 2016 from http://roedentallab.com/downloads/emaxCADData.pdf.

30. VITA., VITABLOCSS: Working Instructions., 2016 Retrieved April 7, 2016 from http://vitanorthamerica.com/wp-content/uploads/2012/06/VITABLOCSS-Working-Instructions_1769E.pdf

31. Helvey G. Clinical Techniques: Monolithic versus Bilayered restorations: a closer look. Vistas Complete & Predictable Dentistry. 2010; 3(2 Supplement):16-23.

32. Urapepon S, Taenguthai P. The effect of zirconia framework design on the failure of all-ceramic crown under static loading., Journal of Advanced Prosthodontics. 2015 Apr; 7(2): 146–150.

33. Kallaya S, Tulapornchai C, Mamani J, Kamchatphai W, Thongpun N. Effect of the shades of background substructures on the overall color of zirconia-based all-ceramic crowns. Journal of Advanced Prosthodontics. 2013 Aug; 5(3): 319–325.

34. Chang J, Ji W, Choi C, Kim S. Catastrophic failure of a monolithic zirconia prosthesis. The Journal of Prosthetic Dentistry. Volume 113, Issue 2, February 2015, Pages 86–90.

35. Lopez S, Carlos GE, Pelaez, J, Rodriguez V, Suarez M. Fracture resistance and failure mode of posterior fixed dental prostheses fabricated with two zirconia CAD/CAM systems. Journal of Clinical Experience Dentistry. 2015;7(2):e250-3.

36. Wang RR, Lu CL, Wang G, Zhang DS. Influence of cyclic loading on the fracture toughness and load bearing capacities of all-ceramic crowns. International Journal of Oral Science. 2013: 6, 99–104.

37. Olio M, Gjerdet NR, Tvinnereim, HM. The firing procedure influences properties of a zirconia core ceramic, Dental Materials. 2008:4, 471-475.

38. Dundar M, Ozcan M, Gokce B, Comlekoglu E, Leite F, Valandro LF. Comparison of Two Bond Strength Testing Methodologies for Bilayered All-Ceramics. Dental Materials. Volume 23, Issue 5, May 2007, 630-636.

39. Wang XD, Jian YT, Guess PC, Swain MV, Zhang XP, Zhao K. Effect of Core Ceramic Grinding on Fracture Behavior of Bilayered Lithium Disilicate Glass-Ceramic under Two Loading Schemes. Science Direct. Journal of Dentistry 42. 2014. 1436-1445.

40. Dibner AC, Kelly RJ. Fatigue Strength of Bilayered Ceramics Under Cyclic Loading as a Function of Core Veneer Thickness Ratios. The Journal of Prosthetics Dentistry. Volume 115, Issue 3, March 2016. 335-340.

41. Giordano, Russell A., Papanagiotou, Harry P., Morgano, Steven M., Pober, Richard. In vitro evaluation of low-temperature aging effects and finishing procedures on the flexural strength and veneer stability of Y-TZP dental ceramics. The Journal of Prosthetic Dentistry. 2006; Vol 96. Issue 3. 154-156.

42. Shahin R, Kern M. Effect of air-abrasion on the retention of zirconia ceramic crowns luted with different cements before and after artificial aging. Dental Materials 2010. Vol 26. Issue 9. 922-928.

43. Komine F, Strub JR, Matsumura H. Bonding between layering materials and zirconia frameworks. Japanese Dental Science Review. 2012. Vol. 48. Issue 2. 153-161.

44. Amaral R, Ozcan M, Felipe VL, Balducci I. Antonio Bottino, Marco., Effect of conditioning methods on the microtensile bond strength of phosphate monomer-based cement on zirconia ceramic in dry and aged conditions. Journal of Biomedical Research. 2008. Vol. 85B. Issue 1. 1-9.

45. Gu XH, Kern M. Marginal discrepancies and leakage of all-ceramic crowns: influence of luting agents and aging conditions. International Journal of Prosthodontics. 2003. Vol. 16. Issue 2. 109-116.

46. Casucci A, Monticelli F, Goracci C, Mazzitelli C, Cantoro A, Papacchini F, Ferrari M. Effect of surface pre-treatments on the zirconia ceramic–resin cement microtensile bond strength. Dental Materials. 2011. Vol.27. Issue 10. 1024-1030.

47. Daou EE. The Zirconia Ceramic: strengths and weaknesses, The Open Dentistry Journal. 2014; 8: 33-42.

48. Allahkarami M, Hanan JC. Mapping the tetragonal to monoclinic phase transformation in zirconia core dental crowns. Dental Materials. Dec. 2011.Vol 27. Issue 12. 1279-1284.

49. Swain MV. Unstable cracking (chipping) of veneering porcelain on all-ceramic dental crowns and fixed partial dentures. Acta Biomaterialia. June 2009. Vol. 5. Issue 5. 1668-1677.

50. Zhang Yu, Pajares A, Lawn B. Fatigue and damage tolerance of Y-TZP ceramics in layered biomechanical systems. Journal of Biomedical Materials Research. Oct 2004. Vol 71B. Issue 1. 166-171.

51. Sikri, Vimal K. Color: Implications in Dentistry. Journal of Conservative Dentistry. Oct 2010. 13(4): 249–255.

52. DiMatteo, Allison M, Reynolds, Tiffany A. The Evolution of Dental Ceramics. Inside Dentistry. June 2013 Vol 9 Issue 6.

53. Sailer I, Feher A, Filser F, et al. Five-year clinical results of zirconia frameworks for posterior fixed partial dentures. International Journal of Prosthodontics 2007;20(4):383-8.

54. Sax C, Hammerle CH, Sailer I. 10-year clinical outcomes of fixed dental prostheses with zirconia frameworks. International Journal of Computerized Dentistry 2011;14(3):183-202.

55. Beuer F, Edelhoff D, Gernet W, Sorensen JA. Three-year clinical prospective evaluation of zirconia-based posterior fixed dental prostheses (FDPs). Clinical Oral Investigations 2009;13(4):445-51.

56. Tsalouchou E, Cattell MJ, Knowles JC, Pittayachawan P, McDonald A. Fatigue and fracture properties of yttria partially stabilized zirconia crown systems. Dental Materials 2008;24(3):308-18.

57. Schmitter M, Mueller D, Rues S. In vitro chipping behaviour of all-ceramic crowns with a zirconia framework and feldspathic veneering: comparison of CAD/CAM-produced veneer with manually layered veneer. Journal of Oral Rehabilitation 2013;40(7):519-25.

58. Alhasanyah A, Vaidyanathan TK, Finton RJ. Effect of core thickness differences on post-fatigue indentation fracture resistance of veneered zirconia crowns. Journal of Prosthodontics. July 2013 22(5):383-90.

59. Tsalouchou E, Cattell MJ, Knowles JC, Pittayachawan P, McDonald A. Fatigue and fracture properties of yttria partially stabilized zirconia crown systems. Dental Materials 2008;24(3):308-18.

60. Beuer F, Schweiger J, Eichberger M, et al. High-strength CAD/CAM-fabricated veneering material sintered to zirconia copings--a new fabrication mode for all-ceramic restorations. Dental Materials 2009;25(1):121-8.

61. Choi YS, Kim SH, Lee JB, Han JS, Yeo IS. In vitro evaluation of fracture strength of zirconia restorations veneered with various ceramic materials. Journal of Advanced Prosthodontics 2012;4(3):162-9.

62. Schmitter M, Mueller D, Rues S. Chipping behaviour of all-ceramic crowns with zirconia framework and CAD/CAM manufactured veneer. Journal of Dentistry 2012;40(2):154-62.

63. Kanat B, Comlekoglu EM, Dundar-Comlekoglu M, et al. Effect of various veneering techniques on mechanical strength of computer-controlled zirconia framework designs. Journal of Prosthodontics 2014;23(6):445-55.

64. Guess PC, Bonfante EA, Silva NR, Coelho PG, Thompson VP. Effect of core design and veneering technique on damage and reliability of Y-TZP-supported crowns. Dental Materials 2013;29(3):307-16

65. Larsson C, El Madhoun S, Wennerberg A, Vult von Steyern P. Fracture strength of yttria-stabilized tetragonal zirconia polycrystal crowns with different design: an in vitro study. Clinical Oral Implants Research 2012;23(7):820-6.

66. Stawarczyk B, Ozcan M, Roos M, Trottmann A, Hammerle CH. Fracture load and failure analysis of zirconia single crowns veneered with pressed and layered ceramics after chewing simulation. Dental Materials Journal 2011;30(4):554-62.

67. Zhang Y, Sailer I, Lawn BR. Fatigue of dental ceramics. Journal of Dentistry 2013;41(12):1135-47.

68. Studart AR, Filser F, Kocher P, Luthy H, Gauckler LJ. Mechanical and fracture behavior of veneer-framework composites for all-ceramic dental bridges. Dental Materials. 2007 Jan;23(1):115-23.

69. Vult von Steyern P, Carlson P, Nilner K. All-ceramic fixed partial dentures designed according to the DC-Zirkon technique. A 2-year clinical study. Journal of Oral Rehabilitation 2005;32(3):180-7.

70. Raigrodski AJ, Chiche GJ, Potiket N, et al. The efficacy of posterior three-unit zirconium-oxide-based ceramic fixed partial dental prostheses: a prospective clinical pilot study. Journal of Prosthetic Dentistry 2006;96(4):237-44.

71. Tinschert J, Schulze KA, Natt G, et al. Clinical behavior of zirconia-based fixed partial dentures made of DC-Zirkon: 3-year results. International Journal of Prosthodontics 2008;21(3):217-22.

72. Sax C, Hammerle CH, Sailer I. 10-year clinical outcomes of fixed dental prostheses with zirconia frameworks. International Journal of Computerized Dentistry 2011;14(3):183-202.

73. Schley JS, Heussen N, Reich S, et al. Survival probability of zirconia-based fixed dental prostheses up to 5 yr: a systematic review of the literature. European Journal of Oral Sciences 2010;118(5):443-50.

74. Wang X, Fan D, Swain MV, Zhao K. A systematic review of all-ceramic crowns: clinical fracture rates in relation to restored tooth type. International Journal of Prosthodontics 2012;25(5):441-50.

75. Larsson C, Wennerberg A. The clinical success of zirconia-based crowns: a systematic review. International Journal of Prosthodontics 2014;27(1):33-43.

76. Renan Belli et. Al. "Mechanical fatigue degradation of ceramics versus resin composites for dental restorations" Dental 30/4 (2014) 424–432.

77. Mohammad Fahmi. Flexural strength, shear bond strength, and thermal shock behanvior of Y-TZP ceramics, including the effects of aging. Boston University Database.Thesis. WU 190 F157f 2012.

78. Vita North America, VM9 Product Information. 2015. http://vitanorthamerica.com/wp-content/uploads/2009/01/VITA_1192E_VM9_PS_EN_V03_en.pdf

79. Ivoclar vivadent, IPS e.max CAD Veneering Solutions/Crystall./connect. 2015. http://www.ivoclarvivadent.us/en-us/p/all/all-ceramics/ips-emax-system-technicians/ips-emax-cad/ips-emax-cad-veneering-solutions.

Curriculum Vita

Abdulrahman Jafar Alhaddad
Phone: +1(774)-266-1587
Fax: +966(2) 2710009
E-mail: alhaddad@bu.edu

Personality

I am an ambitious, hardworking individual with a competitive spirit. I look forward to increase my knowledge and experiences within the laboratory and clinical setting. I am able to organize and prioritize to provide time efficacy. I enjoy social activities and keep an open mind to situational events. I have a passion for academics and its teaching.

Education

Henry M. Goldman School of Dental Medicine

- CAGS/ DScD in Prosthodontics (2016).

King Abdul Aziz University

- Received Bachelors in Dental Medicine and Surgery (BDS), a Second Honor Degree (2007)

Additional Certification

- Attendance Certificates of all Saudi Dental Society from 2004-2011.
- Attendance Certificate at The First Conference of Faculty of Dentistry in Jeddah, Saudi Arabia.
- Attendance Certificate of HI-Tech Dentistry Program" in King Faisal Hospital in 2005.
- Attendance certificate of the 5th pan Arab Association of Oral-Maxillofacial Surgeons.
- Attendance certificate of the 13th international dental congress in Cairo, Egypt.
- Attendance certificate of completion of basic life support-provider course.
- Attendance certificate of the 2nd International King Abdulaziz University and the 19th Saudi

Dental Society Conference for Dental Technology and Research:

- Certificate in English language learning.
- Certificate of workshop attendance at:
- Management of medically compromised patients and emergencies in dental office.
- Difficult airway management.
- Open surgery or minimally invasive precision endoscopes and instruments for the
- Diagnosis and treatment of salivary gland diseases.

Certificate of appreciation to be a presenter for poster " Factors Affecting Shade Selection " and " New Theory on wear of retorative dental materials " that held in the 2nd International King Abdulaziz University and the 19th Saudi Dental Society Conference for Dental Technology and Research.

Work Experience

2011 – June 2016
Resident of the Prosthodontics Department of Henry M. Goldman School of Dental Medicine

2010 – June 2011
Clinical instructor in Prosthodontics department at King Abdulaziz University

2009 – November 2010
General dentist in International Medical Center 'IMC' in cooperate with Cleveland Clinic.

2008 – 2009
National Guard Primary

- Iskan Jeddah
- Al-Madinah
- Al-Madar Dental Clinic " part time"

2007
Al-Kamal Pharmaceutical Company Ltd.

2006
Trainer at Bugshan General Hospital Dental department under the supervision of Dr. Salem Bawazier and Dr. Abdurrahman Albezrah and Al-Magrabi Hospital in the Medical Record Department.

2004 - 2005
Trainer at King Fahad General Hospital Dental department under the supervision of Dr. Ahmed Nasseri and Dr. Salim bin Mahfouz.

2003
Trainer at the Services Department, King Abdul Aziz University

1999 - 2002
Trainer at Research and Consultation center, King Abdul Aziz University

Memberships

- American Academy of Fixed Prosthodontics (AAFP).
- American Collage of Prosthodontists (ACP).
- Professional Accreditation Certificate from Saudi Commission for Health Specialties as Clinical Prosthodontist.
- Member at the Pan Arab Association for Oral-Maxillofacial Surgeons.
- Member of the Saudi Dental Association.
- Member of the World Gold Council Association.
- Member of PADI (Professional Association of Diving Instructors).